

主論文

Multifunctional Ruthenium Catalysts for Selective Organic Synthesis

(選択的有機合成を指向した多官能性ルテニウム触媒に関する研究)–

–

MATSUOKA Aki

松岡亜季

Department of Chemistry, Graduate School of Science

Nagoya University

2015

Preface

This work was carried out under the direction of University Professor Ryoji Noyori at the Graduate School of Science, Nagoya University, from April 2010 to March 2015. This study is concerned with the understanding and development of multifunctional ruthenium catalysts for selective organic synthesis.

The author wishes to express her sincerest gratitude to Professor Ryoji Noyori for his precise guidance, valuable suggestions and encouragement with warm enthusiasm. The author wishes to express her deepest gratitude to Associate Professor Susumu Saito for his continuous advice, helpful discussions and kind encouragement. The author wishes to express her sincerest gratitude to Dr. Hiroshi Naka for his constant and patient guidance, precise suggestions and continuous encouragement throughout this work.

The author would like to express her appreciation to Professor Kenichiro Itami, Professor Mizuki Tada, Professor Shigehiro Yamaguchi, Professor Kunio Awaga and Professor Masato Kitamura for their valuable suggestions and kind encouragement.

The author is deeply grateful to Associate Professor Ken-ichi Shimizu at Hokkaido University, Associate Professor Atsushi Wakamiya at Kyoto University and Associate Professor Michio M. Matsushita for their helpful discussions and technical assistance. The author also gratefully thanks Dr. Christian A. Sandoval at Enantiotech Co. Ltd., Professor Masanobu Uchiyama at University of Tokyo, Professor Satoshi Maeda at Hokkaido University, Professor Irle Stephan and Associate Professor Daisuke Yokogawa for their valuable suggestions. The author is grateful to Dr. Kunihiko Murata at Kanto Chemicals for providing the samples of $[\text{RuCl}\{(S,S)\text{-TsNCH}(\text{C}_6\text{H}_5)\text{CH}(\text{C}_6\text{H}_5)\text{NH}_2\}(\eta^6\text{-}p\text{-cymene})]$. In addition, the author would like to thank Dr. Ken-ichi Oyama and Mr. Yutaka Maeda in guiding the author through many compound

characterization. The author thanks Mr. Toshiaki Noda, Ms. Hideko Natsume, and Mr. Hisakazu Okamoto for their excellent works of scientific glassware.

Part of this research was conducted in collaboration with Dr. Andrew E. H. Wheatley at the University of Cambridge and Professor Akihiko Kudo at Tokyo University of Science. The author is deeply grateful to Dr. Andrew E. H. Wheatley and Mr. Benjamin R. Knappett for their kind collaborations on TEM and EDX analysis of Ru/chitin as well as valuable suggestions and discussions. The author also gratefully thanks Professor Akihiko Kudo and his group members for their friendly collaboration on SEM and XRD analysis of Ru/SrTiO₃/Rh and helpful suggestions and discussions. In addition, the author is deeply grateful to Dr. Zijun Liu, Mr. Takahiro Isogawa, Ms. Yuna Morioka, Mr. Yuki Takada, Dr. Du Ya and Mr. Yusuke Yamazaki for their great assistance and collaborations.

The author would like to express gratitude to Dr. Foo Siong Wan, Dr. Shunsuke Oishi, Dr. Masakazu Nambo, Mr. Yoshio Nishimoto and Mr. Yusuke Nakanishi for their great assistance and fruitful discussions.

The author deeply thanks Mr. Takashi Miura for his kind encouragement and discussions during the doctoral course. The author thanks the former and present members of the Noyori Laboratory for their kind considerations.

Ms. Yuriko Nakamura	Dr. Ingmar E. Held	Dr. Santosh Agrawal
Dr. Adrian Schulte	Dr. Vasily Tsarev	Dr. Joaquim Caner
Dr. Yingsheng Zhao	Dr. Sina Schwendemann	Dr. Friederike Schröter
Mr. Osamu Kose	Ms. Janine Fröhlich	Mr. Thomas Özgün
Mr. Matthias Dahlkamp	Mr. Tadashi Tachinami	Mr. Shun Oishi
Mr. Junki Ando	Ms. Megumi Suzuki	Mr. Kazuhiko Suzuki
Mr. Richiro Ushimaru	Mr. Kazuki Ida	Ms. Erika Isshiki
Mr. Takuho Nishimura	Mr. Masayuki Naruto	Mr. Shinsuke Iwata
Mr. Lyu Ming Wang	Mr. Sota Nimura	Mr. Katsuaki Toda
Mr. Masaki Shibata	Mr. Kiyotaka Mori	Mr. Yuya Akao

Mr. Taiki Shimomura	Mr. Toshiki Iwatsuki	Mr. Atsushi Nakamura
Mr. Takahiro Aoki	Mr. Che-Sheng Hsu	Mr. Alan K. Kimura
Mr. Guliano S. Goto	Ms. Huang Hsiao Ching	Mr. Sunkook Lee
Mr. Lin Francis	Mr. Byeong-Hyeon Jeong	Mr. Tatsuki Koyama

The author also thanks all other members in Professor Itami's group, Professor Yamaguchi's group and Professor Kitamura's group at Nagoya University and Professor Shimizu's group at Hokkaido University for their kind support and encouragement.

The author thanks the Japan Society for the Promotion of Science (JSPS) for the Research Fellowships for Young Scientists (DC2). The author also thanks Integrative Graduate Education and Research Program in Green Natural Sciences (IGER) program for the fellowship and research funding, International Research Training Group Münster-Nagoya (IRTG-MS-NG) program for giving her the opportunity to join the IRTG meetings in Nagoya University and Münster University and Soroptimist International of the Americas Japan Chuo Region for financial support. In addition, the author appreciates a generous allotment of computer time from the RIKEN Intergrated Cluster of Clusters (RICC).

Finally, the author wishes to express the deepest appreciation to her family, Yoshio Matsuoka, Shoko Matsuoka, Sawa Shimizu, Hirotaka Shimizu, Chigusa Matsuoka, Chizu Matsuoka, Hiroshi Kazaoka and Nobuko Kazaoka for their constant assistance and warm encouragement.

MATSUOKA Aki

Department of Chemistry
Graduate School of Science
Nagoya University
2015

Contents

Chapter 1.	General Introduction	1
Chapter 2.	Why <i>p</i> -Cymene? Conformational Effect in Asymmetric Hydrogenation of Aromatic Ketones with a η^6 -Arene/Ruthenium(II) Catalyst	17
Chapter 3.	Hydration of Nitriles to Amides by a Chitin-supported Ruthenium Catalyst	41
Chapter 4.	Aldehyde and Molecular Hydrogen via the Visible-light-promoted Dehydrogenative of Alcohols by Ru/SrTiO ₃ :Rh	65
	Lists of Publications	101

Abbreviations

AH	asymmetric hydrogenation	FT	fourier transformation
aq	aqueous	G	gibbs free energy
ATH	asymmetric transfer hydrogenation	GC	gas chromatography
au	arbitrary unit	h	hour
B3LYP	Becke three-parameter hybrid functional combined with Lee–Yang–Parr correlation functional	h	Planck's constant
BINOL	1,1'-bi-2-naphthol	H	enthalpy
bs	broad singlet	Hz	herz
BS	basis set	HR	high resolution
Cbz	benzyloxycarbonyl group	ICP-AES	inductively coupled plasma atomic emission spectroscopy
Cp*	1,2,3,4,5-pentamethylcyclopentadienyl	IR	infrared spectroscopy
d	doublet	J	coupling constant
δ	chemical shift	λ	wave length
dd	doublet of doublets	l -ADDF	large-anharmonic downward distortion following
DFT	density functional theory	m	multiplet
DV	objective defocus	m	meta
DRS	diffuse reflectance spectra	M	metal
e	electron	min	minute
ϵ	permittivity	MS	mass spectrometry
EDX	energy dispersive X-ray spectrometry	MP2	second-order Møller–Plesset perturbation theory
ee	enantiomeric excess	n	nano
FAB	fast atom bombardment	n	normal
Fmoc	9-fluorenylmethyloxycarbonyl	NMR	nuclear magnetic resonance
		NOEs	nuclear Overhauser effects
		NOESY	NOE correlated spectroscopy

NPA	natural population analysis	TBAF	tetrabutylammonium fluoride
<i>o</i>	ortho		
<i>p</i>	para	TCD-GC	thermal conductivity detector coupled with gas chromatography
PCM	polarizable continuum model		
q	quartet	TEM	transmission electron microscopy
R	an organic group		
rpm	rotation per minute	TGA	thermogravimetric analysis
rt	room temperature	THF	tetrahydrofuran
s	singlet	TS	transition structure
SCRF	self-consistent reaction field	UFF	universal force field
SCS	spin-component-scaled	UV	ultraviolet
SEM	scanning electron microscopy	<i>V</i>	volume
		W	watt
sept	septet	wt	weight
t	triplet	XRD	X-ray diffraction

Chapter 1.

General Introduction

1.1 Concept of multifunctional catalyst

Catalysis is a very important tool for organic synthesis. Most products in chemical industry are prepared by means of catalysis.¹ Establishing a highly efficient catalytic system is an important objective in organic synthesis. The concept of multifunctional catalyst is one of the most attractive principles for catalyst design in homogeneous²⁻⁶ and heterogeneous⁷ catalysis. A multifunctional catalyst should contain two or more catalytic functional groups that work for binding or recognizing reagents/substrates. These catalytic functional groups typically activate electrophiles and nucleophiles simultaneously (Figure 1.1a).²⁻⁵ Various multifunctional catalysts have been developed and contributed to selective organic synthesis by realizing effective molecular transformations.²⁻⁵ They often display higher reaction rate and/or selectivity than those of monofunctional catalysts, presumably because reactions are promoted by positive synergistic effects of the multiple catalytic functional groups.²⁻⁸

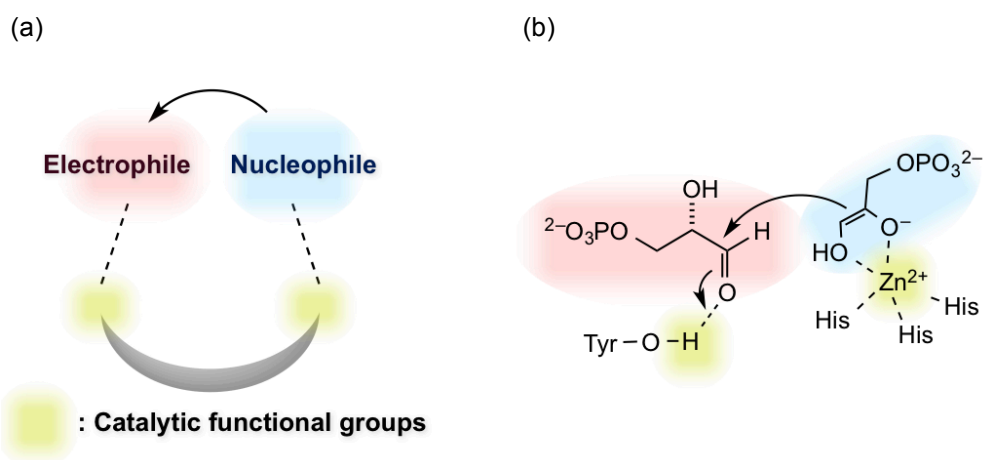


Figure 1.1. (a) Concept of multifunctional catalysts. (b) Proposed transition state of class II aldolase.^{9c}

In Nature, a number of enzymes, such as aldolase, urease and amine oxidase, work as multifunctional catalysts and show high catalytic ability in organic reactions.⁹ Type II zinc enolate aldolase is a representative multifunctional catalyst that promotes asymmetric aldol reaction of dihydroxyacetone phosphate and various aldehydes under neutral conditions. As synergistic effect between the tyrosine residue as a proton donor for aldehydes and the Zn ion as Lewis acid for generating enolate has been proposed in the transition state (Figure 1.1b).^{9c} The high performance of enzymes has been motivating the development of artificial multifunctional catalysts.^{2,10}

1.2 Artificial multifunctional catalysts for organic synthesis

Numerous artificial multifunctional catalysts have been developed to date and various types of synergistic effects have been reported.^{2-46,48-50} In this chapter, the author categorized multifunctional catalysts by the types of active sites: synergies between (1) multiple organic functional groups, (2) organic functional group and metallic species and (3) multiple metallic species. Each category is shown for homogeneous and heterogeneous catalysts.

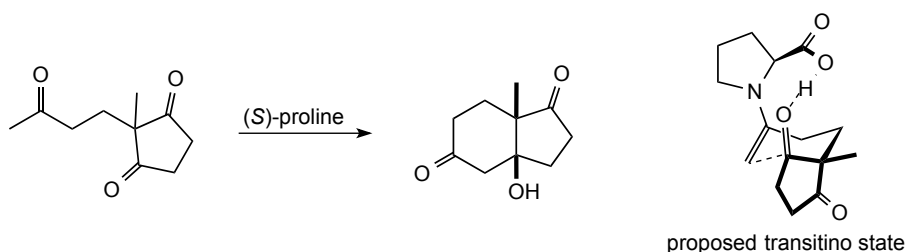
1.2.1 Multifunctional homogeneous catalyst

Type 1. Synergistic effects of multiple organic functional groups

Acid and base are the common catalytic functional groups. Thus, multifunctional acid catalysts,^{11,14} acid-base catalysts^{12,13,15-18} and anionic or cationic¹⁹ catalysts have been studied. Multifunctional acid catalysts displaying cooperative effects between Lewis acids and/or Brønsted acids have been recently reviewed by Yamamoto.¹¹

Multifunctional acid–base catalysts work through cooperative effects between acidic and basic sites in catalysts. Such acid–base cooperative catalysts include proline,^{16,17} thiourea,¹² ammonium salt bearing basic functional group,¹³ chiral Brønsted acids¹⁴ and frustrated Lewis pairs.¹⁵ Proline is a representative example of multifunctional acid–base catalysts. The pioneering work by List and coworkers on aldol reaction with proline in 2000¹⁶ led to the further exploration of this catalyst in other organic reactions, including asymmetric aldol reaction, Mannich reaction, Michael reaction and amination reaction.¹⁷ In these systems, cooperative effects of acidic

carboxylic-acid and basic amine moieties have been proposed by the experimental and theoretical studies (Scheme 1.1).⁸



Scheme 1.1. Intramolecular aldol reaction with proline.

In ion-pairing catalysis, charged catalyst intermediates interact substrates with multiple catalytic functional groups. These catalysts have been recently reviewed in ref. 19.

Type 2. Synergistic effects of organic functional groups and metal ions

Metal–ligand bifunctional catalyst is a leading concept for multifunctional catalysts and have been well studied.³ These catalysts promote the reaction through acid–base cooperative effect between metal ions and organic functional groups in ligand. Figure 1.2. shows typical bifunctional metal-based molecular catalysts.

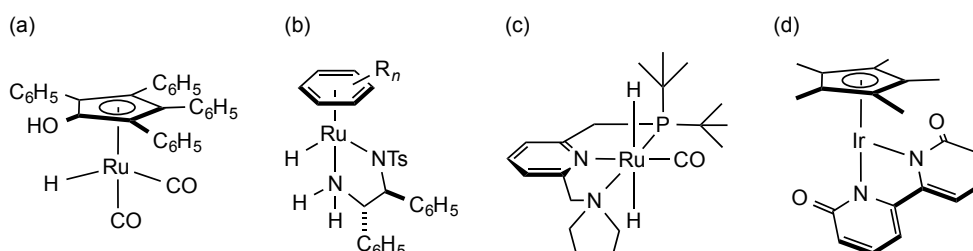


Figure 1.2. Structures of typical bifunctional metal-based molecular catalysts discovered by (a) Shvo,²⁰ (b) Noyori,²² (c) Milstein²⁶ and (d) Fujita.²⁷

The concept of metal–ligand bifunctional catalyst was introduced in 1984 by Shvo and coworkers in the hydrogen transfer reaction with a cyclopentadienone-ligated diruthenium complex (Figure 1.2a).²⁰ A mechanistic study indicated the presence of cooperative effects between ruthenium and ligand in the hydrogenation of ketones to alcohols.²¹ In 1995, Noyori and coworkers developed ruthenium–ligand bifunctional catalysts, $[\text{RuH}\{(S,S)\text{- or } (R,R)\text{-Tsdpen}\}(\eta^6\text{-arene})]$ [$\text{Tsdpen} = \text{TsNCH}(\text{C}_6\text{H}_5)\text{CH}(\text{C}_6\text{H}_5)\text{NH}_2$] (Figure 1.2b)²² These catalysts have long served as a prototype of chiral catalyst for asymmetric hydrogenation²³ and transfer hydrogenation.²⁴ The extensive mechanistic study showed the reaction proceeds through acid–base cooperative effect between ruthenium and NH moiety in the Tsdpen ligand.²³ In addition, the origin of the enantio-face selection has been identified to the CH/ π electronic attraction between catalyst and substrate in the favored transition state (Figure 1.3).^{23b,25} In 2005, Milstein and coworkers reported a ruthenium–ligand bifunctional precatalyst $[(\text{PNP})\text{RuHCl}(\text{CO})]$ promoted sequential dehydrogenation of primary alcohols and aldehyde monohydrate, giving esters (Figure 1.2c).^{26a} The authors proposed that the reaction proceeds through metal–ligand cooperation based on aromatization–dearomatization of pyridine moiety in the pincer ligand. Recently, Fujita and coworkers reported the dehydrogenation of alcohols with iridium–ligand bifunctional catalysts, $\text{Cp}^*\text{Ir}(\text{bpyO})$ ($\text{Cp}^* = 1,2,3,4,5\text{-pentamethylcyclopentadienyl}$, $\text{bpyO} = \alpha,\alpha'\text{-bipyridonate}$, Figure 1.2d). They proposed the bpyO ligand and iridium work cooperatively based on the results of theoretical studies.²⁷

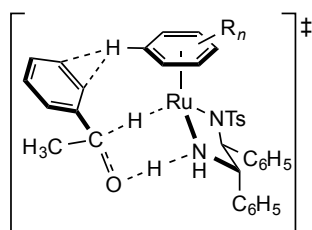


Figure 1.3. CH/ π attraction between catalyst and substrate in favored transition state AH and ATH of acetophenone using $[\text{RuH}\{(S,S)\text{-Tsdpen}\}(\eta^6\text{-arene})]$.

BINOL-based molecular catalysts also have been well studied.^{28,29} In 1992, Shibasaki and coworkers reported the first example of catalytic asymmetric nitroaldol reaction with a BINOL-based lanthanum catalyst.^{29a} Based on the X-ray and MS analysis, they expected the presence of catalyst structure shown in Figure 1.4 and proposed that the catalyst promotes the reaction through cooperative effects of metal and ligand which works as Lewis acid and Brønsted base, respectively.^{29b,c}

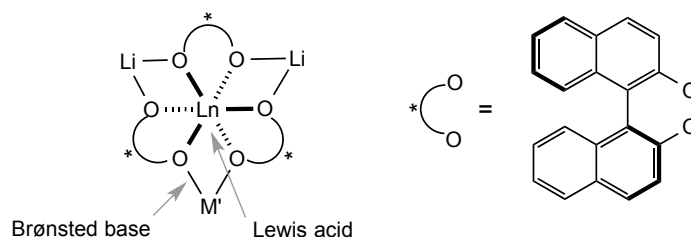


Figure 1.4. Proposed structure of BINOL-based lanthanum catalyst. M' = alkali metal and Ln = rare earth metal.

Type 3. Synergistic effects of metal ions

Various multimetallic catalysts, such as bimetallic catalyst,^{30–32} alloy catalysts³³ and polyoxometalates³⁴ have been developed, expecting synergistic positive effects of multi-metallic ions.

A recent representative work in this field is chiral Schiff base-based transition metal–rare earth metal bimetallic catalysts by Shibasaki and coworkers.³¹ They expected the transition metal and rare earth metal work cooperatively as Lewis acid (Figure 1.5). This concept enabled highly enantioselective α -addition of isocyanides to aldehydes. The multifunctional catalyst showed higher ability than monofunctional analogues.^{31a}

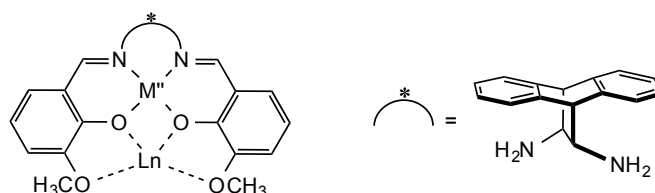


Figure 1.5. Structure of Schiff-base based bimetallic catalyst. M'' = transition metal and Ln = rare earth metal.

1.2.2 Multifunctional heterogeneous catalyst

Type 1. Synergistic effects of multiple organic functional groups

Inspired by the synergistic positive effects of organic functional groups on the activity and selectivity in the homogeneous catalysis,³⁵ various heterogeneous catalysts bearing organic functional groups have been developed, expecting the synergistic effects of acidic and/or basic functional groups on/of support.^{4,36–38} Metal oxide-, typically silica-, supported organic functional groups are one of the well studied multifunctional heterogeneous catalysts.⁷ Silica-supported organocatalysts which contain multiple functional groups have been reported to show cooperative effects between amines and silanols,^{7a,38} amines and urea,³⁹ thiol and sulfonic acid,⁴⁰ or amines and thiol.⁴¹

Figure 1.6 shows a representative acid–base bifunctional catalyst developed by Lin and coworkers in 2005, in which the urea and amine moieties activate substrate and reagent cooperatively and promote the C–C bond formation through aldol reaction, nitroaldol reaction and cyanosilylation.³⁶

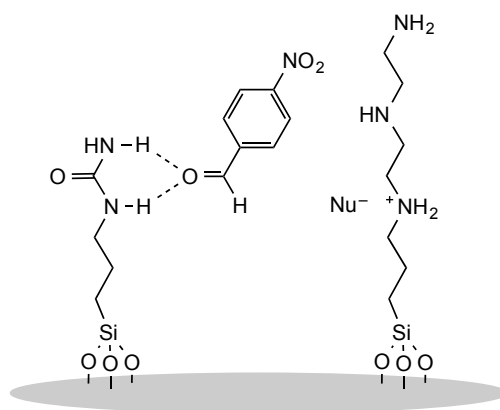


Figure 1.6. Working hypothesis for C–C coupling with urea–amine bifunctional catalyst.

Type 2. Synergistic effects of organic functional groups and metal ions

Cooperative effects between organic functional groups and metal centers in the reaction using metal complexes⁴² and metal nanoparticles including nanoalloys^{43–46} have been reported.

The synergistic effects between support and metallic species in metal-oxide-supported metal nanoparticles^{44,45} have been more widely explored than that of organic-polymer-supported metal nanoparticles.⁴⁴ Recently, chemoselective organic reaction with metal-oxide-supported metal nanoparticles, such as hydrogenation with gold on titania^{45a} or silver on alumina,^{45b} deoxygenation with gold on titania,^{45c} dehydrogenation with platinum^{45d} or nickel^{45e} on alumina, aldol reaction with erbium on silica^{45g} and oxidation with gold–palladium alloy on Mg–Al mixed metaloxide⁴⁶ were discovered.

One of the well-studied reactions is hydrogenation of nitroaromatics to anilines catalyzed by aluminum-oxide-supported silver nanoparticle (Ag/Al₂O₃).^{45b} Satsuma, Shimizu and coworkers found that Ag/Al₂O₃ promotes chemoselective hydrogenation of nitro moiety in nitroaromatics in the presence of olefin, ketone and nitrile groups, which are often hydrogenated with catalysts consisting of platinum group metals.⁴⁷ FTIR studies indicated cooperative effects between acid–base bifunctional support and unsaturated silver species is required for the heterolytic cleavage of H₂ on the Ag atom and Al₂O₃ support, respectively (Figure 1.7).

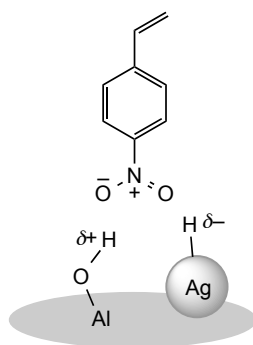


Figure 1.7. Proposed cooperative effect between metal nanoparticle and supports for hydrogenation of nitroaromatics to anilines.

More recently, cooperative effects of metal and support have been noted in the photocatalytic reaction, such as reduction of nitrobenzenes with titanium-oxide-supported gold catalyst.⁴⁸

Type 3. Synergistic effects of metal ions

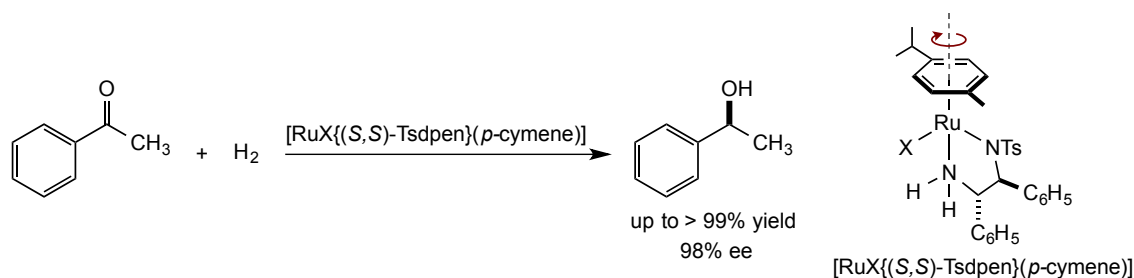
Synergistic effects of metal ions in solid-supported bimetallic nanoparticles such as nanoalloy and core-shell objects have been recently reviewed,⁴⁹ including their application to C–C bond-forming reactions^{50a} and C–heteroatom bond-forming reactions.^{50b}

1.3 Survey of this thesis

Establishing a highly selective and efficient catalytic system is an important objective in organic synthesis. Multifunctional catalyst is a representative concept of catalyst design that has been rationally achieving this objective. Some multifunctional catalysts did contribute to the selective organic synthesis.^{2,3,45,49} Design of the active site is the key to realizing high selectivity and reactivity of these catalysts. Thus, the deep understanding of the nature of active sites as well as creating new types of multifunctional catalysts are important in helping for future catalyst design.

In this thesis, the author focused on the multifunctional ruthenium catalysts because ruthenium has been most commonly used as a metal center in bifunctional molecular catalysts. Her finding of a new functionality in a homogeneous bifunctional catalyst and development of heterogeneous catalysts based on multifunctional catalysts are summarized therein.

Chapter 2 deals with ligand effects on the enantioselectivity in asymmetric hydrogenation of aromatic ketone with $[\text{RuX}\{(S,S)\text{-Tsdpen}\}(p\text{-cymene})]$ ($X = \text{Cl}$ or CF_3SO_3) (Scheme 1.2).^{23a,b,d} Transition states in the chirality-determining elementary step were systematically determined by using global reaction route mapping methods. The author found new functionality of the *p*-cymene ligand, noting that multiple electrostatic CH/ π interactions between *p*-cymene and phenyl ring of ketone are the major origin of enantioselectivity (Figure 1.8).⁵¹



Scheme 1.2. Asymmetric hydrogenation of acetophenone to (*S*)-1-phenylethanol using [RuX{(S,S)-Tsdpen}(p-cymene)].^{23a,b,d}

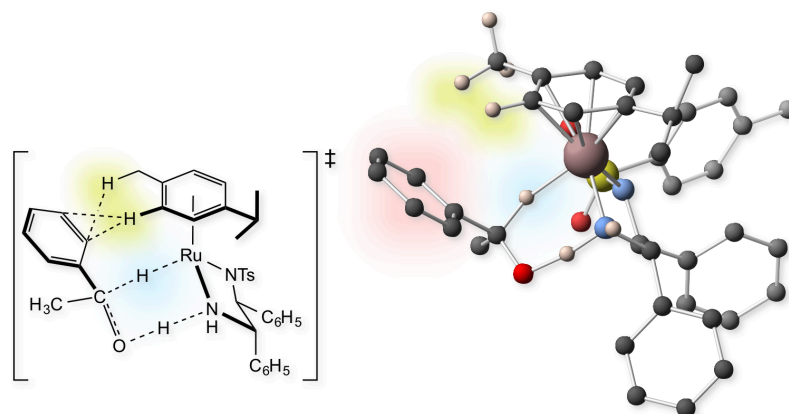


Figure 1.8. Multiple electrostatic CH/π interactions between the *p*-cymene ligand and the phenyl ring of ketone as a origin of enantioselectivity.⁵¹

In chapter 3, the author reports hydration of nitriles to carboxamides with a chitin-supported ruthenium (Ru/chitin) catalyst. The catalyst was designed expecting that the nitrile hydration proceeds through cooperative effect between ruthenium nanoparticles and the organic functionalities of chitin (Figure 1.9). The Ru/chitin catalyst was found to promote the hydration of nitriles under near-neutral, aqueous conditions. The methods are applicable to a wide variety of nitriles with aromatic, heteroaromatic and aliphatic substituents. Importantly, Ru/chitin shows high chemoselectivity in hydration of nitriles bearing redox- or acid/base-sensitive functional groups, such as olefin, aldehyde, methyl ester and benzyloxycarbonyl groups (Scheme 1.3).⁵²

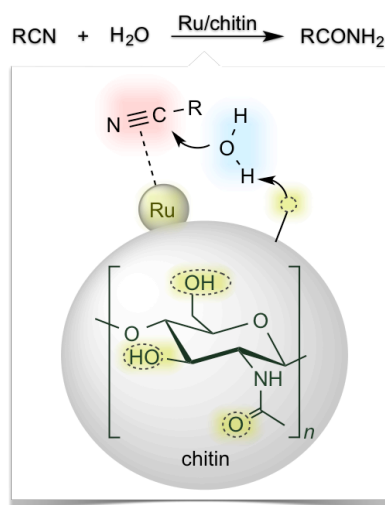
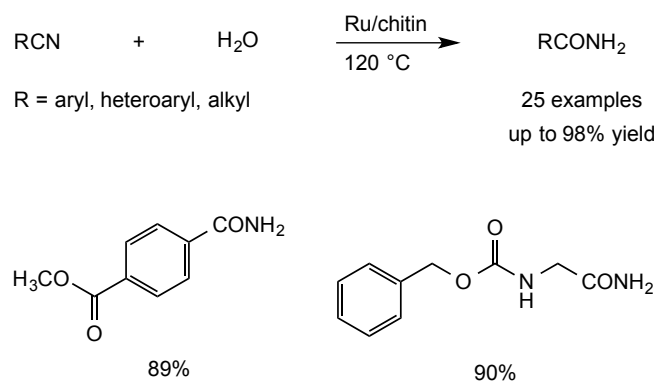


Figure 1.9. Working hypothesis for the hydration of nitriles to amides catalyzed by Ru/chitin.



Scheme 1.3. Hydration of nitriles to amides using Ru/chitin.⁵²

In chapter 4, the author shows the photocatalytic dehydrogenation of alcohols to aldehydes using ruthenium-loaded $\text{SrTiO}_3\text{:Rh}$ ($\text{Ru/SrTiO}_3\text{:Rh}$) (Figure 1.10). This photocatalyst potentially works as a multifunctional photocatalyst through cooperative effect between ruthenium nanoparticles and $\text{SrTiO}_3\text{:Rh}$. The author found that $\text{Ru/SrTiO}_3\text{:Rh}$ promoted dehydrogenation of alcohols to aldehydes under visible light irradiation. The

reaction is compatible with the presence of redox- or base-sensitive functional groups, such as olefin, alkyne, ketone and carbamate. Importantly, various allylic olefins in alcohols are also tolerated and corresponding products with high preservation of stereochemical integrity (Scheme 1.4). This chapter covers structural features of Ru/SrTiO₃:Rh, optimization of reaction conditions, full substrate scope and investigation on the reaction mechanism.

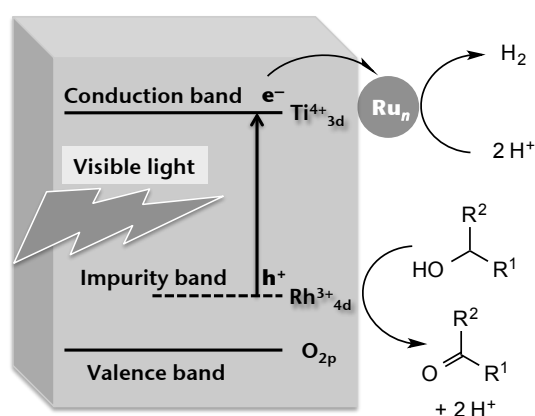
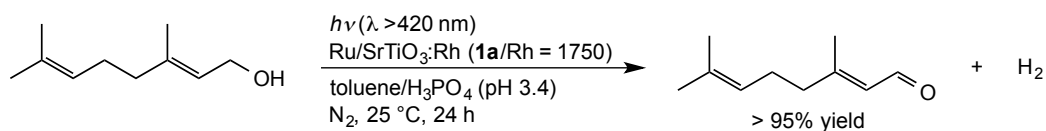


Figure 1.10. Proposed mechanism of dehydrogenation of alcohols to aldehydes using Ru/SrTiO₃:Rh.



Scheme 1.4. Conversion of geraniol to corresponding aldehyde by Ru/SrTiO₃:Rh.

1.4 Notes and References

- 1 a) J. G. de Vries and S. D. Jackson, *Catal. Sci. Technol.*, 2012, **2**, 2009. b) *Nanomaterials in Catalysis*, ed. P. Serp and K. Philippot, Wiley-VCH, Weinheim, 2013.
- 2 *Multimetallic Catalysts in Organic Synthesis*, ed. M. Shibasaki and Y. Yamamoto, Wiley-VCH, Weinheim, 2004.
- 3 *Bifunctional Molecular Catalysis*, ed. T. Ikariya and M. Shibasaki, Springer, New York, 2011.
- 4 C. Yu and J. He, *Chem. Commun.*, 2012, **48**, 4933–4940.
- 5 J.-A. Ma and D. Cahard, *Angew. Chem. Int. Ed.*, 2004, **43**, 4566–4583.
- 6 Synergistic activation of reagent and reactant by two distinct catalysts has been recently reviewed. See: A. E. Allen and D. W. C. MacMillan, *Chem. Sci.*, 2012, **3**, 633–658.
- 7 a) K. Motokura, M. Tada, and Y. Iwasawa, *Chem. Asian J.*, 2008, **3**, 1230–1236. b) E. L. Margelefsky, R. K. Zeidan and M. E. Davis, *Chem. Soc. Rev.*, 2008, **37**, 1118–1126. c) U. Díaz, D. Brunel and A. Corma, *Chem. Soc. Rev.*, 2013, **42**, 4083–4097.
- 8 R. Noyori, M. Yamakawa and S. Hashiguchi, *J. Org. Chem.*, 2001, **66**, 7931–7944.
- 9 a) R. L. Blakeley and B. Zerner, *J. Mol. Catal.*, 1984, **23**, 263–292. b) J. P. Klinman, *Chem. Rev.*, 1996, **96**, 2541–2562. c) T. D. Machajewski and C.-H. Wong, *Angew. Chem. Int. Ed.*, 2000, **39**, 1352–1374.
- 10 a) E. K. van den Beuken and B. L. Feringa, *Tetrahedron*, 1998, **54**, 12985–13011. b) M. Sawamura and Y. Ito, *Chem. Rev.*, 1992, **92**, 857–871. c) M. S. Taylor and E. N. Jacobsen, *Angew. Chem. Int. Ed.*, 2006, **45**, 1520–1543. d) S. Mukherjee, J. W. Yang, S. Hoffmann and B. List, *Chem. Rev.*, 2007, **107**, 5471–5569. e) J. Park and S. Hong, *Chem. Soc. Rev.*, 2012, **41**, 6931–6943.
- 11 H. Yamamoto and K. Futatsugi, *Angew. Chem. Int. Ed.*, 2005, **44**, 1924–1942.
- 12 Y. Takemoto, *Chem. Pharm. Bull.*, 2010, **58**, 593–601.
- 13 a) L. Wang, S. Shirakawa and K. Maruoka, *Angew. Chem. Int. Ed.*, 2011, **50**, 5327–5330. b) J. Novacek and M. Waser, *Eur. J. Org. Chem.*, 2013, 637–648.
- 14 a) F. Lv, S. Liu and W. Hu, *Asian J. Org. Chem.*, 2013, **2**, 824–836. b) M. Rueping, A. Kuenkel and I. Atodiresei, *Chem. Soc. Rev.*, 2011, **40**, 4539–4549.

- 15 a) D. W. Stephan and G. Erker, *Angew. Chem., Int. Ed.*, 2010, **49**, 46–76. b) D. W. Stephan, S. Greenberg, T. W. Graham, P. Chase, J. J. Hastie, S. J. Geier, J. M. Farrell, C. C. Brown, Z. M. Heiden, G. C. Welch and M. Ullrich, *Inorg. Chem.*, 2011, **50**, 12338–12348. c) G. Erker, *Dalton Trans.*, 2012, **41**, 9101–9110. d) O. Eisenstein and R. H. Crabtree, *New J. Chem.*, 2013, **37**, 21–27.
- 16 B. List, R. A. Lerner, and C. F. Barbas III, *J. Am. Chem. Soc.*, 2000, **122**, 2395–2396.
- 17 a) E. R. Jarvo and S. J. Miller, *Tetrahedron*, 2002, **58**, 2481–2495. b) B. List, *Tetrahedron*, 2002, **58**, 5573–5590.
- 18 a) L. Hoang, S. Bahnmanyar, K. N. Houk, B. List, *J. Am. Chem. Soc.*, 2003, **125**, 16–17. b) B. List, L. Hoang, H. J. Martin, *Proc. Natl. Acad. Sci. USA*, 2004, **101**, 5839–5842.
- 19 K. Brak and E. N. Jacobsen, *Angew. Chem. Int. Ed.*, 2013, **52**, 534–561.
- 20 a) Y. Blum and Y. Shvo, *Isr. J. Chem.*, 1984, **24**, 144–148. b) Y. Shvo, D. Czarkie and Y. Rahamim, *J. Am. Chem. Soc.*, 1986, **108**, 7400–7402.
- 21 C. P. Casey, S. W. Singer, D. R. Powell, R. K. Hayashi and M. Kavana, *J. Am. Chem. Soc.*, 2001, **123**, 1090–1100.
- 22 a) S. Hashiguchi, A. Fujii, J. Takehara, T. Ikariya and R. Noyori, *J. Am. Chem. Soc.*, 1995, **117**, 7562–7563. b) A. Fujii, S. Hashiguchi, N. Uematsu, T. Ikariya and R. Noyori, *J. Am. Chem. Soc.*, 1996, **118**, 2521–2522. c) N. Uematsu, A. Fujii, S. Hashiguchi, T. Ikariya and R. Noyori, *J. Am. Chem. Soc.*, 1996, **118**, 4916–4917.
- 23 a) T. Ohkuma, N. Utsumi, K. Tsutsumi, K. Murata, C. Sandoval and R. Noyori, *J. Am. Chem. Soc.*, 2006, **128**, 8724–8725. b) C. A. Sandoval, T. Ohkuma, N. Utsumi, K. Tsutsumi, K. Murata and R. Noyori, *Chem. Asian J.*, 2006, **1–2**, 102–110. c) T. Ohkuma, K. Tsutsumi, N. Utsumi, N. Arai, R. Noyori and K. Murata, *Org. Lett.*, 2007, **9**, 255–257. d) C. A. Sandoval, F. Bie, A. Matsuoka, Y. Yamaguchi, H. Naka, Y. Li, K. Kato, N. Utsumi, K. Tsutsumi, T. Ohkuma, K. Murata and R. Noyori, *Chem. Asian J.*, 2010, **5**, 806–816. e) N. Arai, H. Satoh, N. Utsumi, K. Murata, K. Tsutsumi and T. Ohkuma, *Org. Lett.*, 2013, **15**, 3030–3033.
- 24 a) S. Hashiguchi, A. Fujii, J. Takehara, T. Ikariya and R. Noyori, *J. Am. Chem. Soc.*, 1995, **117**, 7562–7563. b) A. Fujii, S. Hashiguchi, N. Uematsu, T. Ikariya and R. Noyori, *J. Am. Chem. Soc.*, 1996, **118**, 2521–2522.
- 25 a) M. Yamakawa, I. Yamada and R. Noyori, *Angew. Chem. Int. Ed.*, 2001, **40**,

- 2818–2821.
- 26 a) J. Zhang, G. Leitus, Y. B.-David and D. Milstein, *J. Am. Chem. Soc.*, 2005, **127**, 12429–12429. b) J. Zhang, G. Leitus, Y. B.-David and D. Milstein, *Angew. Chem. Int. Ed.*, 2006, **45**, 1113–1115.
- 27 a) R. Kawahara, K. Fujita and R. Yamaguchi, *Angew. Chem. Int. Ed.*, 2012, **51**, 12790–12794. b) K. Fujita, Y. Tanaka, M. Kobayashi and R. Yamaguchi, *J. Am. Chem. Soc.*, 2014, **136**, 4829–4832. c) G. Zeng, S. Sakaki, K. Fujita, H. Sano and R. Yamaguchi, *ACS Catal.*, 2014, **4**, 1010–1020.
- 28 H. Gröger, *Chem. Eur. J.*, 2001, **7**, 5246–5251.
- 29 a) H. Sasai, T. Suzuki, T. Arai, M. Shibasaki, *J. Am. Chem. Soc.*, 1992, **114**, 4418–4419. b) M. Shibasaki, H. Sasai, T. Arai, *Angew. Chem. Int. Ed. Engl.*, 1997, **36**, 1236–1256. c) A. J. Wooten, P. J. Carroll, P. J. Walsh, *J. Am. Chem. Soc.*, 2008, **130**, 7407–7419.
- 30 M. Kitamura, S. Suga, K. Kawai, R. Noyori, *J. Am. Chem. Soc.*, 1986, **108**, 6071–6072.
- 31 a) H. Mihara, Y. Xu, N. E. Shepherd, S. Matsunaga and M. Shibasaki, *J. Am. Chem. Soc.*, 2009, **131**, 8384–8385. b) S. Handa, V. Gnanadesikan, S. Matsunaga and M. Shibasaki, *J. Am. Chem. Soc.*, 2010, **129**, 4900–4901. c) S. Handa, V. Gnanadesikan, S. Matsunaga and M. Shibasaki, *J. Am. Chem. Soc.*, 2010, **132**, 4925–4934. d) S. Matsunaga and M. Shibasaki, *Chem. Commun.*, 2014, **50**, 1044–1057.
- 32 B. M. Trost and H. Ito, *J. Am. Chem. Soc.*, 2000, **122**, 12003–12004. b) R. M. Haak, S. J. Wezenberga and A. W. Kleij, *Chem. Commun.*, 2010, **46**, 2713–2723.
- 33 C. L. Bracey, P. R. Ellisb and G. J. Hutchings, *Chem. Soc. Rev.*, 2009, **38**, 2231–2243.
- 34 a) T. Okuhara, N. Mizuno and M. Misono, *Adv. Catal.*, 1996, **41**, 113–252. b) I. Kozhevnikov, *Catalysts for Fine Chemical Synthesis, Volume 2, Catalysis by Polyoxometalates*, Wiley, Chichester, 2002.
- 35 a) J. E. Jansen, US Pat., 2 468 982, 1949. b) G. T. Williamson, US Pat., 2 730 552, 1956.
- 36 a) S. Huh, H.-T. Chen, J. W. Wiench, M. Pruski and V. S.-Y. Lin, *Angew. Chem. Int. Ed.*, 2005, **44**, 1826–1830.
- 37 a) R. K. Zeidan and M. E. Davis, *J. Catal.*, 2007, **247**, 379–382. b) R. K. Zeidan,

- S.-J. Hwang and M. E. Davis, *Angew. Chem. Int. Ed.*, 2006, **45**, 6332–6335.
- 38 K. Motokura, *J. Jpn. Petrol. Inst.*, 2014, **57**, 95–108.
- 39 a) A. Puglisi, R. Annunziata, M. Benaglia, F. Cozzi, A. Gervasini, V. Bertacche and M. C. Sala, *Adv. Synth. Catal.*, 2009, **351**, 219–229. b) S. Huh, H.-T. Chen, J. W. Wiench, M. Pruski and V. S.-Y. Lin, *Angew. Chem., Int. Ed.*, 2005, **44**, 1826–1830.
- 40 a) E. L. Margelefsky, R. K. Zeidan, V. Dufaud and M. E. Davis, *J. Am. Chem. Soc.*, 2007, **129**, 13691–13697. b) E. L. Margelefsky, A. Bendjériou, R. K. Zeidan, V. r. Dufaud and M. E. Davis, *J. Am. Chem. Soc.*, 2008, **130**, 13442–13449.
- 41 J. D. Bass and A. Katz, *Chem. Mater.*, 2006, **18**, 1611–1620.
- 42 J. M. Notestein and A. Katz, *Chem. Eur. J.*, 2006, **12**, 3954–3965.
- 43 Z. Li, J. Liu, C. Xia and F. Li, *ACS Catal.*, 2013, **3**, 2440–2448.
- 44 a) P. Barbaro, F. Liguori, N. Linares and C. M. Marrodan, *Eur. J. Inorg. Chem.*, 2012, 3807–3823. b) T. Mitsudomea and K. Kaneda, *Green Chem.*, 2013, **15**, 2636–2654.
- 45 a) M. Boronat, P. Concepción, A. Corma, S. González, F. Illas and P. Serna, *J. Am. Chem. Soc.*, 2007, **129**, 16230–16237. b) K.-i. Shimizu, Y. Miyamoto and A. Satsuma, *J. Catal.*, 2010, **270**, 86–94. c) J. Ni, L. He, Y.-M. Liu, Y. Cao, H.-Y. He and K.-N. Fan, *Chem. Commun.*, 2011, **47**, 812–814. d) K. Kon, S. M. A. H. Siddiki, K.-i. Shimizu, *J. Catal.*, 2013, **304**, 63–71. e) K.-i. Shimizu, K. Kon, K. Shimura, S. S. M. A. Hakim, *J. Catal.*, 2013, **300**, 242–250. f) A. Hamasaki, Y. Yasutake, T. Norio, T. Ishida, T. Akita, H. Ohashi, T. Yokoyama, T. Honma, M. Tokunaga, *Appl. Catal. A: General*, 2014, **469**, 146–152. g) M. Oliverio, P. Costanzo, A. Macario, G. D. Luca, M. Nardi and A. Procopio, *Molecules*, 2014, **19**, 10218–10229. h) P. Hirunsit, K.-i. Shimizu, R. Fukuda, S. Namuangruk, Y. Morikawa and M. Ehara, *J. Phys. Chem. C*, 2014, **118**, 7996–8006.
- 46 a) K. Mori, Y. Miura, S. Shironita and H. Yamashita, *Langmuir*, 2009, **25**, 11180–11187. b) J. Feng, C. Ma, P. J. Miedziak, J. K. Edwards, G. L. Brett, Di. Li, Y. Du, D. J. Morganb and G. J. Hutchings, *Dalton Trans.*, 2013, **42**, 14498–14508.
- 47 a) S. Xu, X. Xi, J. Shi and S. Cao, *J. Mol. Catal. A*, 2000, **160**, 287–292. b) M. Takasaki, Y. Motoyama, K. Higashi, S.-H. Yoon, I. Mochida and H. Nagashima, *Org. Lett.*, 2008, **10**, 1601–1604.
- 48 S.-i. Naya, T. Niwa, T. Kume and H. Tada, *Angew. Chem. Int. Ed.*, 2014, **53**, 7305–

7309.

- 49 a) J. Shi, *Chem. Rev.*, 2013, **113**, 2139–2181. b) I. N. Francesco, F. F.-Vive and S. Antoniotti, *ChemCatChem*, 2014, **6**, 2784–2791.
- 50 a) S. Zhou, M. Johnson and J. G. C. Veinot, *Chem. Commun.*, 2010, **46**, 2411–2413.
b) R. Hudson, C.-J. Li, A. Moores, *Green Chem.*, 2012, **14**, 622–624.
- 51 A. Matsuoka, C. A. Sandoval, M. Uchiyama, R. Noyori and H. Naka, *Chem. Asian J.*, 2015, **10**, 112–115.
- 52 A. Matsuoka, T. Isogawa, Y. Morioka, B. R. Knappett, A. E. H. Wheatley, S. Saito and H. Naka, *RSC Adv.*, 2015, **5**, 12152–12160.

Chapter 2.

Why *p*-Cymene? Conformational Effect in Asymmetric Hydrogenation of Aromatic Ketones with a η^6 -Arene/Ruthenium(II) Catalyst

2.1 Abstract

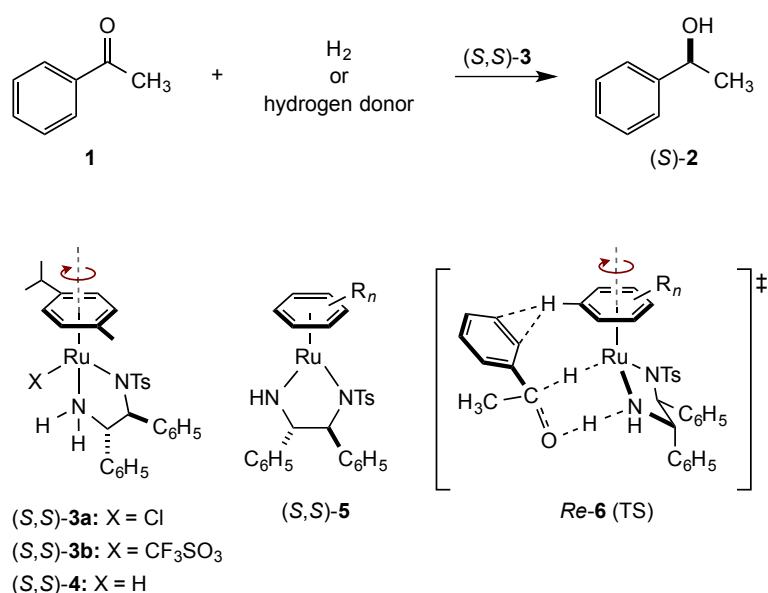
The global reaction route mapping (GRRM) methods conveniently define transition states in asymmetric hydrogenation and transfer hydrogenation of aromatic ketones via $[\text{RuH}\{(S,S)\text{-TsNCH}(\text{C}_6\text{H}_5)\text{CH}(\text{C}_6\text{H}_5)\text{NH}_2\}(\eta^6\text{-}p\text{-cymene})]$ intermediate. The result supports the significance of previously recognized CH/ π interaction between the *p*-cymene and aromatic ring of ketone in the enantioselection. Furthermore, multiple electrostatic CH/ π interactions were identified as the common motif in the preferred diastereometric structures.

2.2 Introduction

Asymmetric hydrogenation (AH) and transfer hydrogenation (ATH) of ketones produce chiral alcohols.^{1,2} $[\text{RuX}\{(S,S)\text{-Tsdpen}\}(\eta^6\text{-}p\text{-cymene})]$ [(S,S) -**3** (X = Cl or CF₃SO₃, Tsdpen = TsNCH(C₆H₅)CH(C₆H₅)NH₂)]³ have been known as excellent catalysts for AH^{1,4} and ATH^{2,5} of aromatic ketones. Typically, AH and ATH of acetophenone (**1**) give (*S*)-1-phenylethanol [(S) -**2**] in 96–98% ee (Scheme 2.1).⁶ The question in this work is why the *p*-cymene/Ru^{II} complex **3** has long served as a prototype for the further development of chiral Ru catalysts besides the ready availability.^{7,8}

Extensive studies of the AH and ATH revealed that the chirality-determining step is commonly the reaction of ketone **1** and 18e Ru hydride ((S,S) -**4** with an *R* configuration at the metallic center, producing the major enantiomer (*S*)-**2** and the 16e Ru complex ((S,S) -**5** (Scheme 2.1).^{4b,9,10} The *Re* and *Si* faces of **1** are clearly

differentiated in the transition states **6**. Notably, the sterically congested *Re*-**6** is favored over the diastereomeric, less crowded *Si*-**6**.^{4b,9b,11} This unique enantio-face selection has been postulated to arise from the CH/ π electronic attraction¹² between the η^6 -arene ligand and the phenyl ring of **1** as depicted in *Re*-**6**.^{4b,13} However, numerous conformers must exist in transition states **6**, because the *p*-cymene ligand can readily rotate around the Ru coordination axis in the ground-state (*S,S*)-**3** and (*S,S*)-**4**.¹⁴ Other single bonds can also rotate. Thus, since these structural isomers similar in energy could affect the enantiomeric outcome, the conformational effects remain to be clarified.



Scheme 2.1. Asymmetric hydrogenation (AH) and transfer hydrogenation (ATH) of acetophenone (**1**) to alcohol (*S*)-**2** using chiral Ru complexes (*S,S*)-**3**.

Theoretical calculation has become a powerful tool for providing better understanding of the mechanisms of asymmetric catalysis. The transition state modeling of the chirality-determining step allows direct comparison of energies of the diastereomeric structures leading to enantiomeric products.^{15,16} However, identifying the major structures that contribute to the enantiomeric outcome is not always straightforward because of the numerous possible geometrical combinations of the substrate and catalytic species.^{17–19} Recently, Maeda and Ohno have developed the global reaction route mapping (GRRM) methods that allow semiautomatic exploration

of transition structures (TSs).^{19,20} With the aid of the GRRM methods, the author has revealed the key conformers in the above-mentioned transition state *Re*- and *Si*-**6** and clarified the effect of *p*-cymene ligand on the enantioselectivity in the asymmetric reaction, noting that multiple CH/ π interactions are the major origin of enantioselectivity.²¹

2.3 Results and discussion

NMR study on the conformation of (*S,S*)-**3a**

First, the author confirmed that the *p*-cymene ligand readily rotates around the Ru coordination axis in the ground-state (*S,S*)-**3a**. This conclusion is supported by the following ¹H NMR analysis of (*S,S*)-**3a** at 20 °C. Numbering scheme for (*S,S*)-**3a** is shown in Figure 2.1. As shown in Figure 2.2, **3a** exists as a single chemical species, where the signals for the following protons are equivalent: C(13)H and C(17)H; C(19)H and C(23)H; C(33)H and C(34)H. The NOESY spectrum of (*S,S*)-**3a** in CD₂Cl₂ at 20 °C showed nuclear Overhauser effects (NOEs) between the C(13)H, C(17)H, C(19)H, and C(23)H protons in Tsdpen and C(31)H, C(33)H, and C(34)H protons in *p*-cymene (Figure 2.3).

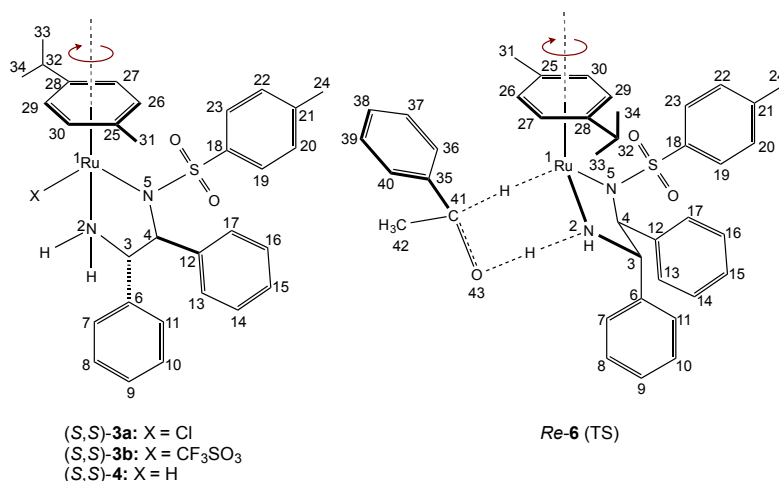


Figure 2.1. Numbering schemes for (*S,S*)-**3**, (*S,S*)-**4**, and *Re*-**6**.

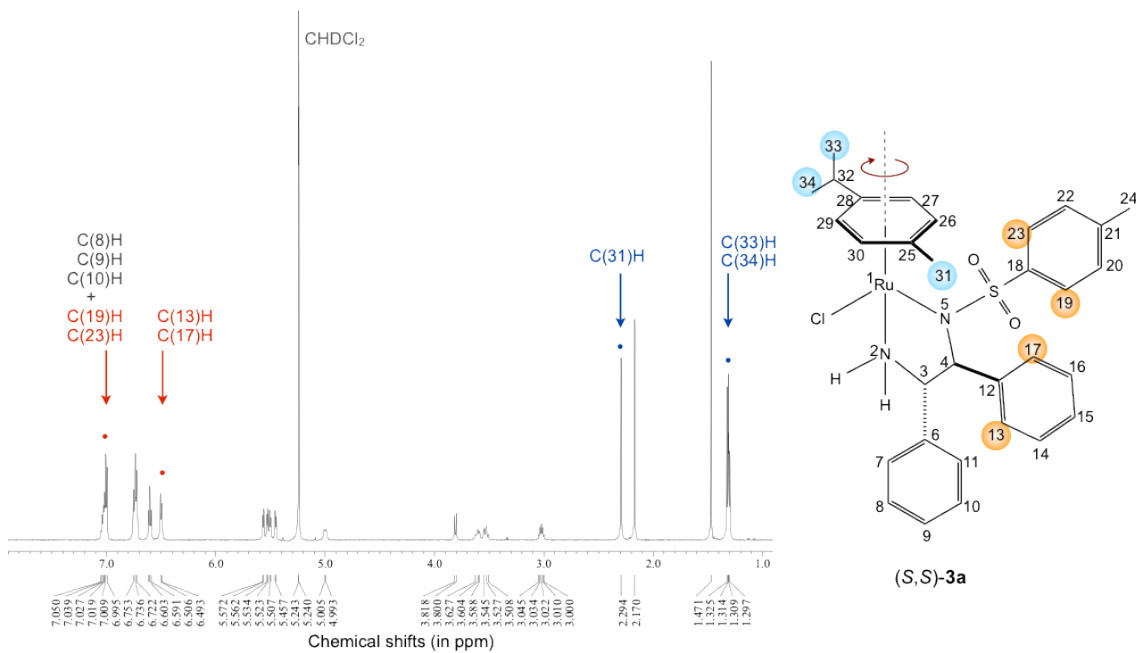


Figure 2.2. ^1H NMR spectrum of (S,S) -**3a** in CD_2Cl_2 at $20\text{ }^\circ\text{C}$.

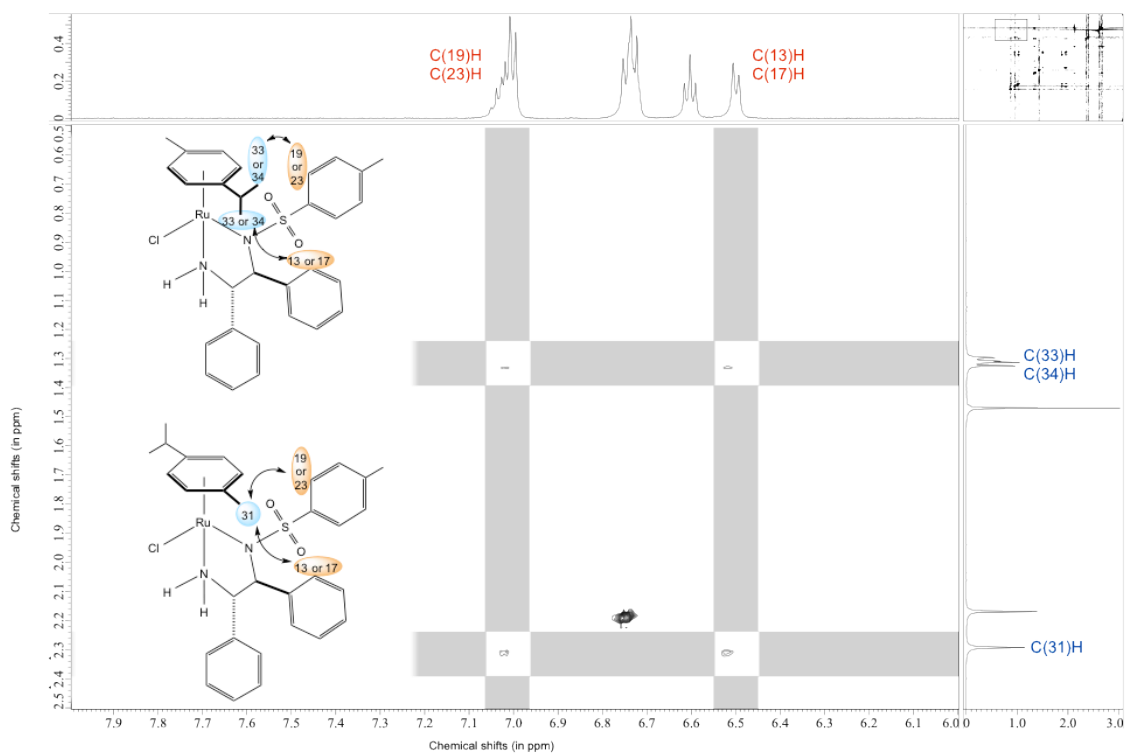


Figure 2.3. ^1H NOESY spectrum of (S,S) -**3a** in CD_2Cl_2 at $20\text{ }^\circ\text{C}$.

Systematic exploration of transition states using GRRM methods

The author identified possible TSs using the GRRM//ADDF methods.¹⁹ Conformational search based on UFF using the GRRM program gave 189 candidates for TSs. The resulting candidates were subsequently optimized to TSs (66 *Re-6* and 123 *Si-6* conformers) at the B3LYP/BS-I level.²² The relative energies for these TSs are shown in Figure 2.4. The *S/R* enantiomeric ratio (er) at 25 °C was predicted to be 99.8:0.2 based on a Boltzmann distribution of these 189 TSs. This theoretical outcome qualitatively agrees with the experimental (98:2–99:1)⁶ preference for the *S* enantiomeric alcohol.²³

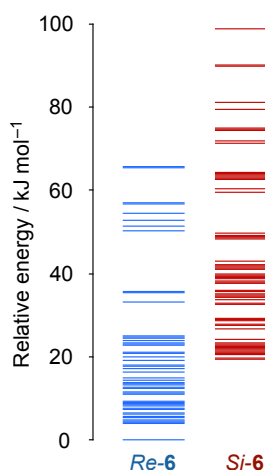


Figure 2.4. Relative energies for 66 *Re-6* and 123 *Si-6* at the B3LYP/BS-I level (kJ mol^{-1}).

In order to further elucidate the major conformers that contribute to the enantiomeric outcome, some low-energy TSs among these structures were optimized with larger basis sets (B3LYP/BS-II) and their energies (ΔG^\ddagger) were evaluated at the B3LYP/BS-II/PCM(methanol)//B3LYP/BS-II level.^{24,25}

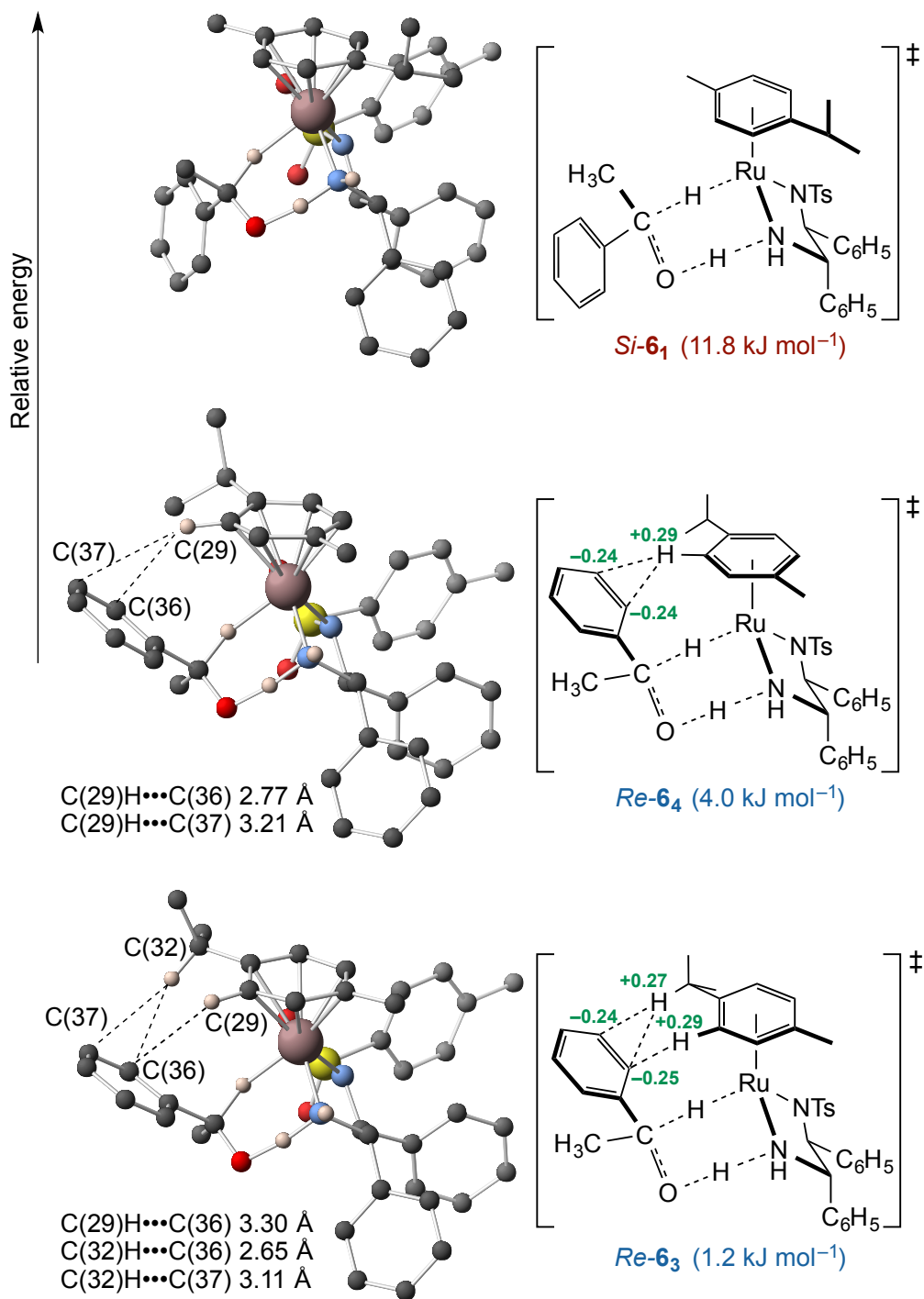


Figure 2.5. Continued on next page.

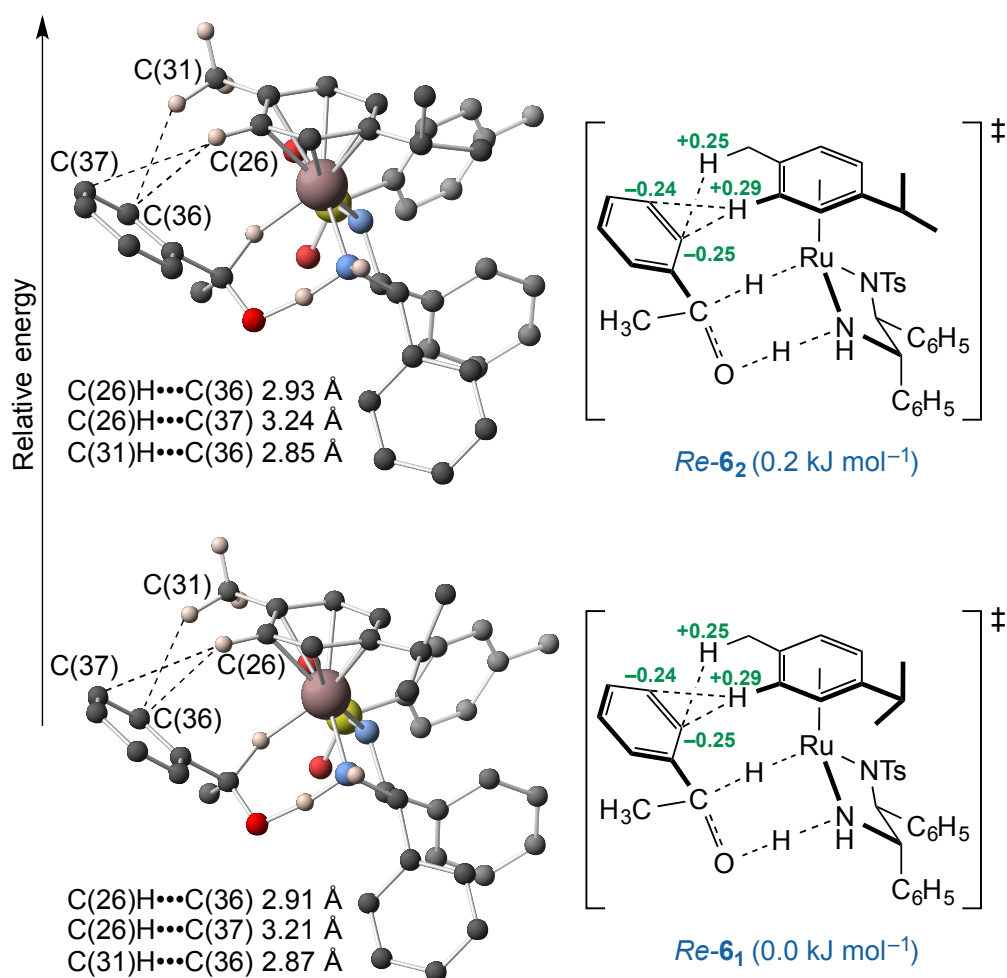


Figure 2.5. The four lowest-energy *S*-directing TSs $Re-6_{1-4}$ and the lowest-energy *R*-directing TS $Si-6_1$ in terms of free energy at the B3LYP/BS-II/PCM(methanol)//B3LYP/BS-II level. Electrostatic interactions are shown in dashed lines. The NPA charges (au) are given in green.

Figure 2.5 shows the four lowest-energy TSs $Re-6_{1-4}$ and diastereomeric $Si-6_1$. The lowest-energy *S*-directing TS $Re-6_1$ ($\Delta G^\ddagger = 120.4$ kJ mol⁻¹) is more stable than the most stable *R*-forming structure $Si-6_1$ ($\Delta G^\ddagger = 132.2$ kJ mol⁻¹) by 11.8 kJ mol⁻¹. The total electron energies of $Re-6_{1-4}$ and $Si-6_1$ with solvation energies at the B3LYP/BS-II/PCM(methanol)//B3LYP/BS-II and the SCS-MP2/BS-II/PCM(methanol)//B3LYP/BS-II levels are similar with each other (Table 2.1).

Table 2.1. Total electron energies of *Re-6*₁₋₄ and *Si-6*₁ relative to those of *Re-6*₁ at the B3LYP/BS-II or SCS-MP2/BS-II levels with the solvation free energies [PCM(methanol)] using the gas-phase geometries optimized at the B3LYP/BS-II level.

	$\Delta(\Delta E_{\text{elec}}^{\ddagger} + \Delta G_{\text{solv}}^{\ddagger}) / \text{kJ mol}^{-1}$	
	B3LYP	SCS-MP2
<i>Si-6</i> ₁	+8.3	+5.0
<i>Re-6</i> ₄	+3.7	+2.9
<i>Re-6</i> ₃	+2.1	+2.3
<i>Re-6</i> ₂	-2.7	-3.6
<i>Re-6</i> ₁	0.0	0.0

How are these TSs stabilized? Both *Re* and *Si* TSs share almost identical conformations around the Tsdpen ligand. As seen in ground-state (*S,S*)-**4**, *Re-6*₁₋₃ and *Si-6*₁ are commonly stabilized by C(sp³)H/O=S (2.29–2.44 Å) and C(sp²)H/O=S (2.44–2.61 Å) interactions between the *p*-cymene ligand and the Ts substituent (Figure 2.6). *Re-6*₄ has a similar geometry but involves only C(sp³)H/O=S attraction (2.39 Å) in this respect.

Notably, *S*-directing TSs *Re-6*₁₋₄ have variable conformations for the *p*-cymene ligand. The author found two geometrical characteristics. First, with respect to the methyl and isopropyl orientation, the structures of *Re-6*₃ and *Re-6*₄ resemble that of crystalline (*S,S*)-**4**,^{9a} whereas the other three TSs in Figure 2.5 have a reversed geometry in this regard. Second, only the 4th stable TS *Re-6*₄ is similar to that of the earlier proposed *Re-6* in Scheme 2.1, with respect to the arene CH conformation for the electrostatic CH/ π interaction. In contrast, the more stable *Re-6*₁, *Re-6*₂ and *Re-6*₃ have a different, *ca.* +160°- or -30°-rotated orientation for the *p*-cymene.²⁶ The newly found TSs *Re-6*₁₋₃ are all stabilized with multiple CH/ π interactions,^{21,27} where the electron-deficient C(sp²)H or benzylic C(sp³)H in the *p*-cymene ring interact with the electron-rich phenyl carbons (*ortho* and *meta*).

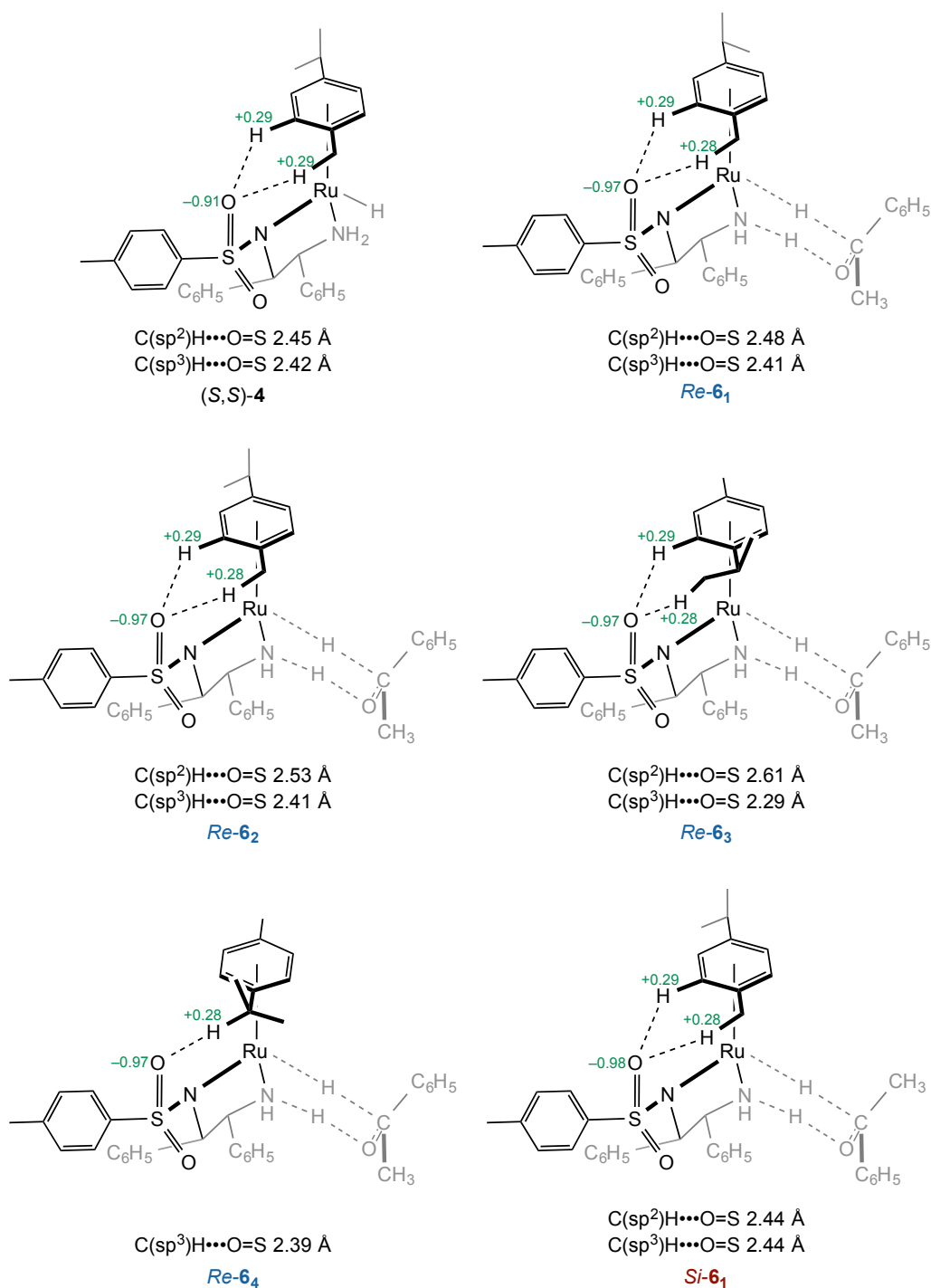


Figure 2.6. Schematic representations of (S,S)-4, Re-6₁₋₄ and Si-6₁. $C(sp^2)H/O=S$ and $C(sp^3)H/O=S$ interactions are shown in dashed lines. NPA charges (au) are shown in green. Sum of the van der Waals radii of hydrogen and oxygen is 2.72 Å.

The most stable *Re-6*₁ is stabilized by the multiple CH/ π attractive interactions as indicated by its geometry and charges (bottom in Figure 2.5). The C(26)H...C(36) and C(31)H...C(36) distances are 2.91 and 2.87 Å, respectively, which are comparable with the sum of the van der Waals radii of carbon and hydrogen (2.90 Å). As shown in Figure 2.7, the NPA²⁸ charges of C(26) and C(31) hydrogens (+0.29 and +0.25 au) are larger than those in the Ru hydride (*S,S*)-**4** (+0.27 and +0.24 au) or the resulting Ru amide (*S,S*)-**5** (+0.27 and +0.24 au), whereas the values on the hydrogen-accepting C(36) for *Re-6*₁ is more negative (−0.25 au) than that for **1** (−0.21 au) or (*S*)-**2** (−0.24 au). A similar electrostatic interaction is seen between C(26)H...C(37) as indicated by its slightly longer distance of 3.21 Å, positive charge at C(26)H (+0.29 au) and negative charge at C(37) (−0.24 au). These results indicate that polarization caused by the hydride transfer from (*S,S*)-**4** to **1** induces the electrostatic attraction in *Re-6*₁, and reminiscent of the secondary molecular orbital interaction in the Diels–Alder reaction favoring the *endo* stereoisomers (Table 2.2).²⁹ Such multiple interactions are also present in the second lowest TS *Re-6*₂, a rotamer around the C(sp²)–CH(CH₃)₂ bond in the *p*-cymene.

*Re-6*₃ has a reversed methyl/isopropyl location with *Re-6*₁ and is 1.2 kJ mol^{−1} higher in energy than *Re-6*₁ (Figure 2.5). *Re-6*₄ has a CH/ π interaction where the phenyl group interacts with only the arene C(sp²)H of the *p*-cymene ring with a C(29)H...C(36) distance of 2.77 Å and a C(29)H...C(37) distance of 3.21 Å. *Re-6*₄ is 4.0 kJ mol^{−1} higher than the most favored *Re-6*₁.³⁰

The lowest-energy *R*-generating TS, *Si-6*₁ (top in Figure 2.5), has a very similar core structure to *Re-6*₁ including the *p*-cymene and Tsdpen conformations. However, this diastereomer is not stabilized by any of attractive secondary interactions. Overall, single CH/ π interaction does stabilize the *S*-directing transition state as postulated earlier, yet the multiple CH/ π interactions are more effective when the geometries are suitably arranged.

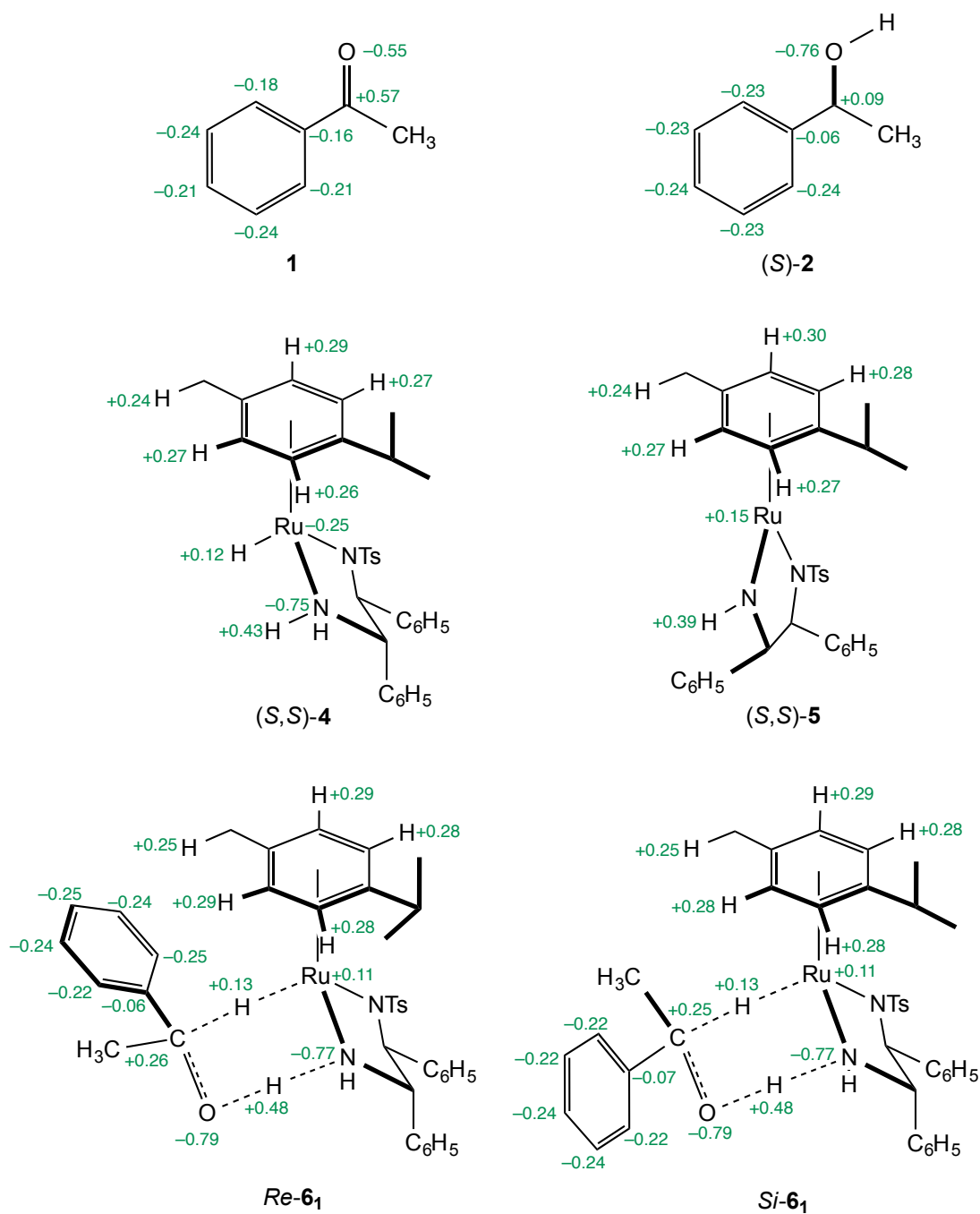


Figure 2.7. NPA charges (au, in green) in 1, (S)-2, (S,S)-4, (S,S)-5, Re-6₁ and Si-6₁ (B3LYP/BS-II).

Table 2.2. Sums of the NPA charges on the CH₃ group at C(41), the C₆H₅ group at C(41), the *p*-cymene ligand and the other moieties.^a

	NPA charges / au			
	CH ₃ at C(41)	C ₆ H ₅ at C(41)	<i>p</i> -cymene	others
1 and (<i>S,S</i>)- 4	-0.01	-0.01	+0.29	-0.28
<i>Si</i> - 6 ₁	0.00	-0.02	+0.46	-0.43
<i>Re</i> - 6 ₁	+0.03	-0.05	+0.47	-0.45
(<i>S</i>)- 2 and (<i>S,S</i>)- 5	0.00	-0.03	+0.41	-0.38

^a The NPA at the B3LYP/BS-II level of theory.

2.4 Conclusion

Transition states in the chirality-determining elementary step for the AH and ATH of acetophenone were systematically determined by using GRRM methods. The result demonstrated the previously reported presence of CH/ π interaction between the cymene and aromatic ring in ketone. In addition, the present study revealed that multiple CH/ π interactions are more effective when the geometries are suitably arranged. These interactions can contribute to the high enantioselectivity in AH and ATH of aromatic ketones catalyzed by **3**. The *p*-cymene complexes act better than the simpler η^6 -benzene and fully alkylated η^6 -hexamethylbenzene analogs.^{4b,13b} The efficacy of the η^6 -mesitylene catalysts is obvious.²¹

2.5 Experimental

Computational Details

Calculations were carried out using the Gaussian 03 or 09 program.³¹ Candidates for TSs were obtained by the GRRM//ADDF methods¹⁹ starting from six input structures for each *Re-6* and *Si-6* with different rotation angles around the *p*-cymene–Ru coordination axis. UFF was used in the conformational search. During this process, the core part [Ru, the C and O atoms in the hydrogenated carbonyl group, the two N atoms, the six C(sp²) atoms in the *p*-cymene ligand, and the two H atoms transferred from (*S,S*)-**4** to **1**] was fixed. The obtained 189 TS candidates were fully optimized at the B3LYP/BS-I level.²² TSs with low energies were selected and optimized at the B3LYP/BS-II level.²⁵ To evaluate the effect of the solvent polarity on the energetics of the transition state models, single point energy calculations were performed with self-consistent reaction field (SCRF) method (based on the PCM,³² $\epsilon = 32.613$ for methanol) on the gas-phase geometries at the B3LYP or SCS-MP2.³³ The NPA was performed at the B3LYP/BS-II level.^{25,28} Images were generated using ChemBioDraw13.0.2.3020 (PerkinElmer, Waltham, MA, USA) and CrystalMaker[®] (CrystalMaker Software Ltd, Oxford, England).

Cartesian Coordinates

<i>Re-6₁</i>						38	1	0	1.677318	-5.682617	-2.335403
Center	Atomic	Atomic	Coordinates (Angstroms)			39	6	0	3.931858	-6.731404	-1.201935
Number	Number	Type	X	Y	Z	40	1	0	4.208265	-5.302484	1.114369
						41	1	0	2.781273	-3.439653	1.947845
1	6	0	2.182599	3.152567	0.502232	42	1	0	3.617161	0.052019	1.852201
2	6	0	2.226625	2.374320	-0.666024	43	1	0	5.931038	-0.772829	1.523107
3	6	0	3.156254	2.701738	-1.661289	44	1	0	6.572329	-1.859214	-0.621409
4	6	0	4.028650	3.779451	-1.501081	45	1	0	4.877432	-2.117360	-2.424067
5	6	0	3.978501	4.548329	-0.338040	46	1	0	2.565566	-1.302814	-2.078747
6	6	0	3.053452	4.231248	0.659414	47	1	0	3.206575	2.098706	-2.564715
7	6	0	1.291828	1.190922	-0.868786	48	1	0	4.745296	4.015809	-2.282801
8	16	0	0.383360	-2.214980	0.923595	49	1	0	4.654435	5.389182	-0.209417
9	8	0	0.963872	-1.839256	2.229239	50	1	0	3.007214	4.827144	1.566766
10	6	0	-1.308020	0.674427	-4.206871	51	1	0	1.456372	2.923680	1.276993
11	6	0	-1.380644	2.206594	-4.257417	52	1	0	-0.249878	0.384121	-4.165181
12	6	0	-4.064850	-2.062441	0.266384	53	1	0	-1.399514	0.479588	-6.378012
13	6	0	1.536750	0.018558	0.103115	54	1	0	-1.811457	-1.014845	-5.520901
14	6	0	2.938180	-0.547468	-0.096871	55	1	0	-2.973455	0.319291	-5.581451
15	6	0	3.897451	-0.415531	0.912814	56	1	0	-2.411254	2.558328	-4.375315
16	6	0	5.199812	-0.883508	0.727093	57	1	0	-0.963991	2.676685	-3.362274
17	6	0	5.559800	-1.493204	-0.475129	58	1	0	-0.812162	2.575338	-5.116213
18	6	0	4.607988	-1.635457	-1.488023	59	1	0	-4.468926	-1.352044	0.990457
19	6	0	3.308944	-1.166347	-1.298606	60	1	0	-4.904656	-2.638403	-0.142060
20	6	0	-1.908870	0.074406	-5.497786	61	1	0	-3.384602	-2.744286	0.779589
21	6	0	1.450918	-3.519394	0.270899	62	6	0	-4.143651	1.151457	2.362362
22	6	0	1.131427	-4.150769	-0.933628	63	6	0	-5.453263	1.636274	2.313320
23	6	0	1.931171	-5.189919	-1.399635	64	6	0	-5.720315	2.884345	1.745965
24	6	0	3.054621	-5.620245	-0.675834	65	6	0	-4.664614	3.646290	1.239273
25	6	0	3.347902	-4.979835	0.533459	66	6	0	-3.357276	3.160150	1.291957
26	6	0	2.555108	-3.935159	1.011026	67	1	0	-3.954986	0.183210	2.815372
27	8	0	-0.978907	-2.787142	0.890083	68	1	0	-6.263732	1.041020	2.725864
28	1	0	-0.345308	2.288237	-1.429637	69	1	0	-6.737972	3.263259	1.710538
29	1	0	1.444616	0.808370	-1.886246	70	1	0	-4.859009	4.627263	0.812871
30	1	0	1.471500	0.413715	1.123733	71	1	0	-2.522014	3.749034	0.928524
31	1	0	-2.059790	-2.995475	-1.337029	72	1	0	-1.902719	-0.265949	3.266223
32	1	0	-0.863634	-1.810278	-3.178536	73	1	0	-0.229102	0.215221	3.005816
33	1	0	-3.209690	1.746584	-2.386951	74	1	0	-1.303564	1.252199	3.975925
34	1	0	-4.276896	0.593340	-0.490560	75	1	0	3.343251	-7.499425	-1.713660
35	6	0	-1.246976	0.592690	3.102813	76	1	0	4.491622	-7.214125	-0.395810
36	6	0	-3.078464	1.903517	1.844294	77	1	0	4.663936	-6.349310	-1.924682
37	1	0	0.261513	-3.834999	-1.499747	78	6	0	-1.986305	0.038727	-3.000102

79	6	0	-1.664457	-1.303641	-2.650327	25	6	0	3.446027	-4.746042	-0.205663
80	6	0	-2.365671	-1.995185	-1.615553	26	6	0	2.660356	-3.784386	0.432404
81	6	0	-3.344885	-1.347048	-0.843887	27	8	0	-0.896924	-2.788590	0.728560
82	6	0	-3.599370	0.039205	-1.130866	28	1	0	-0.734116	2.444366	-1.288478
83	6	0	-2.983896	0.701134	-2.216248	29	1	0	1.111853	1.137789	-1.944942
84	6	0	-1.624819	1.406176	1.856031	30	1	0	1.378036	0.521757	1.013651
85	1	0	-1.630356	0.544911	0.969868	31	1	0	-2.179883	-2.897158	-1.450510
86	44	0	-1.387095	-0.080300	-0.833995	32	1	0	-1.249263	-1.498528	-3.282449
87	7	0	0.435383	-0.952626	-0.146030	33	1	0	-3.642780	1.847641	-1.917559
88	7	0	-0.140056	1.564838	-0.741493	34	1	0	-4.461324	0.466290	-0.039515
89	1	0	-0.370755	2.039466	0.338772	35	6	0	-1.049746	0.447160	3.187503
90	8	0	-0.731822	2.341524	1.526736	36	6	0	-3.148395	1.622462	2.260246

<i>Re-6₂</i>											

Center	Atomic	Atomic	Coordinates (Angstroms)								
Number	Number	Type	X	Y	Z						

1	6	0	2.730031	3.100994	-1.686302	44	1	0	6.447623	-1.301680	-1.265919
2	6	0	1.885267	2.652903	-0.662663	45	1	0	4.640283	-1.510888	-2.962606
3	6	0	1.876200	3.344804	0.559306	46	1	0	2.320557	-0.866425	-2.389295
4	6	0	2.698215	4.457360	0.741508	47	1	0	1.211553	3.023832	1.356299
5	6	0	3.539763	4.894172	-0.284140	48	1	0	2.679118	4.985704	1.690732
6	6	0	3.553941	4.212295	-1.501211	49	1	0	4.178379	5.760582	-0.135883
7	6	0	1.005052	1.433080	-0.894071	50	1	0	4.205264	4.542340	-2.305815
8	16	0	0.435016	-2.150636	0.679477	51	1	0	2.753014	2.566562	-2.632952
9	8	0	1.123473	-1.845485	1.950486	52	1	0	-1.777779	2.148902	-3.555379
10	6	0	-1.951906	1.143679	-3.963462	53	1	0	0.153158	0.534449	-3.909538
11	6	0	-3.087461	1.259727	-5.003916	54	1	0	-0.799318	-0.273015	-5.167565
12	6	0	-4.051753	-2.232138	0.427575	55	1	0	-0.326961	1.412589	-5.369475
13	6	0	1.386098	0.208443	-0.037054	56	1	0	-2.791674	1.932695	-5.814975
14	6	0	2.797547	-0.255831	-0.379629	57	1	0	-3.313153	0.281016	-5.441348
15	6	0	3.819979	-0.152647	0.569474	58	1	0	-4.007788	1.649606	-4.558888
16	6	0	5.128114	-0.525247	0.254026	59	1	0	-3.298746	-2.931632	0.794531
17	6	0	5.430519	-1.010137	-1.018795	60	1	0	-4.398075	-1.615592	1.259683
18	6	0	4.415576	-1.124638	-1.972027	61	1	0	-4.911909	-2.800209	0.051456
19	6	0	3.110833	-0.751411	-1.652923	62	6	0	-4.056317	0.728178	2.847384
20	6	0	-0.654630	0.672474	-4.633407	63	6	0	-5.402202	1.071514	2.999004
21	6	0	1.488862	-3.342940	-0.177325	64	6	0	-5.863300	2.317294	2.567272
22	6	0	1.096575	-3.865384	-1.412559	65	6	0	-4.964176	3.219286	1.992978
23	6	0	1.889185	-4.822141	-2.038477	66	6	0	-3.619701	2.874352	1.844815
24	6	0	3.076348	-5.280675	-1.444587	67	1	0	-3.715229	-0.241531	3.196039

68	1	0	-6.088767	0.367370	3.461746	14	6	0	2.962829	-0.317194	-0.263413
69	1	0	-6.909108	2.585829	2.688212	15	6	0	3.267574	-0.947577	-1.477452
70	1	0	-5.309033	4.198533	1.670476	16	6	0	4.566256	-1.371820	-1.755036
71	1	0	-2.901442	3.570601	1.425612	17	6	0	5.583748	-1.173883	-0.818277
72	1	0	-1.590848	-0.483451	3.374185	18	6	0	5.289882	-0.553792	0.396712
73	1	0	-0.021958	0.182414	2.939926	19	6	0	3.987816	-0.129935	0.670300
74	1	0	-1.053403	1.048902	4.103103	20	6	0	-4.112114	-2.926796	0.874977
75	1	0	3.996009	-6.163129	-3.196218	21	6	0	1.514994	-3.363683	0.211781
76	1	0	3.471732	-7.336655	-1.989370	22	6	0	1.028670	-4.101477	-0.870420
77	1	0	4.925432	-6.375613	-1.703634	23	6	0	1.793494	-5.138271	-1.397520
78	6	0	-2.420778	0.270659	-2.808821	24	6	0	3.047063	-5.461604	-0.854962
79	6	0	-2.008374	-1.078625	-2.634940	25	6	0	3.505423	-4.719750	0.240078
80	6	0	-2.558786	-1.893525	-1.596503	26	6	0	2.749890	-3.676258	0.776196
81	6	0	-3.481911	-1.378009	-0.671584	27	8	0	-0.853809	-2.602585	1.005246
82	6	0	-3.829810	0.011984	-0.794977	28	1	0	-0.477509	2.404251	-1.412826
83	6	0	-3.359069	0.801449	-1.864432	29	1	0	1.340088	0.995978	-1.956174
84	6	0	-1.664416	1.285048	2.056420	30	1	0	1.547080	0.601781	1.047102
85	1	0	-1.702121	0.482098	1.118294	31	1	0	-2.900223	1.820972	-2.594455
86	44	0	-1.592755	-0.000936	-0.736840	32	1	0	-4.249996	0.958957	-0.708573
87	7	0	0.325736	-0.808163	-0.282547	33	1	0	-2.385769	-2.912151	-1.088213
88	7	0	-0.434973	1.707016	-0.649903	34	1	0	-0.891227	-1.998904	-2.849634
89	1	0	-0.622715	2.115225	0.473461	35	6	0	-1.152018	0.657645	3.132571
90	8	0	-0.918696	2.330521	1.689433	36	6	0	-3.050031	1.968100	1.969382
-----						37	1	0	0.049284	-3.880834	-1.281336
-----						38	1	0	1.408722	-5.715286	-2.235234
<i>Re-6₃</i>						39	6	0	3.883879	-6.569093	-1.449987
-----						40	1	0	4.467402	-4.962149	0.684597
Center	Atomic	Atomic	Coordinates (Angstroms)			41	1	0	3.105324	-3.105996	1.626144
Number	Number	Type	X	Y	Z	42	1	0	2.473765	-1.127724	-2.196709
-----						43	1	0	4.784305	-1.862745	-2.699741
1	6	0	2.109004	3.360995	0.400402	44	1	0	6.596150	-1.504907	-1.032867
2	6	0	2.122419	2.588218	-0.772255	45	1	0	6.072909	-0.400200	1.134183
3	6	0	2.985175	2.954061	-1.813206	46	1	0	3.759937	0.346887	1.619196
4	6	0	3.821638	4.065050	-1.693848	47	1	0	3.011926	2.355353	-2.720543
5	6	0	3.801845	4.828638	-0.526393	48	1	0	4.486837	4.331316	-2.510607
6	6	0	2.943518	4.473026	0.516690	49	1	0	4.449844	5.695335	-0.429575
7	6	0	1.224539	1.370425	-0.931095	50	1	0	2.921398	5.064589	1.427751
8	16	0	0.510405	-2.041824	0.926879	51	1	0	1.434149	3.101628	1.211275
9	8	0	1.197638	-1.647752	2.174072	52	1	0	-4.563831	-0.829247	0.980176
10	6	0	-4.505387	-1.603987	0.206762	53	1	0	-4.152861	-3.761084	0.164173
11	6	0	-5.904245	-1.710021	-0.442722	54	1	0	-3.106120	-2.884711	1.296940
12	6	0	-0.998542	0.459769	-4.093801	55	1	0	-4.822169	-3.155197	1.676152
13	6	0	1.560412	0.207344	0.024311	56	1	0	-5.908643	-2.465491	-1.236582

57	1	0	-6.643152	-2.006720	0.308445	4	6	0	3.720844	3.976735	-1.209235	
58	1	0	-6.229975	-0.759547	-0.877150	5	6	0	3.646639	4.624711	0.023984	
59	1	0	-0.802933	1.532047	-4.002302	6	6	0	2.746216	4.168941	0.989724	
60	1	0	-0.039943	-0.062414	-4.148447	7	6	0	1.116186	1.209934	-0.819180	
61	1	0	-1.521532	0.301035	-5.045003	8	16	0	0.364502	-2.369922	0.664952	
62	6	0	-4.076418	1.228186	2.575097	9	8	0	0.859363	-2.053109	2.021661	
63	6	0	-5.390081	1.705411	2.589941	10	6	0	-3.759407	-3.003073	-0.587607	
64	6	0	-5.700117	2.931244	1.997885	11	6	0	-4.937398	-3.573176	-1.407489	
65	6	0	-4.682488	3.681349	1.402531	12	6	0	-1.834328	1.612028	-3.751175	
66	6	0	-3.370992	3.204618	1.393818	13	6	0	1.412886	-0.030809	0.045620	
67	1	0	-3.853776	0.277677	3.049471	14	6	0	2.845234	-0.500825	-0.180151	
68	1	0	-6.169444	1.121020	3.072000	15	6	0	3.786714	-0.396521	0.849297	
69	1	0	-6.720641	3.303781	2.012160	16	6	0	5.116065	-0.770299	0.642278	
70	1	0	-4.909201	4.646677	0.956876	17	6	0	5.520729	-1.257281	-0.600936	
71	1	0	-2.563249	3.788731	0.966185	18	6	0	4.586685	-1.372511	-1.633713	
72	1	0	-1.778777	-0.221837	3.298564	19	6	0	3.260583	-0.997855	-1.422976	
73	1	0	-0.128207	0.311320	2.991272	20	6	0	-4.166822	-2.750814	0.868576	
74	1	0	-1.193850	1.296318	4.021902	21	6	0	1.546663	-3.549629	-0.026536	
75	1	0	4.577531	-6.985785	-0.713999	22	6	0	1.321694	-4.108156	-1.286856	
76	1	0	4.483931	-6.202029	-2.292358	23	6	0	2.205340	-5.059967	-1.786454	
77	1	0	3.260210	-7.384938	-1.828693	24	6	0	3.320420	-5.474636	-1.041295	
78	6	0	-3.520983	-1.100071	-0.834519	25	6	0	3.517575	-4.910617	0.224407	
79	6	0	-3.584852	0.284863	-1.237285	26	6	0	2.640076	-3.953637	0.736088	
80	6	0	-2.814283	0.776538	-2.309795	27	8	0	-0.951335	-3.025944	0.523660	
81	6	0	-1.835080	-0.052861	-2.951868	28	1	0	-0.574729	2.268317	-1.288348	
82	6	0	-1.688308	-1.376434	-2.457381	29	1	0	1.288067	0.927834	-1.866193	
83	6	0	-2.557729	-1.908658	-1.451726	30	1	0	1.311531	0.264904	1.096691	
84	6	0	-1.592131	1.486511	1.917777	31	1	0	-3.768723	1.603645	-1.768277	
85	1	0	-1.626714	0.631626	1.018865	32	1	0	-4.447206	-0.277483	-0.334110	
86	44	0	-1.404898	0.013102	-0.773497	33	1	0	-1.637274	-2.871729	-2.295969	
87	7	0	0.476672	-0.795287	-0.157849	34	1	0	-0.838039	-0.961791	-3.685618	
88	7	0	-0.211632	1.692955	-0.731375	35	6	0	-1.539208	0.178618	3.081756	
89	1	0	-0.407175	2.157130	0.362522	36	6	0	-3.295429	1.608978	1.837912	
90	8	0	-0.724962	2.436026	1.564188	37	1	0	0.460313	-3.802905	-1.870931	
-----							38	1	0	2.025364	-5.495297	-2.766685
<i>Re-6₄</i>							39	6	0	4.291302	-6.486072	-1.602694
-----							40	1	0	4.369400	-5.224323	0.822565
Center	Atomic	Atomic	Coordinates (Angstroms)			41	1	0	2.791591	-3.518661	1.716941	
Number	Number	Type	X	Y	Z	42	1	0	3.471481	-0.023951	1.819655	
-----							43	1	0	5.833388	-0.682517	1.453661
1	6	0	1.924930	3.071099	0.731561	44	1	0	6.554405	-1.549730	-0.763918	
2	6	0	1.994286	2.412940	-0.507234	45	1	0	4.891594	-1.759717	-2.602295	
3	6	0	2.897828	2.879989	-1.470264	46	1	0	2.531493	-1.113797	-2.219653	

47	1	0	2.967857	2.371185	-2.428757	90	8	0	-0.931968	2.030053	1.671959
48	1	0	4.418533	4.321577	-1.967403	-----					
49	1	0	4.284734	5.479273	0.231342						
50	1	0	2.680903	4.670410	1.951380	<i>Si-6_t</i>					
51	1	0	1.218105	2.733999	1.484021	-----					
52	1	0	-2.954327	-3.742699	-0.572093	Center	Atomic	Atomic	Coordinates (Angstroms)		
53	1	0	-4.491037	-3.690680	1.326411	Number	Number	Type	X	Y	Z
54	1	0	-3.315340	-2.372758	1.437535	-----					
55	1	0	-5.002363	-2.046462	0.948974	1	6	0	-2.219960	-2.177792	2.400257
56	1	0	-5.307439	-4.495149	-0.947051	2	6	0	-2.274407	-2.316678	1.004554
57	1	0	-5.771462	-2.862886	-1.451188	3	6	0	-3.303453	-3.082967	0.441553
58	1	0	-4.640455	-3.805005	-2.435869	4	6	0	-4.264022	-3.695563	1.247531
59	1	0	-2.404411	1.622152	-4.687799	5	6	0	-4.203972	-3.551478	2.634008
60	1	0	-2.000017	2.574350	-3.258639	6	6	0	-3.179257	-2.793455	3.204934
61	1	0	-0.775210	1.526909	-4.008580	7	6	0	-1.248152	-1.657060	0.095161
62	6	0	-4.400988	0.827114	2.205029	8	16	0	-0.002298	1.952383	-0.959671
63	6	0	-5.696940	1.345102	2.141245	9	8	0	-0.642680	2.670296	0.155728
64	6	0	-5.910001	2.656440	1.710158	10	6	0	1.400666	-3.787375	-2.535503
65	6	0	-4.814983	3.446592	1.353419	11	6	0	2.381779	-4.692057	-3.312590
66	6	0	-3.521072	2.926859	1.420009	12	6	0	4.414418	1.059127	-0.942827
67	1	0	-4.255379	-0.192269	2.546661	13	6	0	-1.320192	-0.115843	0.052395
68	1	0	-6.539736	0.725554	2.436818	14	6	0	-2.687888	0.325456	-0.457583
69	1	0	-6.917429	3.060807	1.664506	15	6	0	-3.553775	1.031949	0.384130
70	1	0	-4.968032	4.474690	1.034840	16	6	0	-4.832079	1.391942	-0.046227
71	1	0	-2.656635	3.534524	1.175196	17	6	0	-5.261045	1.050869	-1.329680
72	1	0	-2.237659	-0.656534	3.178296	18	6	0	-4.401186	0.353729	-2.181535
73	1	0	-0.534835	-0.234278	2.982782	19	6	0	-3.125220	-0.004081	-1.747818
74	1	0	-1.591431	0.785108	3.992672	20	6	0	0.119828	-3.555029	-3.347351
75	1	0	5.047522	-6.000206	-2.232271	21	6	0	-0.910547	2.435915	-2.447675
76	1	0	3.782331	-7.229632	-2.223978	22	6	0	-0.514488	1.964546	-3.701365
77	1	0	4.822475	-7.015391	-0.806387	23	6	0	-1.195716	2.380581	-4.841699
78	6	0	-3.205256	-1.783792	-1.303199	24	6	0	-2.272183	3.277398	-4.755027
79	6	0	-3.724134	-0.464487	-1.119749	25	6	0	-2.648670	3.738983	-3.488306
80	6	0	-3.334056	0.625217	-1.939695	26	6	0	-1.975485	3.327156	-2.337245
81	6	0	-2.287674	0.461456	-2.891693	27	8	0	1.412864	2.239647	-1.279092
82	6	0	-1.674820	-0.822731	-3.010258	28	1	0	0.255027	-3.029528	0.349621
83	6	0	-2.144648	-1.916399	-2.225719	29	1	0	-1.432859	-2.011722	-0.925816
84	6	0	-1.850608	1.085775	1.882835	30	1	0	-1.195844	0.260248	1.075475
85	1	0	-1.817514	0.287735	0.934790	31	1	0	2.538464	0.822783	-2.914387
86	44	0	-1.504933	-0.178565	-0.899936	32	1	0	1.221746	-1.178798	-3.577836
87	7	0	0.369459	-1.032379	-0.311862	33	1	0	3.149719	-3.468123	-0.445676
88	7	0	-0.331618	1.502501	-0.659716	34	1	0	4.361706	-1.433681	0.263596
89	1	0	-0.575680	1.868841	0.466300	35	6	0	3.139648	-0.669962	2.768113

36	6	0	1.289267	1.059497	2.881275	64	6	0	0.653409	3.582390	3.936013
37	1	0	0.319976	1.276514	-3.784894	65	6	0	0.068755	2.431768	4.467773
38	1	0	-0.886699	2.009392	-5.816189	66	6	0	0.381911	1.177949	3.941063
39	6	0	-2.984278	3.751290	-5.999849	67	1	0	2.537642	2.147146	1.498259
40	1	0	-3.483376	4.429571	-3.397577	68	1	0	1.991009	4.364020	2.435450
41	1	0	-2.270764	3.679093	-1.355675	69	1	0	0.404575	4.559620	4.340775
42	1	0	-3.215685	1.308659	1.378225	70	1	0	-0.633013	2.509976	5.294296
43	1	0	-5.490610	1.940863	0.621252	71	1	0	-0.057953	0.273731	4.347891
44	1	0	-6.255507	1.330467	-1.666652	72	1	0	3.851315	0.069265	2.386401
45	1	0	-4.722811	0.094308	-3.186606	73	1	0	3.219501	-0.687314	3.859905
46	1	0	-2.451676	-0.521682	-2.424765	74	1	0	3.399496	-1.664227	2.393684
47	1	0	-3.361157	-3.189065	-0.638973	75	1	0	-2.475331	4.617888	-6.440601
48	1	0	-5.056810	-4.282785	0.792332	76	1	0	-4.012365	4.054592	-5.781645
49	1	0	-4.948816	-4.028004	3.265392	77	1	0	-3.015502	2.970761	-6.766526
50	1	0	-3.123528	-2.680938	4.284203	78	6	0	2.119712	-2.513605	-2.116868
51	1	0	-1.412820	-1.608607	2.851600	79	6	0	1.957420	-1.271147	-2.788798
52	1	0	1.125580	-4.318056	-1.613466	80	6	0	2.730728	-0.123996	-2.426711
53	1	0	-0.400170	-4.505205	-3.500902	81	6	0	3.626326	-0.157857	-1.345087
54	1	0	-0.565048	-2.870782	-2.838993	82	6	0	3.735192	-1.394950	-0.619886
55	1	0	0.340830	-3.143195	-4.338083	83	6	0	3.045203	-2.555697	-1.024342
56	1	0	1.898204	-5.638056	-3.575968	84	6	0	1.678125	-0.337055	2.396888
57	1	0	2.703738	-4.206592	-4.240375	85	1	0	1.713174	-0.222962	1.172781
58	1	0	3.275801	-4.921080	-2.724743	86	44	0	1.541922	-0.928743	-0.635643
59	1	0	4.693821	1.018214	0.113082	87	7	0	-0.169870	0.310730	-0.794776
60	1	0	5.339576	1.119849	-1.529561	88	7	0	0.151524	-2.018816	0.442861
61	1	0	3.827622	1.962973	-1.114913	89	1	0	0.404644	-1.760836	1.574969
62	6	0	1.867579	2.218672	2.350547	90	8	0	0.824517	-1.309928	2.718716
63	6	0	1.550575	3.472014	2.871801	-----					

2.6 Notes and References

- 1 a) T. Ohkuma, R. Noyori, in *The Handbook of Homogeneous Hydrogenation, Vol. 3, Chap. 32*, ed. J. G. de Vries and C. J. Elsevier, Wiley-VCH, Weinheim, 2007. b) J. F. Hartwig, *Organotransition Metal Chemistry*, University Science Books, Sausalito, CA, 2011, Chap. 15.
- 2 a) R. Noyori and S. Hashiguchi, *Acc. Chem. Res.*, 1997, **30**, 97–102. b) M. J. Palmer, and M. Wills, *Tetrahedron: Asymmetry*, 1999, **10**, 2045–2061. c) S. E. Clapham, A. Hadzovic and R. H. Morris, *Coord. Chem. Rev.*, 2004, **248**, 2201–2237. d) S. Gladiali and E. Alberico, *Chem. Soc. Rev.*, 2006, **35**, 226–236. e) T. Ikariya and A. J. Blacker, *Acc. Chem. Res.*, 2007, **40**, 1300–1308. f) C. Wang, X. Wu and J. Xiao, *Chem. Asian J.*, 2008, **3**, 1750–1770. g) T. Ikariya, *Bull. Chem. Soc. Jpn.*, 2011, **84**, 1–16.
- 3 Commercially available from Kanto Chemicals and other suppliers.
- 4 a) T. Ohkuma, N. Utsumi, K. Tsutsumi, K. Murata, C. Sandoval and R. Noyori, *J. Am. Chem. Soc.*, 2006, **128**, 8724–8725. b) C. A. Sandoval, T. Ohkuma, N. Utsumi, K. Tsutsumi, K. Murata and R. Noyori, *Chem. Asian J.*, 2006, **1–2**, 102–110. c) T. Ohkuma, K. Tsutsumi, N. Utsumi, N. Arai, R. Noyori and K. Murata, *Org. Lett.*, 2007, **9**, 255–257. d) C. A. Sandoval, F. Bie, A. Matsuoka, Y. Yamaguchi, H. Naka, Y. Li, K. Kato, N. Utsumi, K. Tsutsumi, T. Ohkuma, K. Murata and R. Noyori, *Chem. Asian J.*, 2010, **5**, 806–816. e) N. Arai, H. Satoh, N. Utsumi, K. Murata, K. Tsutsumi and T. Ohkuma, *Org. Lett.*, 2013, **15**, 3030–3033.
- 5 a) S. Hashiguchi, A. Fujii, J. Takehara, T. Ikariya and R. Noyori, *J. Am. Chem. Soc.*, 1995, **117**, 7562–7563. b) A. Fujii, S. Hashiguchi, N. Uematsu, T. Ikariya and R. Noyori, *J. Am. Chem. Soc.*, 1996, **118**, 2521–2522.
- 6 AH of the ketone **1** with (*S,S*)-**3a** in methanol at 50 °C gives (*S*)-**2** in 96% ee.^{4d} ATH of ketone **1** with (*S,S*)-**3a** using formic acid at 25 °C gave (*S*)-**2** in 98% ee under the similar reaction conditions to ref. 5b.
- 7 a) M. Miyagi, J. Takehara, S. Collet and K. Okano, *Org. Proc. Res. Dev.*, 2000, **4**, 346–348. b) I. C. Lennon and J. A. Ramsden, *Org. Proc. Res. Dev.*, 2005, **9**, 110–112. c) H. Zhou, Z. Li, Z. Wang, T. Wang, L. Xu, Y. He, Q.-H. Fan, J. Pan, L. Gu and A. S. C. Chan, *Angew. Chem. Int. Ed.*, 2008, **47**, 8464–8467.

- 8 a) J. Hannedouche, G. J. Clarkson and M. Wills, *J. Am. Chem. Soc.*, 2004, **126**, 986–987. b) J. B. Sortais, V. Ritleng, A. Voelklin, A. Holuigue, H. Smail, L. Barloy, C. Sirlin, G. K. M. Verzijl, J. A. F. Boogers, A. H. M. de Vries, J. G. de Vries and M. Pfeffer, *Org. Lett.*, 2005, **7**, 1247–1250. c) J. Canivet, G. Labat, H. Stoeckli-Evans and G. Süss-Fink, *Eur. J. Inorg. Chem.*, 2005, 4493–4500. d) A. M. Hayes, D. J. Morris, G. J. Clarkson and M. Wills, *J. Am. Chem. Soc.*, 2005, **127**, 7318–7319. e) M. Ito, Y. Endo, T. Ikariya, *Organometallics*, 2008, **27**, 6053–6055. f) J. E. D. Martins, G. J. Clarkson and M. Wills, *Org. Lett.*, 2009, **11**, 847–850. g) T. Touge, T. Hakamata, H. Nara, T. Kobayashi, N. Sayo, T. Saito, Y. Kayaki and T. Ikariya, *J. Am. Chem. Soc.*, 2011, **133**, 14960–14963.
- 9 a) K.-J. Haack, S. Hashiguchi, A. Fujii, T. Ikariya and R. Noyori, *Angew. Chem. Int. Ed. Engl.*, 1997, **36**, 285–288. b) M. Yamakawa, H. Ito and R. Noyori, *J. Am. Chem. Soc.*, 2000, **122**, 1466–1478.
- 10 a) D. A. Alonso, P. Brandt, S. J. M. Nordin and P. G. Andersson, *J. Am. Chem. Soc.*, 1999, **121**, 9580–9588. b) D. G. I. Petra, J. N. H. Reek, J.-W. Handgraaf, E. J. Meijer, P. Dierkes, P. C. J. Kamer, J. Brussee, H. E. Schoemaker and P. W. N. M. van Leeuwen, *Chem. Eur. J.*, 2000, **6**, 2818–2829.
- 11 J. Václavík, M. Kuzma, J. Přečh and P. Kačer, *Organometallics*, 2011, **30**, 4822–4829.
- 12 a) M. Nishio, M. Hirota and Y. Umezawa, *The CH/ π Interaction, Evidence Nature, and Consequences*, Wiley-VCH, New York, 1998. b) O. Takahashi, Y. Kohno and M. Nishio, *Chem. Rev.*, 2010, **110**, 6049–6076. c) M. Nishio, *Phys. Chem. Chem. Phys.*, 2011, **13**, 13873–13900.
- 13 a) M. Yamakawa, I. Yamada and R. Noyori, *Angew. Chem. Int. Ed.*, 2001, **40**, 2818–2821. b) R. Noyori, M. Yamakawa and S. Hashiguchi, *J. Org. Chem.*, 2001, **66**, 7931–7944.
- 14 a) E. L. Muetterties, J. R. Bleeke, E. J. Wucherer and T. A. Albright, *Chem. Rev.*, 1982, **82**, 499–525. b) R. K. Pomeroy and D. J. Harrison, *J. Chem. Soc. Chem. Commun.*, 1980, 661–663.
- 15 a) *Transition State Modeling for Catalysis. ACS Symp. Ser. 721*, ed. D. G. Truhlar and K. Morokuma, American Chemical Society, DC, 1999. b) D. Balcells and F. Maseras, *New J. Chem.*, 2007, **31**, 333–343. c) K. N. Houk, P. H.-Y. Cheong,

- Nature*, 2008, **455**, 309–313. d) J. M. Brown and R. J. Deeth, *Angew. Chem. Int. Ed.*, 2009, **48**, 4476–4479.
- 16 a) S. Mori, T. Vreven and K. Morokuma, *Chem. Asian J.*, 2006, **1**, 391–403. b) I. D. Gridnev, T. Imamoto, G. Hoge, M. Kouchi and H. Takahashi, *J. Am. Chem. Soc.*, 2008, **130**, 2560–2572. c) P. J. Donoghue, P. Helquist, P.-O. Norrby and O. Wiest, *J. Am. Chem. Soc.*, 2009, **131**, 410–411.
- 17 a) T. Matsubara, S. Sieber and K. Morokuma, *Int. J. Quant. Chem.*, 1996, **60**, 1101–1109. b) M. M. Khaledy, M. Y. S. Kalani, K. S. Khuong, K. N. Houk, V. Aviyente, R. Neier, N. Soldermann and J. Velker, *J. Org. Chem.*, 2003, **68**, 572–577. c) M. A. Rangelov, G. P. Petrova, V. M. Yomtova and G. N. Vayssilov, *J. Mol. Graph. Model.*, 2010, **29**, 246–255.
- 18 H. Yang and M. W. Wong, *J. Am. Chem. Soc.*, 2013, **135**, 5808–5818.
- 19 a) S. Maeda and K. Ohno, *J. Phys. Chem. A*, 2007, **111**, 13168–13171. b) S. Maeda and K. Ohno, *J. Am. Chem. Soc.*, 2008, **130**, 17228–17229. c) K. Ohno and S. Maeda, *J. Mol. Catal. A: Chem.*, 2010, **324**, 133–140.
- 20 a) K. Ohno and S. Maeda, *Chem. Phys. Lett.*, 2004, **384**, 277–282. b) S. Maeda and K. Ohno, *J. Phys. Chem. A*, 2005, **109**, 5742–5753. c) K. Ohno and S. Maeda, *J. Phys. Chem. A*, 2006, **110**, 8933–8941.
- 21 P. A. Dub and T. Ikariya, *J. Am. Chem. Soc.*, 2013, **135**, 2604–2619.
- 22 BS-I (basis set I) represents LANL2DZ with *f*-type pseudopotentials for Ru; 6-31G* for the C and O atoms in the hydrogenated carbonyl group, the two N atoms, the six C(sp²) atoms in the *p*-cymene ligand, and the two H atoms transferred from (*S,S*)-**4** to **1**; 3-21G for the other atoms.
- 23 The difference between the experimental and theoretical *er* values may be due partly to the limited level of calculations, the neglect of solvent effects [alcoholic or HCOOH/N(C₂H₅)₃], and/or the presence of unknown reaction pathways.
- 24 The 40 lowest TSs for each *Re*- and *Si*-TSs at the B3LYP/BS-I level were considered for optimization except for TSs with overlapping conformations.
- 25 BS-II (basis set II) represents LANL2DZ with *f*-type pseudopotentials for Ru, 6-31G** for the other atoms. PCM = polarized continuum model. The free energies at the B3LYP/BS-II/PCM(methanol)//B3LYP/BS-II level are more accurate than and different from those at the B3LYP/BS-I level.

- 26 A similar structure to TS *Re-6*₁ is presented in ref.11, though its details are not discussed therein.
- 27 a) P. Sozzani, A. Comotti, S. Bracco and R. Simonutti, *Chem. Commun.*, 2004, 768–769. b) Y. Kobayashi and K. Saigo, *J. Am. Chem. Soc.*, 2005, **127**, 15054–15060. c) J. Ran and M. W. Wong, *J. Phys. Chem. A*, 2006, **110**, 9702–9709.
- 28 NPA = natural population analysis. See: A. E. Reed, R. B. Weinstock, F. Weinhold, *J. Chem. Phys.*, 1985, **83**, 735–746.
- 29 R. B. Woodward, R. Hoffmann, *Angew. Chem. internat. Edit.*, 1969, **8**, 781–853.
- 30 The result with the B3LYP calculations is to be treated with caution because dispersion forces are neglected. Further structural optimization of *Re-6*₁₋₃ at the M06/BS-II level of theory did not result in significant conformational change, but the optimization of *Re-6*₄ at the same level led to a structure stabilized by multiple CH/ π interactions.
- 31 a) Gaussian 03, Revision E.01, M. J. Frisch, G. W. Trucks, H. B. Schlegel, G. E. Scuseria, M. A. Robb, J. R. Cheeseman, J. A. Montgomery, Jr., T. Vreven, K. N. Kudin, J. C. Burant, J. M. Millam, S. S. Iyengar, J. Tomasi, V. Barone, B. Mennucci, M. Cossi, G. Scalmani, N. Rega, G. A. Petersson, H. Nakatsuji, M. Hada, M. Ehara, K. Toyota, R. Fukuda, J. Hasegawa, M. Ishida, T. Nakajima, Y. Honda, O. Kitao, H. Nakai, M. Klene, X. Li, J. E. Knox, H. P. Hratchian, J. B. Cross, V. Bakken, C. Adamo, J. Jaramillo, R. Gomperts, R. E. Stratmann, O. Yazyev, A. J. Austin, R. Cammi, C. Pomelli, J. W. Ochterski, P. Y. Ayala, K. Morokuma, G. A. Voth, P. Salvador, J. J. Dannenberg, V. G. Zakrzewski, S. Dapprich, A. D. Daniels, M. C. Strain, O. Farkas, D. K. Malick, A. D. Rabuck, K. Raghavachari, J. B. Foresman, J. V. Ortiz, Q. Cui, A. G. Baboul, S. Clifford, J. Cioslowski, B. B. Stefanov, G. Liu, A. Liashenko, P. Piskorz, I. Komaromi, R. L. Martin, D. J. Fox, T. Keith, M. A. Al-Laham, C. Y. Peng, A. Nanayakkara, M. Challacombe, P. M. W. Gill, B. Johnson, W. Chen, M. W. Wong, C. Gonzalez, and J. A. Pople, Gaussian, Inc., Wallingford CT, 2004; b) Gaussian 09, Revision B.01 and C.01, M. J. Frisch, G. W. Trucks, H. B. Schlegel, G. E. Scuseria, M. A. Robb, J. R. Cheeseman, G. Scalmani, V. Barone, B. Mennucci, G. A. Petersson, H. Nakatsuji, M. Caricato, X. Li, H. P. Hratchian, A. F. Izmaylov, J. Bloino, G. Zheng, J. L. Sonnenberg, M. Hada, M. Ehara, K. Toyota, R. Fukuda, J. Hasegawa, M. Ishida, T. Nakajima, Y. Honda, O. Kitao, H. Nakai, T. Vreven, J. A. Montgomery,

- Jr., J. E. Peralta, F. Ogliaro, M. Bearpark, J. J. Heyd, E. Brothers, K. N. Kudin, V. N. Staroverov, T. Keith, R. Kobayashi, J. Normand, K. Raghavachari, A. Rendell, J. C. Burant, S. S. Iyengar, J. Tomasi, M. Cossi, N. Rega, J. M. Millam, M. Klene, J. E. Knox, J. B. Cross, V. Bakken, C. Adamo, J. Jaramillo, R. Gomperts, R. E. Stratmann, O. Yazyev, A. J. Austin, R. Cammi, C. Pomelli, J. W. Ochterski, R. L. Martin, K. Morokuma, V. G. Zakrzewski, G. A. Voth, P. Salvador, J. J. Dannenberg, S. Dapprich, A. D. Daniels, O. Farkas, J. B. Foresman, J. V. Ortiz, J. Cioslowski, and D. J. Fox, Gaussian, Inc., Wallingford CT, 2010.
- 32 a) S. Miertuš, E. Scrocco and J. Tomasi, *Chem. Phys.*, 1981, **55**, 117–129. b) S. Miertuš and J. Tomasi, *Chem. Phys.*, 1982, **65**, 239–245. c) V. Barone, M. Cossi and J. Tomasi, *J. Comput. Chem.*, 1998, **19**, 404–417.
- 33 SCS-MP2 = spin-component-scaled second-order Møller–Plesset perturbation theory. Energies were calculated using the result of MP2 calculation with Gaussian09 program and the parameters shown in S. Grimme, *J. Chem. Phys.*, 2003, **118**, 9095–9102.

Chapter 3.

Hydration of Nitriles to Amides by a Chitin-supported Ruthenium Catalyst

3.1 Abstract

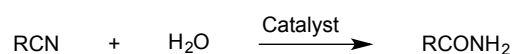
Chitin-supported ruthenium (Ru/chitin) promotes the hydration of nitriles to carboxamides under aqueous conditions. The nitrile hydration can be performed on a gram-scale and is compatible with the presence of various functional groups including olefins, aldehydes, carboxylic esters, nitro and benzyloxycarbonyl groups. The Ru/chitin catalyst is easily prepared from commercially available chitin, ruthenium(III) chloride and sodium borohydride. Analysis of Ru/chitin by high-resolution transmission electron microscopy indicated the presence of ruthenium nanoparticles on the chitin support.

3.2 Introduction

The catalytic hydration of nitriles (RCN) to carboxamides (RCONH₂) represents a fundamentally important pathway to these products in both laboratory and industrial contexts (Scheme 3.1).¹⁻³ Since the discovery of alumina-supported ruthenium hydroxide catalysts [Ru(OH)_x/Al₂O₃] by Yamaguchi *et al.*,⁴ solid-supported Ru has become an important class of catalyst for nitrile hydration, demonstrating high selectivity for carboxamide formation as well as other practical advantages.⁵⁻⁸ Although RuCl₃·*n*H₂O itself catalyzes nitrile hydration, the choice of solid support is critically important for achieving sufficient reactivity as well as for retaining Ru species on support.^{4,6} Examples of supports successfully used for Ru species include inorganic γ -Al₂O₃,⁴ nanoferrite^{5a} and magnetic silica,^{5b} as well as organic chitosan,^{5c} Amberlite⁶ and Nafion.⁷ However, these systems typically require the use of microwave

irradiation^{5,6} or high reaction temperatures (~ 175 °C).⁷ Moreover, the tolerance of base-sensitive functional groups such as carboxylic esters has not been documented in these reports.⁴⁻⁷ Such chemoselectivity is important in modern organic synthesis,⁹ but is generally considered elusive in nitrile hydration promoted by metal-loaded heterogeneous catalysts, a single exception (Au/TiO₂)^{8f} notwithstanding.

To address this issue, the author establishes that the chemoselective hydration of various nitriles to carboxamides is effectively catalyzed by chitin-supported ruthenium nanoparticles (abbreviated as Ru/chitin).



Scheme 3.1. Catalytic hydration of nitriles to carboxamides.

After cellulose, chitin is the second most abundant polysaccharide in Nature (Figure 3.1).¹⁰ It has a wide range of applications in materials, food, medical and environmental contexts, including the preparation of chitosan, affinity chromatography, wound-dressing and metal-extraction in water purification.¹¹ Whereas chitin has been intensively used as a catalyst support for enzymes,¹² its use as a support for metal catalysts has been less widely explored than has that of chitosan.^{13,14} So far, chitin has been used as a support for Pt in asymmetric arene hydrogenation,¹⁵ Pd in the hydrogenation of nitrobenzene and unsaturated fatty acid esters¹⁶ and Re in the epoxidation of olefins.^{14d} The author expected that chitin would represent a potentially attractive support for the Ru-catalyzed hydration of nitriles because chitin is highly stable under aqueous conditions, effectively adsorbs Ru species with its carboxamide functionality¹⁷ and the presence of both hydroxyl and amide groups in chitin potentially activate water as a mild base. With this hypothesis in mind, the author here proved that Ru/chitin serves as a versatile catalyst for the hydration of nitriles to carboxamides, the details of which are discussed herein.

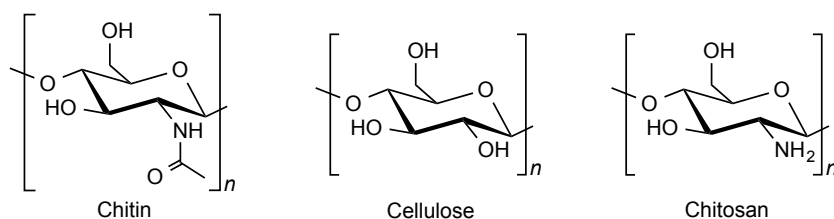
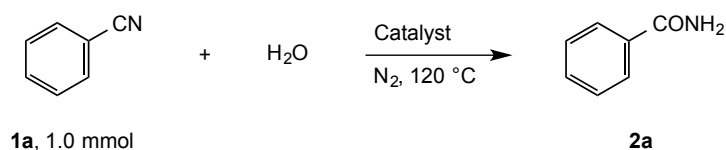


Figure 3.1. Chemical structures of chitin, cellulose and chitosan.

3.3 Results and discussion

Catalytic tests

Ru/chitin was prepared as follows: impregnation of commercially available chitin with an aqueous solution of $\text{RuCl}_3 \cdot 3\text{H}_2\text{O}$ gave a catalyst precursor. After drying, the catalyst precursor was reduced with NaBH_4 under aqueous conditions to give the Ru/chitin catalyst.¹⁸ Ru/chitin was tested for its effectiveness in the hydration of benzonitrile (**1a**, Table 3.1). When a mixture of **1a** (1.0 mmol), H_2O (1.0 mL) and Ru/chitin (0.016 mmol Ru, 1.6 mol % Ru) was heated at 120 °C for 3 h, the corresponding amide **2a** was obtained in 33% ¹H NMR yield (Table 3.1, entry 1). The presence of ruthenium was found to be essential, with the reaction hardly proceeding without catalyst or using only chitin (entries 2 and 3). Meanwhile, the chitin support was also found to be critical, with $\text{RuCl}_3 \cdot 3\text{H}_2\text{O}$ alone catalyzing the hydration of **1a** but with significantly lower efficiency (entry 4). The optimization of reaction conditions using Ru/chitin increased the yield of **2a** from 33% to 87% (entries 5–7). Here again, use of chitin support gave for better result than $\text{RuCl}_3 \cdot 3\text{H}_2\text{O}$ (entry 7 vs entry 8). Ru/chitin with a higher Ru content [2.3 mol % Ru, prepared from catalyst precursor (202 mg, 1.2 wt % Ru)] gave slightly better yield (entry 9). The result shown in entry 9 proved to be reproducible (¹H NMR yields of separate runs: 97%, 91%, 89% and 89%). Analogously prepared Ru catalysts that utilized other polysaccharide supports such as chitosan and cellulose (abbreviated as Ru/chitosan and Ru/cellulose, respectively) were found to be less reactive than Ru/chitin (entries 10 and 11 vs entry 9).

Table 3.1. Hydration of benzonitrile (**1a**) to benzamide (**2a**).^a

Entry	Catalyst (mol % Ru)	H ₂ O (mL)	<i>t</i> (h)	Yield (%) ^b
1	Ru/chitin (1.6)	1	3	33
2	None	1	3	< 1
3	Chitin	1	3	< 1
4	RuCl ₃ •3H ₂ O (2.0)	1	3	17
5	Ru/chitin (1.6)	1	20	77
6	Ru/chitin (1.6)	1	30	87
7	Ru/chitin (1.6)	4	20	87
8	RuCl ₃ •3H ₂ O (2.0)	4	20	45
9	Ru/chitin (2.3) ^c	4	20	97
10	Ru/chitosan (3.2) ^d	4	20	74
11	Ru/cellulose (3.2) ^e	4	20	17

^a Conditions: **1a** (1.0 mmol), H₂O (1.0 mL, 56 equiv) and catalyst [1.6 mol % Ru, prepared from catalyst precursor (202 mg, 0.8 wt % Ru)] at 120 °C under a N₂ atmosphere unless otherwise stated. The mol % Ru was confirmed by ICP-AES analysis.

^b Of **2a**, determined by ¹H NMR using mesitylene as an internal standard. ^c Ru/chitin (2.3 mol % Ru), prepared from catalyst precursor (1.2 wt % Ru). ^d Ru/chitosan (3.2 mol % Ru), prepared from catalyst precursor (1.7 wt % Ru). ^e Ru/cellulose (3.2 mol % Ru), prepared from catalyst precursor (1.6 wt % Ru).

Scope and limitation

The scope of the Ru/chitin-catalyzed hydration of nitriles is outlined in Table 3.2. These reactions were run under comparable conditions to those in entry 9 of Table 3.1. Benzamide (**2a**) was obtained in 87% isolated yield (Table 3.2, entry 1). Various substituted benzonitriles could be converted to the corresponding amides in

good-to-excellent yields (entries 2–13). *o*-Methyl-substituted **1i** was somewhat less reactive (entry 9) though *m*- and *p*-substituted analogues reacted in satisfying yields (entries 7 and 8). Benzonitrile **1l**, which bore an electron-withdrawing *p*-nitro group, was completely hydrated in shorter reaction times than **1b**, **1c**, **1f** and **1g**, each of which bore electron-donating groups at the *para* positions. *p*-Formylbenzonitrile (**1k**) could be converted to the corresponding amide **2k** with an intact formyl moiety in 76% yield. Furthermore, heteroaromatic nitriles could be efficiently hydrated to the corresponding amides (entries 14 and 15).

The Ru/chitin system was also applied to the hydration of aliphatic nitriles (Table 3.2, entries 16–23). Although the hydration reaction proved susceptible to steric hindrance (entry 19), primary and secondary nitriles **1p–r** and **1t–w** could all be converted to amides (entries 16–18 and 20–23) with retention of olefin (entry 21), β -hydroxy (entry 22) and α -methoxy (entry 23) groups in fair-to-good yields.

Table 3.2. Catalytic hydration of nitriles with Ru/chitin.^a

	RCN	+	H ₂ O	$\xrightarrow[\text{N}_2, 120\text{ }^\circ\text{C}]{\text{Ru/chitin (2.3 mol \% Ru)}}$	RCONH ₂	
	1 , 1.0 mmol		4 mL		2	

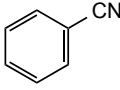
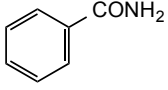
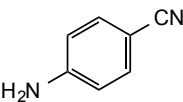
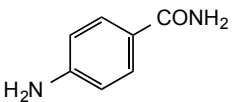
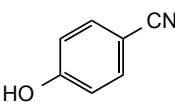
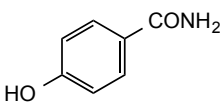
Entry	Nitrile (1)	<i>t</i> (h)	Amide (2)	Isolated yield (%)
1	 1a	20	 2a	87
2	 1b	60	 2b	89
3	 1c	40	 2c	98

Table 3.2. Continued.^a

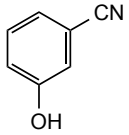
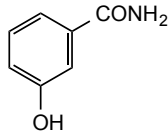
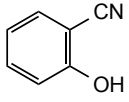
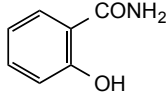
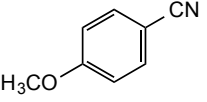
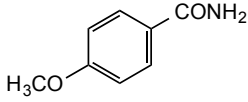
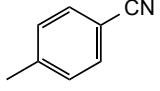
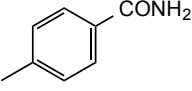
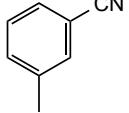
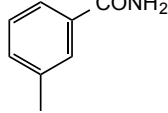
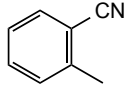
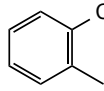
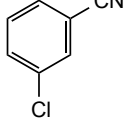
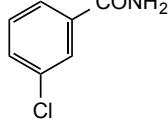
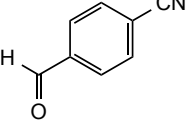
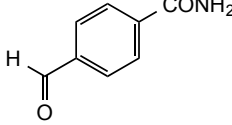
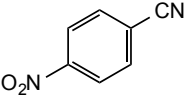
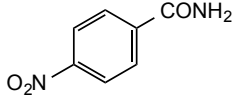
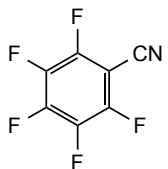
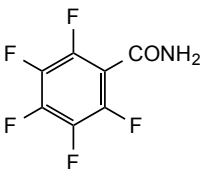
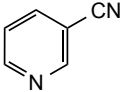
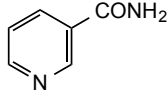
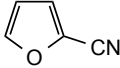
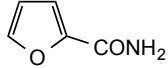
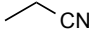
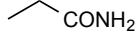
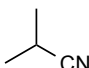
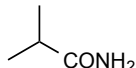
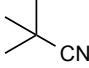
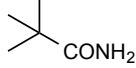
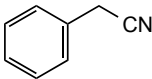
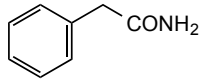
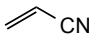

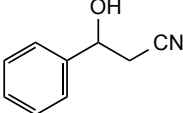
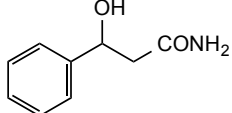
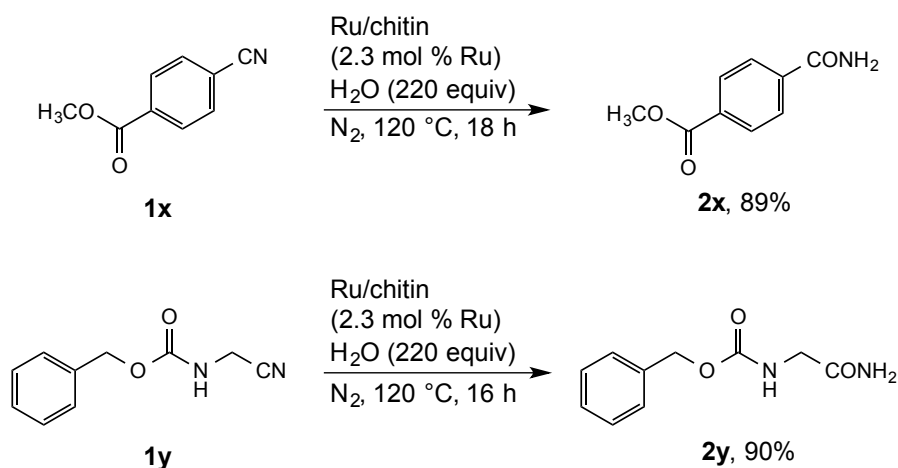
4		1d	32		2d	97
5		1e	32		2e	79
6		1f	40		2f	88
7		1g	50		2g	96
8		1h	60		2h	92
9		1i	60		2i	49
10		1j	24		2j	80
11		1k	40		2k	76
12		1l	18		2l	92
13		1m	50		2m	65

Table 3.2. *Continued.*^a

14		1n	24		2n	94
15		1o	20		2o	91
16	CH ₃ CN	1p	36	CH ₃ CONH ₂	2p	65
17		1q	36		2q	55
18		1r	48		2r	65
19		1s	48		2s	23
20		1t	36		2t	85
21		1u	24		2u	66
22		1v	30		2v	46
23	H ₃ COCH ₂ CN	1w	24	H ₃ COCH ₂ CONH ₂	2w	81

^a Conditions: **1** (1.0 mmol), H₂O (4 mL, 220 equiv) and Ru/chitin (2.3 mol % Ru) at 120 °C under a N₂ atmosphere.

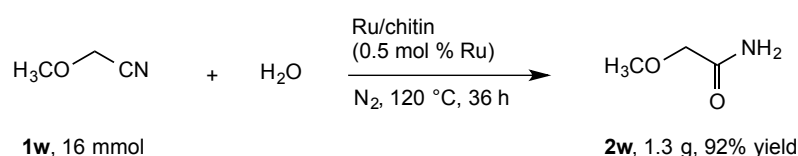
Importantly, the presence of a base-sensitive carbonyl functionality in methyl ester **1x** was tolerated by virtue of the near-neutral conditions that could be used for catalyst preparation (Scheme 3.2).^{6,18} Similarly, an α -amino acetonitrile conjugated with a redox-sensitive benzyloxycarbonyl (Cbz) group (as in **1y**) was converted to protected α -amino acetoamide **2y** with retention of the carbamoyl linkage. The tolerance to carboxylic ester and CbzN functionality shown in Scheme 3.2 illustrates the applicability of the present method to the nitrile hydration of complex molecules bearing redox- or base-sensitive functional groups.



Scheme 3.2. Hydration nitriles bearing carboxylic ester and carbamate functionalities.

Upscale experiment

To verify the scalability of this method, a gram-scale hydration was carried out (Scheme 3.3). The hydration of **1w** using a decreased loading of Ru/chitin catalyst (0.5 mol % Ru) yielded the amide **2w** in an excellent yield [conditions: **1w** (16 mmol), H₂O (13 mL), Ru/chitin (0.5 mol % Ru), 120 °C, 36 h, 92% isolated yield (77% isolated yield after 24 h under otherwise identical conditions)].



Scheme 3.3. Gram-scale hydration of nitrile **1w**.

High-resolution transmission electron microscopy (HRTEM) analysis

To elucidate the nature of the Ru/chitin catalyst, the catalyst was analyzed with HRTEM. The presence of nanoparticles with a mean size of 2.1 ± 0.4 nm was established (Figures 3.2a–c). Energy dispersive X-ray spectroscopy (EDX) confirms the existence of ruthenium and measurement of the d -spacings ($d = 0.23$ nm) indicated the presence of both Ru⁰ and RuO₂ [Figures 3.2c, inset, and 3.2d). EDX also revealed the presence of Ca and P in both Ru/chitin (Figure 3.2d) and chitin (Figures 3.2e and 3.2f). This was attributed to calcium phosphate on account of the crustaceous origin of the chitin^{10a} and was found not to incur significant catalytic activity (Table 3.1, entry 3).

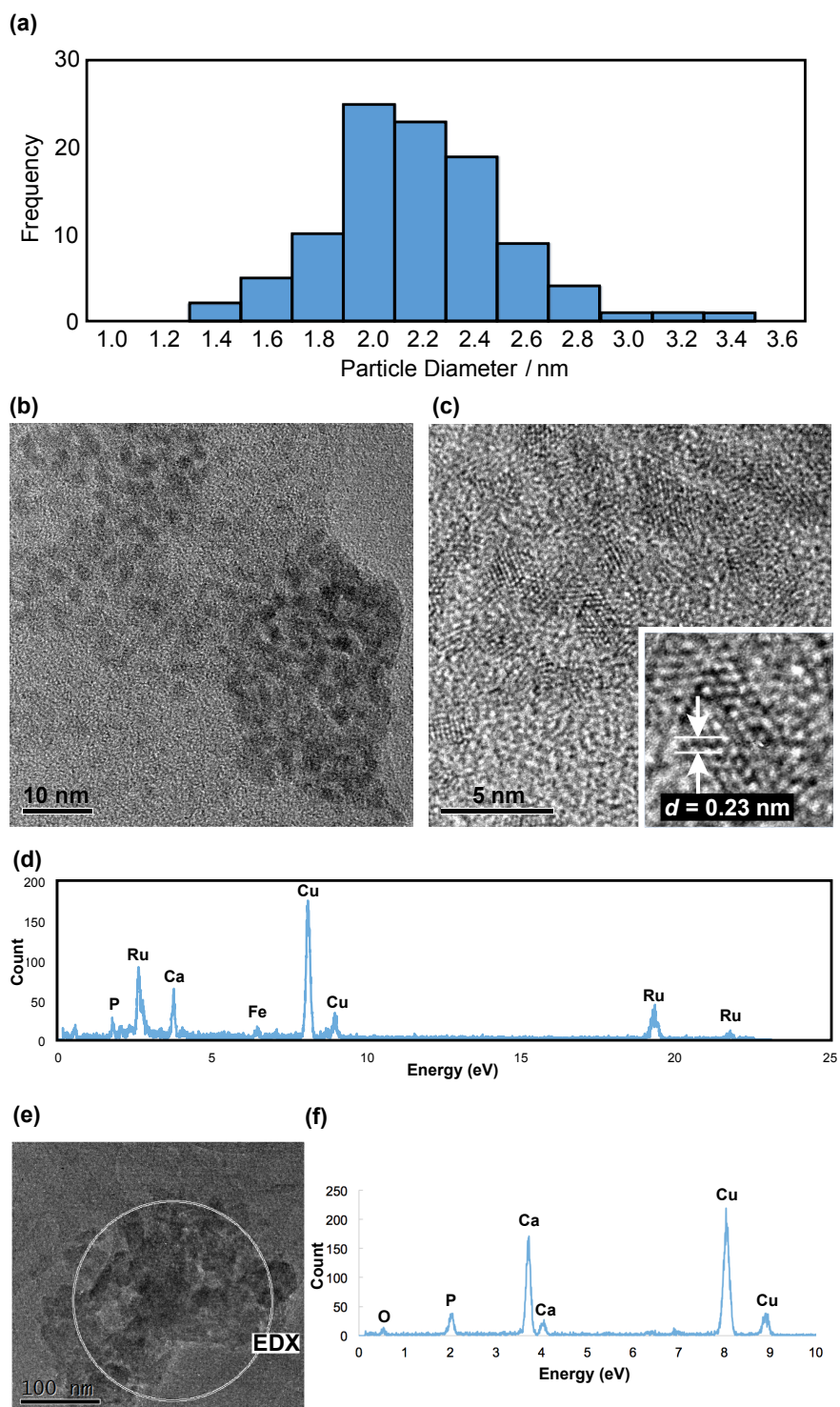


Figure 3.2. (a) A histogram representing the particle size distribution of Ru nanoparticles on chitin. (b) Low-magnification and (c and inset) high-resolution TEM images of chitin-supported Ru nanoparticles. (d) EDX of Ru/chitin. (e) A low-magnification TEM image of chitin. (f) EDX of chitin.

HRTEM analysis of the Ru nanoparticles after hydration of **1w** showed that they remained morphologically essentially unchanged (Figure 3.3). In fact, the Ru/chitin catalyst could be reused without significant loss of catalytic activity at least three times. (Figure 3.4).

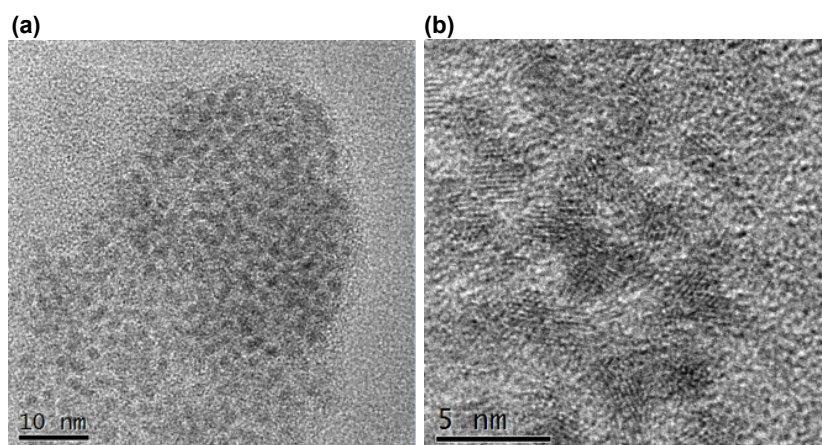


Figure 3.3. (a) Low-magnification and (b) high-resolution TEM images of Ru/chitin after nitrile hydration.

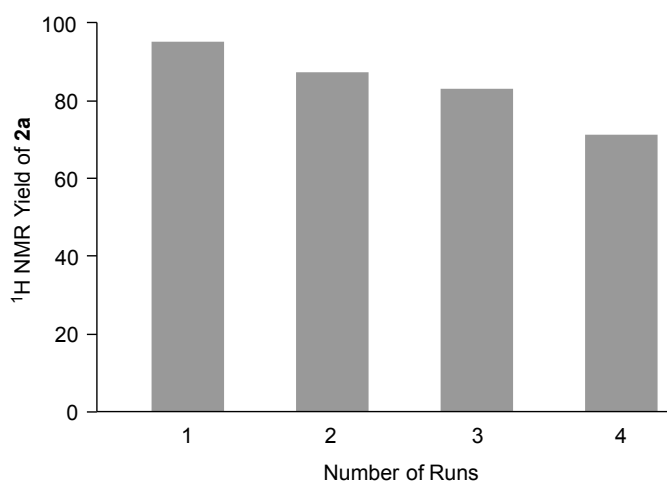


Figure 3.4. Reuse experiment of Ru/chitin in the hydration of **1a** to **2a**. Conditions: **1a** (1.0 mmol), H₂O (4 mL, 220 equiv) and Ru/chitin (2.3 mol % Ru) at 120 °C for 20 h under a N₂ atmosphere.

3.4 Conclusions

The author has established that chitin-supported ruthenium displays high catalytic activity towards the hydration of nitriles to amides under near-neutral, aqueous conditions. The catalyst is easily prepared, and applicable to the hydration of a wide variety of nitriles with aromatic, heteroaromatic and aliphatic substituents. HRTEM analysis of Ru/chitin revealed the presence of ruthenium nanoparticles before and after hydration reactions, indicating that chitin could serve as an effective solid support for ruthenium nanoparticles.

3.5 Experimental section

General comments

^1H and ^{13}C NMR spectra were recorded on a JEOL ECA-600 (600 MHz for ^1H , 150 MHz for ^{13}C , 564 MHz for ^{19}F) or a JEOL ECA-500 (500 MHz for ^1H , 125 MHz for ^{13}C) at 25 °C. Chemical shifts are reported as δ in ppm and are internally referenced to tetramethylsilane (TMS, 0.00 ppm for ^1H), CD_2HOH (3.30 ppm for ^1H), $\text{CD}_2\text{HSOCD}_3$ (2.50 ppm for ^1H), HOD (4.79 ppm for ^1H), CDCl_3 (77.2 ppm for ^{13}C), CD_3OD (49.0 ppm for ^{13}C), dioxane (67.2 ppm in D_2O for ^{13}C), or dimethyl sulfoxide- d_6 ($\text{DMSO-}d_6$, 39.5 ppm for ^{13}C). Chemical shifts for ^{19}F NMR were externally referenced to CF_3COOH (-78.5 ppm, neat). Infrared (IR) spectra were recorded on a FT-IR6100 (JASCO). High-resolution mass spectrometry (HRMS) was recorded with a Bruker Daltonik micrOTOF-QII spectrometer. Inductively coupled plasma-atomic emission spectroscopy (ICP-AES) spectra were recorded on an Agilent VISTA-PRO. Elemental analyses were recorded on a Yanaco CHN recorder MT-6. These analytical experiments were carried out at the Chemical Instrumental Center, Research Center for Materials Science, Nagoya University. Melting points were recorded on an OptiMelt automated melting point system (Stanford Research Systems). Ruthenium content was analyzed by ICP-AES using yttrium as an internal standard after digestion of samples (10 mg) in concd HNO_3 (2 mL) at 150 °C for 12 h. Products **2a–y** were known compounds and their identities were confirmed by comparing with literature data.^{6,7,8g,19–34}

HRTEM analysis

High-resolution transmission electron microscopy (HRTEM) analysis was performed on a JEOL JEM-3011 microscope. Samples illustrated in Figures 3.1a–d and 3.2 were prepared as per the typical procedure for the preparation of Ru/chitin (0.016 mmol Ru, vide infra) and by the hydration of **1w** (0.5 mmol) using Ru/chitin (0.016 mmol Ru) at 120 °C for 6 h, respectively. Sample preparation required droplet coating of particle dispersions obtained by sonicating in CH₃CH₂OH on carbon-coated Cu grids (Agar Scientific, 300 mesh). Electron optical parameters: C_S = 0.6 mm, C_C = 1.2 mm, electron energy spread = 1.5 eV, beam divergence semi-angle = 1 mrad. Elemental analysis was by energy dispersive X-ray spectroscopy (EDX) using a PGT prism Si/Li detector and an Avalon 2000 analytical system. Spectra were analyzed using the PGT eXcalibur 4.03.00 software. Observed Cu K α and K β emission lines were attributed to scattered electrons impinging on the copper grid. Any minor Fe K α and Co K α emission lines of similar intensity were due to parasitic scattering from the lens pole piece. Detailed analysis of particle morphology was performed using Digital Micrograph 3.6.5 by counting the diameters of 100 particles (N), defining intervals of 0.25 nm between $d_{\min} \leq d \leq d_{\max}$ and counting the number of particles falling into these intervals. Particle size distributions were constructed using DataGraph 3.0. Values of average d -spacing were obtained from Fourier transforms of high magnification images ($\times 800k$, $\times 1M$) using $d = 20/D$ where D is the diameter (nm) of rings obtained. Average d -spacing was confirmed using the profile tool in Digital Micrograph by averaging over 10 d -spacings. To determine the error in the value of d -spacing thus obtained, detailed TEM examination of CeO₂ and Au nanoparticles was undertaken. The relationship between FT ring diameter and DV value (a measure of objective lens focusing voltage) was established for DV values between -6 and $+6$ and the standard deviation in d -spacing was established to be 10% when compared to the literature.

Materials

RuCl₃•3H₂O was purchased from Furuya Metal Co., Ltd. Benzonitrile (**1a**), *m*-hydroxybenzonitrile (**1d**), *p*-methylbenzonitrile (**1g**), *m*-methylbenzonitrile (**1h**), *o*-methylbenzonitrile (**1i**), *m*-chlorobenzonitrile (**1j**), *p*-nitrobenzonitrile (**1l**), 2,3,4,5,6-pentafluorobenzonitrile (**1m**), acetonitrile (**1p**), pivalonitrile (**1s**),

2-phenylacetonitrile (**1t**), 3-hydroxy-3-phenylpropanonitrile (**1v**), α -methoxyacetonitrile (**1w**) and 4-(methoxycarbonyl)benzonitrile (**1x**), were purchased from TCI. *p*-Aminobenzonitrile (**1b**), *p*-methoxybenzonitrile (**1f**), 2-furonitrile (**1o**), yttrium standard solution [$\text{Y}(\text{NO}_3)_3$ in HNO_3 aq, 1.00 mg Y mL^{-1} ; 1000 ppm] and concd HNO_3 were purchased from Wako Chemicals. *p*-Hydroxybenzonitrile (**1c**), *p*-formylbenzonitrile (**1k**), propionitrile (**1q**), 2-methylpropanenitrile (**1r**) and acrylonitrile (**1u**) were purchased from Aldrich. *o*-Hydroxybenzonitrile (**1e**) was purchased from Merck. Nicotinonitrile (**1n**) and chitin were purchased from Kanto Chemicals. Ruthenium standard solution (1 mg Ru mL^{-1} in HCl aq) for ICP-AES was purchased from Acros. α -(Benzyloxycarbonylamino)acetonitrile (**1y**) was prepared according to the literature procedure by protecting α -aminoacetonitrile with CbzCl.³⁵

Catalyst preparation

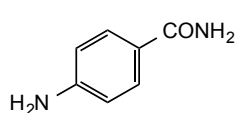
A typical procedure for the preparation of Ru/chitin (0.016 mmol Ru). To a 300 mL round-bottom flask, $\text{RuCl}_3 \cdot 3\text{H}_2\text{O}$ (71.6 mg, 0.30 mmol Ru), H_2O (50 mL) and chitin (2980.4 mg) were added. The mixture was heated at 50 °C for 30 min, and concentrated using a rotary evaporator at 50 °C for 25 min (17 mmHg). The solid was dried at 50 °C *in vacuo* overnight to afford the catalyst precursor (0.8 wt % Ru as determined by ICP-AES analysis, dark green solid, 2784.0 mg). To a 10 mL test tube with a screw cap, a magnetic stirring bar and the catalyst precursor (202 mg, 0.8 wt % Ru), deaerated H_2O (8 mL) was added under a N_2 atmosphere. Under vigorous stirring, a solution [1.0 mL; a mixture of NaBH_4 (39.4 mg, 1.0 mmol) and deaerated H_2O (5.2 mL)] was introduced dropwise to the test tube. The mixture was stirred at rt for 3.5 h. The liquid phase was separated by centrifugation (3500 rpm, 5 min) and replaced with H_2O (8 mL) via syringe. After the mixture was stirred at rt overnight, the solid was washed with water (2 times) and dried *in vacuo* at rt for 2 h to afford Ru/chitin as a grey solid, which was directly used for nitrile hydration.

Ru/chitin (0.023 mmol Ru). As per the above-mentioned typical procedure, the catalyst precursor was prepared using $\text{RuCl}_3 \cdot 3\text{H}_2\text{O}$ (107.4 mg, 0.45 mmol Ru), H_2O (50 mL), and chitin (2957 mg). Dark green solid (1.2 wt % Ru determined by ICP-AES analysis, 2813 mg). As per the above-mentioned typical procedure, the Ru/chitin (0.023 mmol Ru) was prepared using precursor (202 mg, 1.2 wt % Ru), deaerated H_2O (7.5 mL) and a reducing solution [1.5 mL; a mixture of NaBH_4 (103.0 mg, 2.7 mmol) and

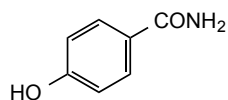
deaerated H₂O (20 mL)].

Hydration of nitriles to amides

A typical procedure for hydration of nitriles: benzamide (2a, Table 3.1, entry 9; Table 3.2, entry 1).¹⁹ As per the above-mentioned procedure, Ru/chitin (0.023 mmol Ru) was prepared in a screw-cap 10 mL test tube equipped with a rubber septum and a magnetic stirring bar. To this tube were added nitrile **1a** (0.986 mmol, 101.6 mg) and deaerated H₂O (2.2×10^2 mmol, 4 mL) under a N₂ atmosphere. After the septum inlet was replaced with a plastic screw cap and the cap was wrapped with Teflon tape, the mixture was shaken at 120 °C for 20 h [*ca.* 100 rpm, with a constant temperature oven (EYELA MG-2300, Tokyo Rikakikai Co. Ltd.)] on a rotary shaker (EYELA Multi Shaker MMS, Tokyo Rikakikai Co. Ltd.). The mixture was cooled down with ice water, and mixed with CH₃OH (4 mL) under air. The liquid phase was separated by centrifugation (3500 rpm, 10 min). Extraction of the product was carried out by repeating this process (CH₃OH, 6 × 4 mL). Liquid phases were combined and concentrated *in vacuo*. ¹H NMR analysis of this crude mixture using mesitylene as an internal standard indicated the formation of amide **2a** in 97% yield. The product was purified by sequential column chromatography on silica gel (acetone/dichloromethane 3:7; tetrahydrofuran/diethyl ether 1:10) to afford amide **2a** as colorless plates (103.8 mg, 87% yield). Mp 126.5–127.1 °C (lit.¹⁹ 125–128 °C); IR (KBr) 1405, 1577, 1625, 1660, 3175, 3369 cm⁻¹; ¹H NMR (600 MHz, DMSO-*d*₆) δ 7.36 (bs, 1H), 7.42–7.47 (m, 2H), 7.51 (tt, *J* = 1.5, 7.3 Hz, 1H), 7.85–7.89 (m, 2H), 7.97 (bs, 1H); ¹³C{¹H} NMR (150 MHz, DMSO-*d*₆) δ 127.4, 128.2, 131.2, 134.3, 167.9; elemental analysis calcd for [C₇H₇NO•0.1H₂O]: C, 68.39; H, 5.90; N, 11.39, found: C, 68.64; H, 5.92; N, 11.15.

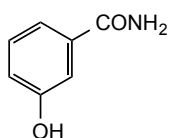


p-Aminobenzamide (2b).¹⁹ Light yellow blocks, purified by column chromatography on silica gel (methanol/chloroform 1:8); mp 176.3–180.9 °C (lit.¹⁹ 180–183 °C); IR (KBr) 780, 1397, 1563, 1600, 3219, 3326, 3464 cm⁻¹; ¹H NMR (600 MHz, DMSO-*d*₆) δ 5.59 (s, 2H), 6.53 (d, *J* = 8.6 Hz, 2H), 6.86 (bs, 1H), 7.53 (bs, 1H), 7.60 (d, *J* = 8.6 Hz, 2H); ¹³C{¹H} NMR (150 MHz, DMSO-*d*₆) δ 112.5, 121.0, 129.2, 151.7, 168.2; elemental analysis calcd for [C₇H₈N₂O]: C, 61.75; H, 5.92; N, 20.58, found: C, 61.79; H, 5.87; N, 20.30.

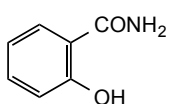


p-Hydroxybenzamide (2c).²⁰ White powder, purified by column chromatography on silica gel (tetrahydrofuran/diethyl ether 4:6–10:0,

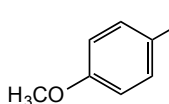
gradient); mp 157.1–159.2 °C (lit.²⁰ 148 °C); IR (KBr) 1247, 1403, 1558, 1618, 1649, 3124, 3340, 3417 cm⁻¹; ¹H NMR (600 MHz, DMSO-*d*₆) δ 6.78 (d, *J* = 8.6 Hz, 2H), 7.08 (bs, 1H), 7.68–7.79 (m, 3H), 9.94 (s, 1H); ¹³C{¹H} NMR (150 MHz, DMSO-*d*₆) δ 114.7, 125.0, 129.5, 160.2, 167.7; elemental analysis calcd for [C₇H₇NO₂]: C, 61.31; H, 5.15; N, 10.21, found: C, 61.13; H, 5.14; N, 10.01.



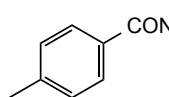
***m*-Hydroxybenzamide (2d).**²¹ White powder, purified by column chromatography on silica gel (2-propanol/*n*-hexane/ethyl acetate 1:20:200); mp 165.1–168.0 °C (lit.²¹ 167–168 °C); IR (KBr) 1256, 1450, 1580, 1653, 3247, 3400 cm⁻¹; ¹H NMR (600 MHz, DMSO-*d*₆) δ 6.88–6.92 (m, 1H), 7.20–7.24 (m, 1H), 7.24–7.30 (m, 3H), 7.86 (s, 1H), 9.60 (s, 1H); ¹³C{¹H} NMR (150 MHz, DMSO-*d*₆) δ 114.5, 118.0, 118.1, 129.2, 135.8, 157.3, 168.0; elemental analysis calcd for [C₇H₇NO₂]: C, 61.31; H, 5.15; N, 10.21, found: C, 61.23; H, 5.12; N, 10.05.



***o*-Hydroxybenzamide (2e).**⁷ Colorless plates, purified by column chromatography on silica gel (chloroform only); mp 138.2–139.2 °C; IR (KBr) 1253, 1359, 1424, 1447, 1493, 1590, 1630, 1675, 3189, 3395 cm⁻¹; ¹H NMR (600 MHz, DMSO-*d*₆) δ 6.83–6.89 (m, 2H), 7.37–7.42 (m, 1H), 7.84 (dd, *J* = 1.6, 8.0 Hz, 1H), 7.89 (bs, 1H), 8.39 (bs, 1H), 13.0 (s, 1H); ¹³C{¹H} NMR (150 MHz, DMSO-*d*₆) δ 114.4, 117.4, 118.3, 128.1, 134.1, 161.1, 172.1; elemental analysis calcd for [C₇H₇NO₂]: C, 61.31; H, 5.15; N, 10.21, found: C, 61.22; H, 5.21; N, 10.01.

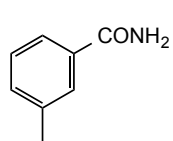


***p*-Methoxybenzamide (2f).**⁶ Colorless plates, purified by column chromatography on silica gel (tetrahydrofuran/diethyl ether 0:10–10:0, gradient); mp 164.3–169.3 °C; IR (KBr) 1146, 1253, 1396, 1422, 1573, 1643, 3170, 3391 cm⁻¹; ¹H NMR (600 MHz, CD₃OD) δ 3.82 (s, 3H), 6.93–6.97 (m, 2H), 7.81–7.85 (m, 2H); ¹³C{¹H} NMR (150 MHz, CD₃OD) δ 55.9, 114.7, 126.9, 130.6, 164.1, 172.0; elemental analysis calcd for [C₈H₉NO₂]: C, 63.56; H, 6.00; N, 9.27, found: C, 63.37; H, 6.00; N, 9.23.

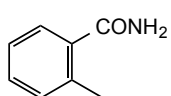


***p*-Methylbenzamide (2g).**^{8g} Colorless plates, purified by column chromatography on silica gel (acetone/dichloromethane 2:5); mp 157.6–159.0 °C (lit.^{8g} 159–160 °C); IR (KBr) 1397, 1414, 1571, 1618, 1671, 3168, 3343 cm⁻¹; ¹H NMR (600 MHz, DMSO-*d*₆) δ 2.34 (s, 3H), 7.22–7.30 (m, 3H), 7.75–7.80 (m, 2H), 7.89 (bs, 1H); ¹³C{¹H} NMR (150 MHz, DMSO-*d*₆) δ 20.9, 127.5, 128.7, 131.5, 141.0, 167.8; elemental analysis calcd for [C₈H₉NO]: C, 71.09; H,

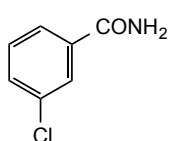
6.71; N, 10.36, found: C, 70.99; H, 6.66; N, 10.26.



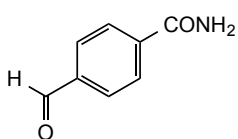
***m*-Methylbenzamide (2h).**^{8g} Colorless plates, purified by column chromatography on silica gel (*n*-hexane/ethyl acetate 2:3); mp 91.0–92.4 °C (lit.^{8g} 92–93 °C); IR (KBr) 687, 1114, 1387, 1432, 1616, 1650, 3195, 3376 cm⁻¹; ¹H NMR (600 MHz, DMSO-*d*₆) δ 2.34 (s, 3H), 7.25–7.35 (m, 3H), 7.64–7.69 (m, 1H), 7.69–7.72 (m, 1H), 7.91 (bs, 1H); ¹³C{¹H} NMR (150 MHz, DMSO-*d*₆) δ 20.9, 124.6, 128.1 (2C), 131.7, 134.3, 137.4, 168.0; elemental analysis calcd for [C₈H₉NO]: C, 71.09; H, 6.71; N, 10.36, found: C, 71.04; H, 6.78; N, 9.98.



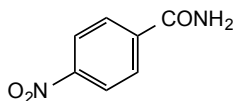
***o*-Methylbenzamide (2i).**^{8g} Colorless needles, purified by column chromatography on silica gel (ethyl acetate/*n*-hexane 2:3); mp 140.1–140.5 °C (lit.^{8g} 140 °C); IR (KBr) 1140, 1395, 1623, 1656, 3187, 3368 cm⁻¹; ¹H NMR (600 MHz, DMSO-*d*₆) δ 2.36 (s, 3H), 7.18–7.24 (m, 2H), 7.28–7.37 (m, 3H), 7.68 (bs, 1H); ¹³C{¹H} NMR (150 MHz, DMSO-*d*₆) δ 19.6, 125.4, 127.0, 129.1, 130.4, 135.1, 137.1, 171.0; elemental analysis calcd for [C₈H₉NO]: C, 71.09; H, 6.71; N, 10.36, found: C, 71.35; H, 6.72; N, 10.36.



***m*-Chlorobenzamide (2j).**^{8g} Colorless plates, purified by sequential column chromatography on silica gel (*n*-hexane/ethyl acetate 1:1; ethyl acetate only; tetrahydrofuran only) and activated carbon treatment; mp 132.6–133.4 °C (lit.^{8g} 134–136 °C); IR (KBr) 1123, 1389, 1432, 1569, 1626, 1658, 3181, 3366 cm⁻¹; ¹H NMR (600 MHz, DMSO-*d*₆) δ 7.46–7.52 (m, 1H), 7.54 (bs, 1H), 7.56–7.61 (m, 1H), 7.81–7.86 (m, 1H), 7.89–7.94 (m, 1H), 8.10 (bs, 1H); ¹³C{¹H} NMR (150 MHz, DMSO-*d*₆) δ 126.2, 127.3, 130.3, 131.1, 133.1, 136.3, 166.4; elemental analysis calcd for [C₇H₆NCIO]: C, 54.04; H, 3.89; N, 9.00, found: C, 53.96; H, 3.89; N, 8.95.

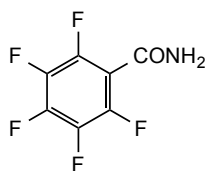


***p*-Formylbenzamide (2k).**²² White powder, purified by column chromatography on silica gel (*n*-hexane/ethyl acetate 1:3); mp 155.4–159.2 °C; IR (KBr) 1212, 1397, 1607, 1670, 1698, 3194, 3288, 3354 cm⁻¹; ¹H NMR (600 MHz, DMSO-*d*₆) δ 7.60 (bs, 1H), 7.96–8.00 (m, 2H), 8.03–8.08 (m, 2H), 8.17 (bs, 1H), 10.08 (s, 1H); ¹³C{¹H} NMR (150 MHz, DMSO-*d*₆) δ 128.1, 129.3, 137.8, 139.3, 167.0, 192.9; elemental analysis calcd for [C₈H₇NO₂]: C, 64.42; H, 4.73; N, 9.39, found: C, 64.69; H, 4.85; N, 9.16.



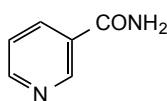
***p*-Nitrobenzamide (2l).**⁶ Colorless needles, purified by column chromatography on silica gel (triethylamine/2-propanol/chloroform

0.05:3:7); mp 197.1–200.0 °C; IR (KBr) 1346, 1413, 1526, 1600, 1678, 3177, 3477 cm^{-1} ; ^1H NMR (600 MHz, CD_3OD) δ 8.05–8.08 (m, 2H), 8.29–8.33 (m, 2H); $^{13}\text{C}\{^1\text{H}\}$ NMR (150 MHz, CD_3OD) δ 124.6, 130.0, 140.9, 151.2, 170.1; elemental analysis calcd for $[\text{C}_7\text{H}_6\text{N}_2\text{O}_3]$: C, 50.61; H, 3.64; N, 16.86, found: C, 50.67; H, 3.69; N, 16.64.



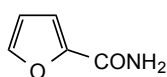
2,3,4,5,6-Pentafluorobenzamide (2m).⁷ Colorless plates, purified by column chromatography on silica gel (ethyl acetate/*n*-hexane 1:2); mp 146.8–147.2 °C; IR (KBr) 1001, 1493, 1675, 3186, 3358 cm^{-1} ; ^1H NMR (600 MHz, $\text{DMSO}-d_6$) δ 8.16 (bs, 1H), 8.30 (bs, 1H); $^{13}\text{C}\{^1\text{H}\}$

NMR (150 MHz, $\text{DMSO}-d_6$) δ 112.9 (t, $J = 21.6$ Hz), 135.9–137.9 (m), 139.9–141.9 (m), 141.8–143.9 (m), 158.3; $^{13}\text{C}\{^{19}\text{F}\}$ NMR (150 MHz, $\text{DMSO}-d_6$); δ 112.9 (d, $J = 8.7$ Hz), 136.9, 140.9, 142.9, 158.3; ^{19}F NMR (564 MHz, $\text{DMSO}-d_6$) δ -162.0–161.3 (m, 2F), -154.0–153.4 (m, 1F), -142.3–141.9 (m, 2F); elemental analysis calcd for $[\text{C}_7\text{H}_2\text{F}_5\text{NO}]$: C, 39.83; H, 0.96; N, 6.64, found: C, 40.00; H, 6.65; N, 1.09.



Nicotinamide (2n).²³ Colorless needles, purified by column chromatography on silica gel (ethyl acetate only) and recrystallization (from dichloromethane); mp 126.0–127.7 °C; IR (KBr) 1620, 1682,

3159, 3370 cm^{-1} ; ^1H NMR (500 MHz, $\text{DMSO}-d_6$) δ 7.48–7.51 (m, 1H), 7.59 (bs, 1H), 8.15 (bs, 1H), 8.19–8.21 (m, 1H), 8.69–8.70 (m, 1H), 9.02–9.03 (m, 1H); $^{13}\text{C}\{^1\text{H}\}$ NMR (150 MHz, $\text{DMSO}-d_6$) δ 123.3, 129.6, 135.1, 148.6, 151.8, 166.4; elemental analysis calcd for $[\text{C}_6\text{H}_6\text{N}_2\text{O}]$: C, 59.01; H, 4.95; N, 22.94, found: C, 59.00; H, 4.91; N, 22.70.



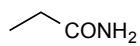
2-Francarbamide (2o).²⁴ White powder, purified by column chromatography on silica gel (dichloromethane/acetone 1:4) and recrystallization (from water); mp 139.6–140.9 °C (lit.²⁴ 141–142 °C);

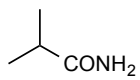
IR (KBr) 1626, 1665, 3171, 3351 cm^{-1} ; ^1H NMR (600 MHz, CDCl_3) δ 5.53 (bs, 1H), 6.26 (bs, 1H), 6.52–6.53 (m, 1H), 7.16–7.18 (m, 1H), 7.46–7.49 (m, 1H); $^{13}\text{C}\{^1\text{H}\}$ NMR (125MHz, CDCl_3) δ 112.5, 115.3, 144.6, 147.6, 160.4; elemental analysis calcd for $[\text{C}_5\text{H}_5\text{NO}_2]$: C, 54.05; H, 4.54; N, 12.61, found: C, 53.73; H, 4.55; N, 12.49.

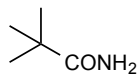


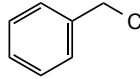
Acetamide (2p).²⁵ White powder, purified by recrystallization (from dichloromethane/*n*-hexane); mp 79.2–80.1 °C; IR (KBr) 1665, 3212,

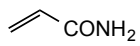
3389 cm^{-1} ; ^1H NMR (600 MHz, D_2O) δ 2.00 (s, 3H); $^{13}\text{C}\{^1\text{H}\}$ NMR (125 MHz, D_2O) δ 21.9, 178.0; elemental analysis calcd for $[\text{C}_2\text{H}_5\text{NO}\cdot 0.001\text{H}_2\text{O}]$: C, 40.66; H, 8.53; N, 23.71, found: C, 40.26; H, 8.54; N, 23.53.

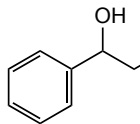
 **Propionamide (2q).**²⁶ Colorless plates, purified by recrystallization (from dichloromethane/*n*-hexane); mp 79.1–80.5 °C; IR (KBr) 1664, 3202, 3370 cm^{-1} ; ^1H NMR (600 MHz, CDCl_3) δ 1.18 (t, $J = 7.6$ Hz, 3H), 2.27 (q, $J = 7.6$ Hz, 2H), 5.04–5.58 (m, 2H); $^{13}\text{C}\{^1\text{H}\}$ NMR (150 MHz, CDCl_3) δ 9.8, 29.1, 176.3; elemental analysis calcd for $[\text{C}_3\text{H}_7\text{NO}\cdot 0.02\text{H}_2\text{O}]$: C, 49.05; H, 9.66; N, 19.07, found: C, 48.70; H, 9.56; N, 18.82.

 **2-Methylpropanamide (2r).**²⁷ White powder, purified by recrystallization (from dichloromethane/*n*-hexane); mp 124.7–127.3 °C; IR (KBr) 1641, 3179, 3355 cm^{-1} ; ^1H NMR (500 MHz, CDCl_3) δ 1.19 (d, $J = 6.9$ Hz, 6H), 2.43 (sept, $J = 6.9$ Hz, 1H), 5.10–5.75 (m, 2H); $^{13}\text{C}\{^1\text{H}\}$ NMR (125 MHz, CDCl_3) δ 19.7, 35.2, 179.8; elemental analysis calcd for $[\text{C}_4\text{H}_9\text{NO}]$: C, 55.15; H, 10.41; N, 16.08, found: C, 54.95; H, 10.45; N, 15.89.

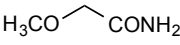
 **Pivalamide (2s).**²⁸ Colorless needles, purified by recrystallization (from dichloromethane/*n*-hexane); mp 148.7–152.0 °C; IR (KBr) 1627, 1656, 3204, 3398 cm^{-1} ; ^1H NMR (600 MHz, CDCl_3) δ 1.23 (s, 9H), 5.21 (bs, 1H), 5.59 (bs, 1H); $^{13}\text{C}\{^1\text{H}\}$ NMR (150 MHz, CDCl_3) δ 27.8, 38.8, 181.5; elemental analysis calcd for $[\text{C}_5\text{H}_{11}\text{NO}\cdot 0.08\text{H}_2\text{O}]$: C, 58.54; H, 10.97; N, 13.65, found: C, 58.29; H, 10.85; N, 13.36.

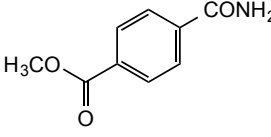
 **2-Phenylacetamide (2t).**²⁹ White powder, purified by washing with *n*-hexane; mp 157.9–158.5 °C (lit.²⁹ 155 °C); IR (KBr) 1637, 3178, 3355 cm^{-1} ; ^1H NMR (600 MHz, CDCl_3) δ 3.60 (s, 2H), 5.13–5.64 (m, 2H), 7.28–7.38 (m, 5H); $^{13}\text{C}\{^1\text{H}\}$ NMR (150 MHz, CDCl_3) δ 43.5, 127.6, 129.2, 129.6, 135.0, 173.7; elemental analysis calcd for $[\text{C}_8\text{H}_9\text{NO}]$: C, 71.09; H, 6.71; N, 10.36, found: C, 71.07; H, 6.76; N, 10.28.

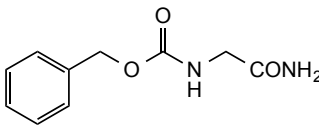
 **Acrylamide (2u).**³⁰ Colorless plates, purified by recrystallization (from dichloromethane/*n*-hexane); mp 78.2–80.3 °C; IR (KBr) 1613, 1675, 3193, 3357 cm^{-1} ; ^1H NMR (600 MHz, D_2O) δ 5.83 (d, $J = 10.3$ Hz, 1H), 6.22–6.33 (m, 2H); $^{13}\text{C}\{^1\text{H}\}$ NMR (125 MHz, D_2O) δ 129.1, 130.1, 171.6; elemental analysis calcd for $[\text{C}_3\text{H}_5\text{NO}\cdot 0.07\text{H}_2\text{O}]$: C, 49.81; H, 7.16; N, 19.36, found: C, 49.52; H, 7.02; N, 18.99.

 **3-Hydroxy-3-phenylpropanamide (2v).**³¹ Colorless needles, purified by column chromatography on silica gel (*n*-hexane/ethyl acetate 1:6–0:7, gradient); mp 121.0–121.7 °C; IR (KBr) 1624, 1658, 3194, 3386 cm^{-1} ; ^1H NMR (600 MHz, CD_3OD) δ 2.52 (dd, $J = 4.8, 14.4$ Hz, 1H),

2.63 (dd, $J = 8.9, 14.5$ Hz, 1H), 5.05 (dd, $J = 4.8, 8.9$ Hz, 1H), 7.22–7.39 (m, 5H); $^{13}\text{C}\{^1\text{H}\}$ NMR (125 MHz, CD_3OD) δ 46.1, 71.9, 126.9, 128.5, 129.4, 145.4, 176.4; elemental analysis calcd for $[\text{C}_9\text{H}_{11}\text{NO}_2]$: C, 65.44; H, 6.71; N, 8.48, found: C, 65.41; H, 6.71; N, 8.45.

 **α -Methoxyacetamide (2w).**³² Colorless needles, purified by short-column chromatography on silica gel (dichloromethane only); mp 96.2–96.9 °C; IR (KBr) 1638, 3198, 3384 cm^{-1} ; ^1H NMR (500 MHz, D_2O) δ 3.45 (s, 3H), 4.02 (s, 2H); $^{13}\text{C}\{^1\text{H}\}$ NMR (125 MHz, D_2O) δ 59.6, 71.1, 176.4; elemental analysis calcd for $[\text{C}_3\text{H}_7\text{NO}_2]$: C, 40.44; H, 7.92; N, 15.72, found: C, 40.28; H, 8.02; N, 15.78.

 **p -(Methoxycarbonyl)benzamide (2x).**³³ Off-white plates, purified by column chromatography on silica gel (*n*-hexane/ethyl acetate 1:4); mp 205.0–206.6 °C (lit.³³ 200–201 °C); IR (KBr) 1281, 1660, 1725, 3195, 3406 cm^{-1} ; ^1H NMR (600 MHz, $\text{DMSO-}d_6$) δ 3.87 (s, 3H), 7.57 (bs, 1H), 7.96–8.04 (m, 4H), 8.15 (bs, 1H); $^{13}\text{C}\{^1\text{H}\}$ NMR (150 MHz, $\text{DMSO-}d_6$) δ 52.3, 127.8, 129.1, 131.8, 138.4, 165.7, 167.0; elemental analysis calcd for $[\text{C}_9\text{H}_9\text{NO}_3]$: C, 60.33; H, 5.06; N, 7.82, found: C, 60.32; H, 5.14; N, 7.72.

 **α -(Benzyloxycarbonylamino)acetamide (2y).**³⁴ White needles, purified by column chromatography on silica gel (chloroform/methanol 95:5–92:8, gradient); mp 135.0–136.6 °C (lit.³⁴ 138–139 °C); IR (KBr) 1537, 1652, 1688, 3191, 3324, 3381 cm^{-1} ; ^1H NMR (600 MHz, $\text{DMSO-}d_6$) δ 3.55 (d, $J = 6.2$ Hz, 2H), 5.03 (s, 2H), 7.01 (s, 1H), 7.26–7.40 (m, 7H); $^{13}\text{C}\{^1\text{H}\}$ NMR (150 MHz, $\text{DMSO-}d_6$) δ 43.3, 65.4, 127.7, 127.8, 128.3, 137.1, 156.4, 171.1; HRMS (ESI-TOF) m/z calcd for $\text{C}_{10}\text{H}_{12}\text{N}_2\text{O}_3\text{Na}$ $[\text{M} + \text{Na}]^+$ 231.0746, found 231.0757.

Gram-scale hydration

To a 30 mL test tube with a screw cap, a magnetic stirring bar and catalyst precursor (657 mg, 1.2 wt % Ru), deaerated H_2O (13 mL) was added under a N_2 atmosphere. Under vigorous stirring, a solution [4.9 mL; a mixture of NaBH_4 (82.1 mg, 2.2 mmol) and deaerated H_2O (10.9 mL)] was introduced dropwise to the test tube. The mixture was stirred at rt for 3.5 h. The liquid phase was separated by centrifugation (3500 rpm, 5 min) and replaced with H_2O (13 mL) via syringe. After the mixture was stirred at rt

overnight, the solid was washed with water (2 times) and dried *in vacuo* at rt for 2 h to afford Ru/chitin as a grey solid. To this Ru/chitin in the test tube were added **1w** (16.3 mmol, 1.16 g) and deaerated H₂O (7.2×10^2 mmol, 13 mL) under a N₂ atmosphere. After this the septum inlet was replaced with plastic screw cap and the cap was wrapped with Teflon tape. The mixture was then shaken at 120 °C for 36 h (*ca.* 100 rpm). After cooling with ice water, the catalyst was removed by filtration and washed with methanol (300 mL). The solvent was concentrated *in vacuo*. The product was purified by short-column chromatography on silica gel (ethyl acetate only) to afford **2w** as colorless needles (1.34 g, 92% yield).

Reuse experiment

As per the typical procedure, Ru/chitin (0.023 mmol Ru) was prepared in a screw-cap 10 mL test tube equipped with a rubber septum and a magnetic stirring bar. To this tube was added nitrile **1a** (1.01 mmol, 104.1 mg) and deaerated H₂O (2.2×10^2 mmol, 4.0 mL) under a N₂ atmosphere. After this septum inlet was replaced with a plastic screw cap and the cap was wrapped with Teflon tape. The mixture was shaken at 120 °C for 20 h (*ca.* 100 rpm). The mixture was cooled down with ice water, mixed with deaerated H₂O (4 mL) under a N₂ atmosphere, and stirred at 100 °C for 1 min. The liquid phase was separated by centrifugation (3500 rpm, 3 min). Extraction of the product was carried out by repeating this process (deaerated H₂O, 7×4 mL). The combined liquid phases were concentrated *in vacuo*. ¹H NMR analysis of this crude mixture using mesitylene as an internal standard indicated the formation of **2a** in 95% yield. Ru/chitin in the test tube was directly reused for the next run [conditions: **1a** (1.04 mmol, 107.2 mg), deaerated H₂O (2.2×10^2 mmol, 4.0 mL) and the reused catalyst at 120 °C for 20 h under a N₂ atmosphere]. ¹H NMR analysis of this crude mixture showed the formation of **2a** in 87% yield. Crude yields of **2a** in 3rd and 4th runs were 87% and 71%, respectively.

3.6. Notes and references

- 1 a) C. E. Mabermann, in *Encyclopedia of Chemical Technology*, ed. J. I. Kroschwitz, Wiley, New York, 1991, vol. 1, pp. 251–266. b) D. Lipp, in *Encyclopedia of Chemical Technology*, ed. J. I. Kroschwitz, Wiley, New York, 1991, Vol. 1, pp. 266–287. c) R. Opsahl, in *Encyclopedia of Chemical Technology*, ed. J. I. Kroschwitz, Wiley, New York, 1991, Vol. 2, pp. 346–356.
- 2 a) C. L. Allen and J. M. J. Williams, *Chem. Soc. Rev.*, 2011, **40**, 3405–3415. b) C. Singh, V. Kumar, U. Sharma, N. Kumar and B. Singh, *Curr. Org. Synth.*, 2013, **10**, 241–264.
- 3 a) V. Y. Kukushkin and A. J. L. Pombeiro, *Inorg. Chim. Acta*, 2005, **358**, 1–21. b) T. J. Ahmed, S. M. M. Knapp and D. R. Tyler, *Coord. Chem. Rev.*, 2011, **255**, 949–974. c) T. Tu, Z. Wang, Z. Liu, X. Feng and Q. Wang, *Green Chem.*, 2012, **14**, 921–924. d) R. García-Álvarez, P. Crochet and V. Cadierno, *Green Chem.*, 2013, **15**, 46–66. e) E. L. Downs and D. R. Tyler, *Coord. Chem. Rev.*, 2014, **280**, 28–37.
- 4 K. Yamaguchi, M. Matsushita and N. Mizuno, *Angew. Chem. Int. Ed.*, 2004, **43**, 1576–1580.
- 5 a) V. Polshettiwar and R. S. Varma, *Chem. Eur. J.*, 2009, **15**, 1582–1586. b) R. B. N. Baig and R. S. Varma, *Chem. Commun.*, 2012, **48**, 6220–6222. c) R. B. N. Baig, M. N. Nadagouda and R. S. Varma, *Green Chem.*, 2014, **16**, 2122–2127.
- 6 S. Kumar and P. Das, *New J. Chem.*, 2013, **37**, 2987–2990.
- 7 G. K. S. Prakash, S. B. Munoz, A. Papp, K. Masood, I. Bychinskaya, T. Mathew and G. A. Olah, *Asian J. Org. Chem.*, 2012, **1**, 146–149
- 8 Recent examples based on other metals: a) A. Ishizuka, Y. Nakazaki and T. Oshiki, *Chem. Lett.*, 2009, **38**, 360–361. b) T. Mitsudome, Y. Mikami, H. Mori, S. Arita, T. Mizugaki, K. Jitsukawa and K. Kaneda, *Chem. Commun.*, 2009, 3258–3260. c) S. Ichikawa, S. Miyazoe and O. Matsuoka, *Chem. Lett.*, 2011, **40**, 512–514. d) M. Tamura, H. Wakasugi, K.-i. Shimizu and A. Satsuma, *Chem. Eur. J.*, 2011, **17**, 11428–11431. e) A. Y. Kim, H. S. Bae, S. Park, S. Park and K. H. Park, *Catal. Lett.*, 2011, **141**, 685–690. f) Y.-M. Liu, L. He, M.-M. Wang, Y. Cao, H.-Y. He and K.-N. Fan, *ChemSusChem*, 2012, **5**, 1392–1396. g) Y. Gangarajula and B. Gopal, *Chem. Lett.*, 2012, **41**, 101–103. h) K. Yamaguchi,

- Y. Wang, H. Kobayashi and N. Mizuno, *Chem. Lett.*, 2012, **41**, 574–576. i) K.-i. Shimizu, T. Kubo, A. Satsuma, T. Kamachi and K. Yoshizawa, *ACS Catal.*, 2012, **2**, 2467–2474. j) T. Hirano, K. Uehara, K. Kamata and N. Mizuno, *J. Am. Chem. Soc.*, 2012, **134**, 6425–6433. k) M. B. Gawande, P. S. Branco, I. D. Nogueira, C. A. A. Ghumman, N. Bundaleski, A. Santos, O. M. N. D. Teodoro and R. Luque, *Green Chem.*, 2013, **15**, 682–689. l) C. Battilocchio, J. M. Hawkins and S. V. Ley, *Org. Lett.*, 2014, **16**, 1060–1063.
- 9 a) N. A. Afagh and A. K. Yudin, *Angew. Chem. Int. Ed.*, 2010, **49**, 262–310. b) J. Mahatthananchai, A. M. Dumas and J. W. Bode, *Angew. Chem. Int. Ed.*, 2012, **51**, 10954–10990.
- 10 a) *Chitin: Formation and Diagenesis*, ed. N. S. Gupta, Springer, New York, 2011. b) V. S. Yeul and S. S. Rayalu, *J. Polym. Environ.*, 2013, **21**, 606–614.
- 11 a) M. N. V. R. Kumar, *React. Funct. Polym.*, 2000, **46**, 1–27. b) M. Rinaudo, *Prog. Polym. Sci.*, 2006, **31**, 603–632.
- 12 B. Krajewska, *Enzyme Microbial Technol.*, 2004, **35**, 126–139.
- 13 a) E. Guibal, *Prog. Polym. Sci.*, 2005, **30**, 71–109. b) D. J. Macquarrie and J. J. E. Hardy, *Ind. Eng. Chem. Res.*, 2005, **44**, 8499–8520.
- 14 a) F. Quignard, A. Choplin and A. Domard, *Langmuir*, 2000, **16**, 9106–9108. b) V. Calò, A. Nacci, A. Monopoli, A. Fornaro, L. Sabbatini, N. Cioffi and N. Ditaranto, *Organometallics*, 2004, **23**, 5154–5158. c) A. Corma, P. Concepción, I. Domínguez, V. Fornés and M. J. Sabater, *J. Catal.*, 2007, **251**, 39–47. d) A. D. Giuseppe, M. Crucianelli, M. Passacantando, S. Nisi and R. Saladino, *J. Catal.*, 2010, **276**, 412–422. e) A. Ricci, L. Bernardi, C. Gioia, S. Vierucci, M. Robitzer and F. Quignard, *Chem. Commun.*, 2010, **46**, 6288–6290. f) A. C. Kathalikkattil, J. Tharun, R. Roshan, H.-G. Soek and D.-W. Park, *Appl. Catal. A: General*, 2012, **447–448**, 107–114.
- 15 G.-L. Yuan, M.-Y. Yin, T.-T. Jiang, M.-Y. Huang and Y.-Y. Jiang, *J. Mol. Catal. A: Chemical*, 2000, **159**, 45–50.
- 16 a) Y. Ito and M. Inoue, *Kagaku to Kyoiku*, 2010, **58**, 486–489. b) D. Abiru and M. Inoue, *Kagaku to Kyoiku*, 2014, **62**, 36–39.
- 17 a) B. J. Arena, US Patent 4274980, 1981. b) B. J. Arena, US Patent 4367355, 1983. c) R. A. A. Muzzarelli, *Water Res.*, 1970, **4**, 451–455.
- 18 M. Zahmakıran and S. Özkar, *J. Mol. Catal. A: Chem.*, 2006, **258**, 95–103.

- 19 Q. Song, Q. Feng and K. Yang, *Org. Lett.*, 2014, **16**, 624–627
- 20 J. Lee, M. Kim, S. Chang and H.-Y. Lee, *Org. Lett.*, 2009, **11**, 5598–5601.
- 21 D. R. Brown, I. Collins, L. G. Czaplowski and D. J. Hayden, WO Patent 2007/107758, 2007.
- 22 X.-b. Jiang, A. J. Minnaard, B. L. Feringa and J. G. de Vries, *J. Org. Chem.*, 2004, **69**, 2327–2331.
- 23 SDBSWeb: <http://sdb.sdb.aist.go.jp/> (National Institute of Advanced Industrial Science and Technology, accessed August 2014) SDBS No. 553.
- 24 L. Zhang, S. Wang, S. Zhou, G. Yang and E. Sheng, *J. Org. Chem.*, 2006, **71**, 3149–3153.
- 25 SDBSWeb: <http://sdb.sdb.aist.go.jp/> (National Institute of Advanced Industrial Science and Technology, accessed August 2014) SDBS No. 1491.
- 26 SDBSWeb: <http://sdb.sdb.aist.go.jp/> (National Institute of Advanced Industrial Science and Technology, accessed August 2014) SDBS No. 1431.
- 27 K. Y. Koltunov, S. Walspurger and J. Sommer, *Eur. J. Org. Chem.*, 2004, 4039–4047.
- 28 SDBSWeb: <http://sdb.sdb.aist.go.jp/> (National Institute of Advanced Industrial Science and Technology, accessed August 2014) SDBS No. 4737.
- 29 S. S. Deshmukh, S. N. Huddar, D. S. Bhalerao and K. G. Akamanchi, *ARKIVOC*, 2010, **2**, 118–126.
- 30 SDBSWeb: <http://sdb.sdb.aist.go.jp/> (National Institute of Advanced Industrial Science and Technology, accessed August 2014) SDBS No. 1461.
- 31 A. Kamal, G. B. R. Khanna, T. Krishnaji and R. Ramu, *Bioorg. Med. Chem. Lett.*, 2005, **15**, 613–615.
- 32 K. L. Breno, M. D. Pluth and D. R. Tyler, *Organometallics*, 2003, **22**, 1203–1211.
- 33 B. F. Plummer, M. Menendez and M. Songster, *J. Org. Chem.*, 1989, **54**, 718–719.
- 34 S.-T. Chen, S.-H. Wu and K.-T. Wang, *Synthesis*, 1989, 37–38.
- 35 P. Chen, L. B. Horton, R. L. Mikulski, L. Deng, S. Sundriyal, T. Palzkill and Y. Song, *Bioorg. Med. Lett.*, 2012, **22**, 6229–6232.

Chapter 4.

Aldehydes and Molecular Hydrogen

via the Visible-light-promoted

Dehydrogenation of Alcohols by Ru/SrTiO₃:Rh

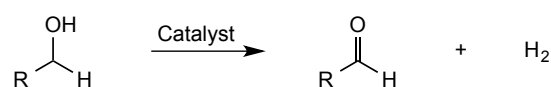
4.1 Abstract

The discovery, scope, and study of the Ru/SrTiO₃:Rh-promoted photocatalytic dehydrogenation of alcohols to aldehydes are reported. This reaction proceeds in a mixture of aqueous phosphoric acid and toluene at ambient temperature under visible light irradiation, yielding aldehydes and molecular hydrogen (H₂). The dehydrogenation is compatible with the presence of redox-sensitive functional groups such as allylic and non-allylic olefins, alkyne, ketone, amide and carbamate. A reproducible solid-phase synthesis of SrTiO₃:Rh is established by means of scanning electron microscopy (SEM) and X-ray diffraction (XRD) analysis.

4.2 Introduction

Catalytic dehydrogenation of primary alcohols is one of the most effective methods for preparing aldehydes and hydrogen (H₂, Scheme 4.1).¹ This reaction is distinct from oxidation of alcohols using stoichiometric amount of oxidants (Scheme 4.2),² because the dehydrogenation of alcohols does not require any external oxidants. Accordingly, the dehydrogenation of alcohols yields both aldehydes and H₂ in a highly atom-economical manner without being affected by the contamination of byproducts. Whereas catalysts for dehydrogenation of secondary alcohols to ketones have been intensively developed to date,³ selective dehydrogenation of primary alcohols to aldehydes has been considered elusive presumably due to the instability of aldehydes

under the reaction conditions.⁴ For example, primary alcohols (RCH₂OH) are converted to carboxylic esters (RCOOCH₂R) when heated with typical catalysts used for dehydrogenation of secondary alcohols such as ruthenium complexes,⁵ iridium complexes⁶ and supported copper⁷ catalysts. Carboxylic acids (RCOOH)^{7a} and acetals [RCH(OR)₂]⁸ could also form under aqueous and acidic conditions, respectively. Only very recently, some homogeneous Ru^{4b} and Ir^{3a,4a,d} catalysts as well as hydrotalcite-supported Au catalysts⁹ have been found to promote dehydrogenation of primary alcohols to aldehydes under thermal conditions (70–130 °C). However, the tolerance of redox-sensitive functional groups, typically, unsaturated carbon–carbon bonds, remains unclear and seems considered not straightforward. Conjugated and non-conjugated olefins are reduced by the co-produced H₂ under typical dehydrogenation conditions.^{4a,c,d} This issue of chemoselectivity seems to underlie all dehydrogenation catalysis and has limited the use of acceptorless dehydrogenation in the synthesis of carbonyl compounds bearing such redox-sensitive functional groups.



Scheme 4.1. Dehydrogenation of primary alcohols to aldehydes and hydrogen.



Scheme 4.2. Oxidation of primary alcohols to aldehydes using stoichiometric oxidant.

Development of selective dehydrogenation catalysis has been partially hampered by the unfavorable thermodynamics of this transformation. Since alcohol-dehydrogenation is endergonic ($\Delta G > 0$) and endothermic ($\Delta H > 0$) in most cases, these methods require thermal energy input and/or removal of H₂ gas from the reaction system to shift the equilibrium to the right. For instance, conversion of

methanol (*l*) to hydrogen (*g*) and formaldehyde (*g*) is endergonic ($\Delta G^\circ = + 63.7 \text{ kJ mol}^{-1}$) and endothermic ($\Delta H^\circ = + 130.1 \text{ kJ mol}^{-1}$).

Such unfavorable thermodynamics could be potentially overcome by photocatalytic dehydrogenation of alcohols using sunlight energy.¹⁰ Use of visible light for this reaction is advantageous compared with UV light because the former not only leaves many functional groups intact but also covers more than 50% of the solar energy. Numerous methods for visible-light-promoted oxidation of alcohols have been developed using oxidant.¹¹ However, allylic alcohols are decomposed into smaller carbon pieces, such as acetone or CO₂.^{11j} In addition, oxidation of alcohols using oxidants to carbonyls is thermodynamically downward (down-hill process). Conversion of methanol (*l*) and dioxygen (*g*) to water (*l*) and formaldehyde (*g*) is exergonic ($\Delta G^\circ = -173.4 \text{ kJ mol}^{-1}$) and exothermic ($\Delta H^\circ = -155.7 \text{ kJ mol}^{-1}$).^{10a}

Recently, effective photocatalytic dehydrogenation of aromatic alcohols to aldehydes under visible light irradiation has been achieved using heterogeneous photocatalysts. Pt/TiO₂ nanofilm catalyzes oxidation of aromatic alcohols to aldehydes and hydrogen in water through reduction of protons.¹² CdS promotes dehydrogenation of benzyl alcohols to aldehydes but also gives homo-coupling products.¹³ Modified CdS promotes both dehydrogenation and hydrogenolysis of benzyl alcohol at the same time.¹⁴ Au–Pd/ZrO₂ enhances dehydrogenation of aromatic alcohols and gives corresponding aldehydes in high selectivity.¹⁵ However, the redox- and chemoselectivity, substrate scope and scalability in these systems have yet to be fully explored.

More recently, Ru/SrTiO₃:Rh has been identified as an excellent photocatalyst for dehydrogenation of primary alcohols to aldehydes under visible light irradiation.¹⁶ The author here reports a full account of this study, including preparation and characterization of Ru/SrTiO₃:Rh, effect of reaction conditions on the catalytic activity of Ru/SrTiO₃:Rh, expanded substrate scope and proposed reaction mechanism. Ru/SrTiO₃:Rh is a visible-light responsible photocatalyst developed by Kudo for hydrogen evolution in the Z-scheme type water splitting.^{17,18} The conduction band level of SrTiO₃:Rh is 0.2 eV, which is higher than the redox potential for H₂ evolution in the aqueous and/or alcoholic media.^{17b}

4.3 Results and discussion

Preparation of Ru/SrTiO₃:Rh

Typically, SrTiO₃:Rh (1 mol % Rh) can be prepared by mixing dry SrCO₃, TiO₂ and Rh₂O₃ in a solid phase, followed by calcination under air at 900 °C for 1 h and at 1000 °C for 10 h. However, because of the technical difficulties in the solid phase synthesis of SrTiO₃:Rh, a reproducible protocol for preparing SrTiO₃:Rh has remained to be developed. To address this issue, the author developed a reliable synthetic method of SrTiO₃:Rh in high purity by controlling the heating rate in calcination and clarified a critical factor in the solid phase synthesis of SrTiO₃:Rh. A series of SrTiO₃:Rh was prepared based on the above-mentioned typical procedure at a different heating rate between 900–1000 °C (0.5, 1.0, 2.0, 4.0, 5.3 and 16 °C min⁻¹). The X-ray diffraction (XRD) analysis of the products indicated that pure SrTiO₃:Rh could be synthesized when calcination was conducted at a slow heating rate (< 4 °C min⁻¹, Figure 4.1a–d). In contrast, impurities such as Sr₄Ti₃O₁₀ and/or Sr₂TiO₄ was present when the calcination was carried out at a faster heating rate (5.3 or 16 °C min⁻¹, Figure 4.1e and f). This result is consistent with that of the scanning electron microscopy (SEM) analysis of these SrTiO₃:Rh samples (Figure 4.2). The SEM image of SrTiO₃:Rh prepared at a slow reaction rate (0.5–4.0 °C min⁻¹) indicates the presence of blocks of SrTiO₃:Rh with a size of 100–300 nm (Figure 4.2a–d), while samples prepared at 5.3 or 16 °C min⁻¹ consist of fused clusters of these blocks with round edges (Figure 4.2e and f).

To shed light on the origin of these differences, the author monitored the calcination process by thermogravimetric analysis (TGA) of a gridded mixture of SrCO₃, TiO₂ and Rh₂O₃ under the typical reaction conditions (Figure 4.3). The weight loss started from around 870 °C, and an immediate, significant weight loss occurred at 900 °C (up to *ca.* 15% decrease). The decreased amount of weight (15%) broadly agrees with the approximate weight of CO₂ from SrCO₃ (theoretical value: 19%). No further decrease was observed between 900 °C and 1000 °C. These results suggest that (1) the decarboxylation from a mixture of SrCO₃, TiO₂ and Rh₂O₃ occurs over 890 °C and completes at around 900 °C and that (2) the purity of Ru/SrTiO₃:Rh was affected by the process after decarboxylation from SrCO₃.

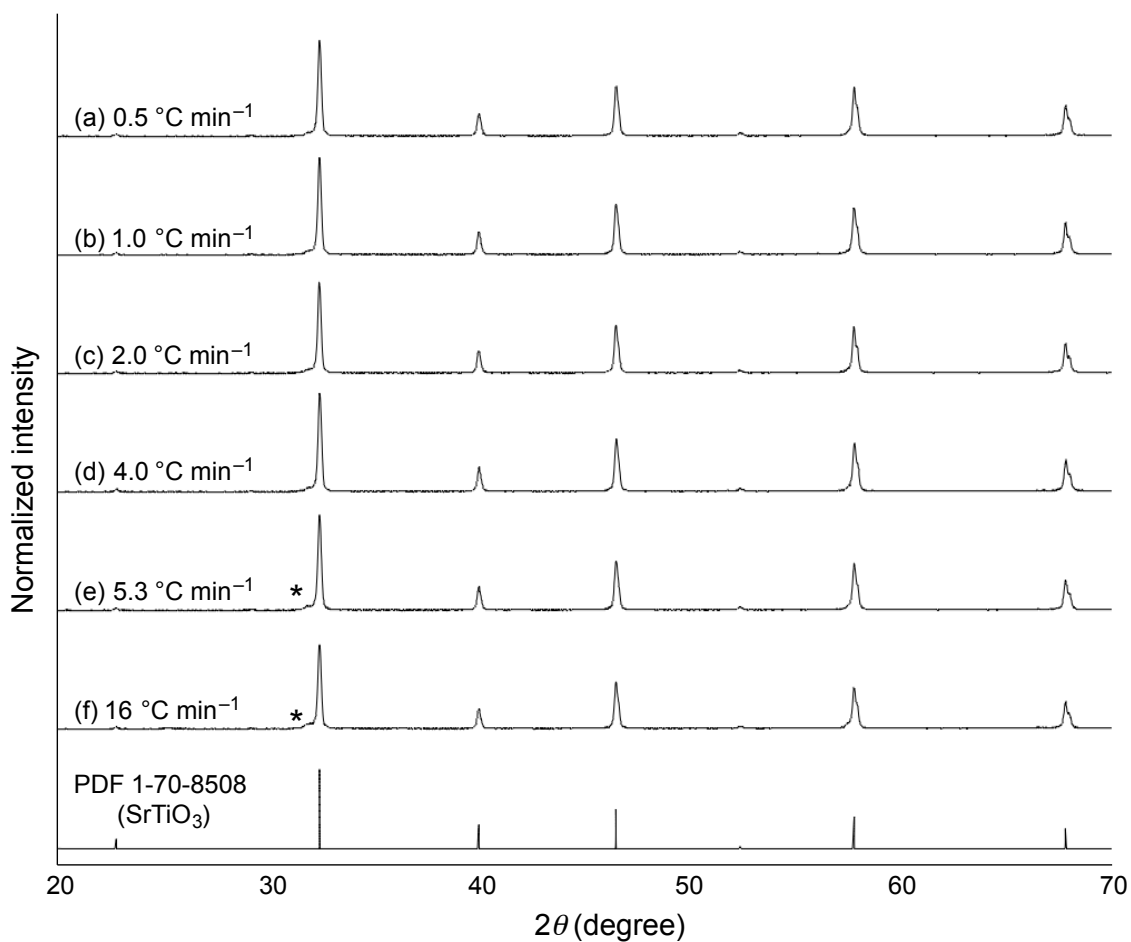
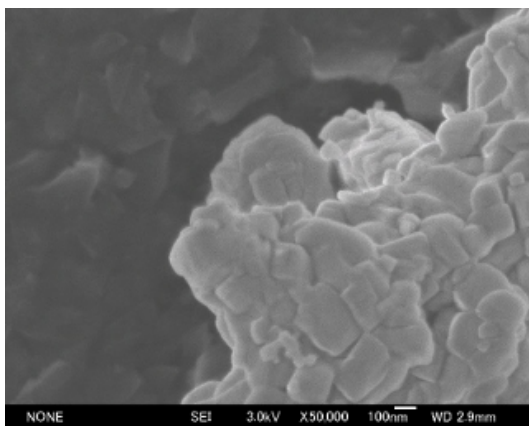
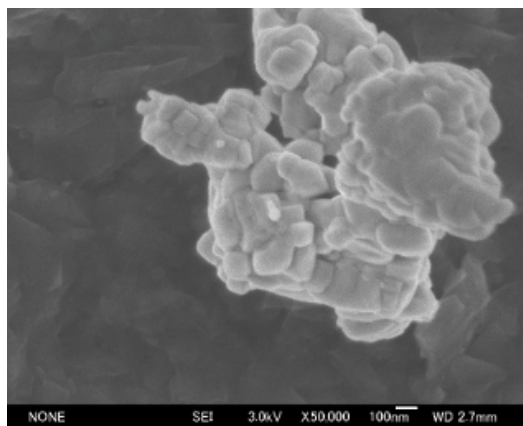


Figure 4.1. X-ray diffraction patterns of SrTiO₃:Rh prepared by calcination at (a) 0.5 °C min⁻¹, (b) 1.0 °C min⁻¹, (c) 2.0 °C min⁻¹, (d) 4.0 °C min⁻¹, (e) 5.3 °C min⁻¹, (f) 16 °C min⁻¹ between 900–1000 °C. Asterisk indicates an impurity phase of Sr₂TiO₄ and/or Sr₄Ti₃O₁₀.

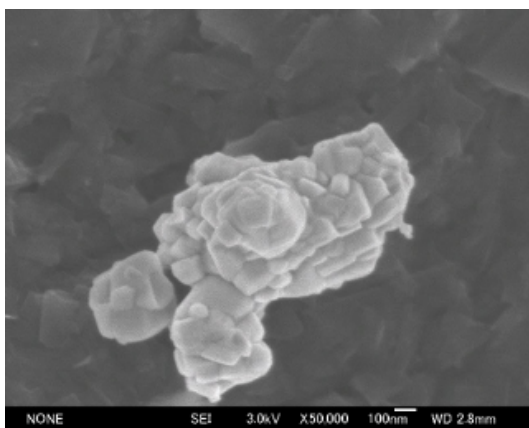
(a) 0.5 °C min⁻¹



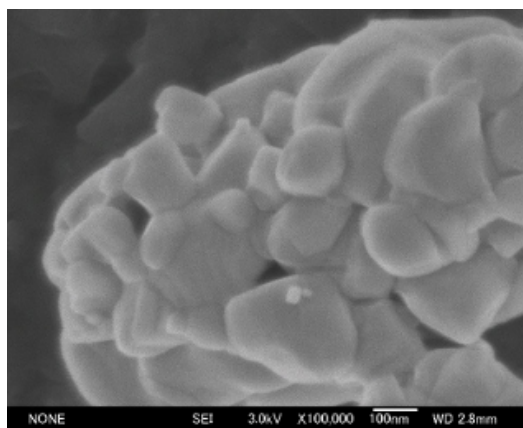
(b) 1.0 °C min⁻¹



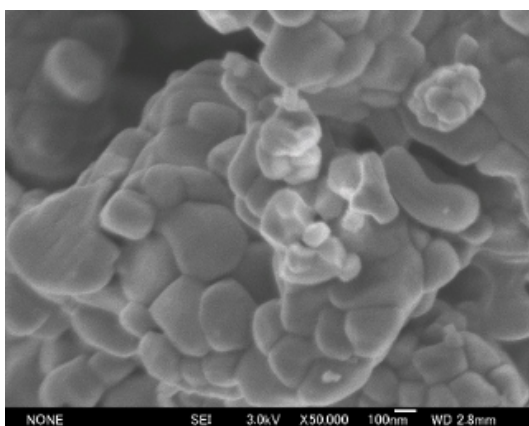
(c) 2.0 °C min⁻¹



(d) 4.0 °C min⁻¹



(e) 5.3 °C min⁻¹



(f) 16 °C min⁻¹

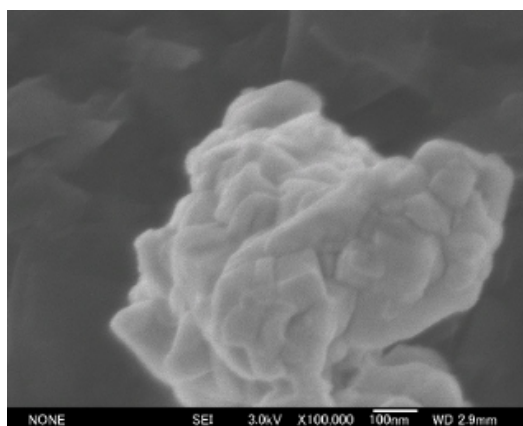


Figure 4.2. SEM images of SrTiO₃:Rh prepared by calcination at (a) 0.5 °C min⁻¹, (b) 1.0 °C min⁻¹, (c) 2.0 °C min⁻¹, (d) 4.0 °C min⁻¹, (e) 5.3 °C min⁻¹, (f) 16 °C min⁻¹ between 900–1000 °C.

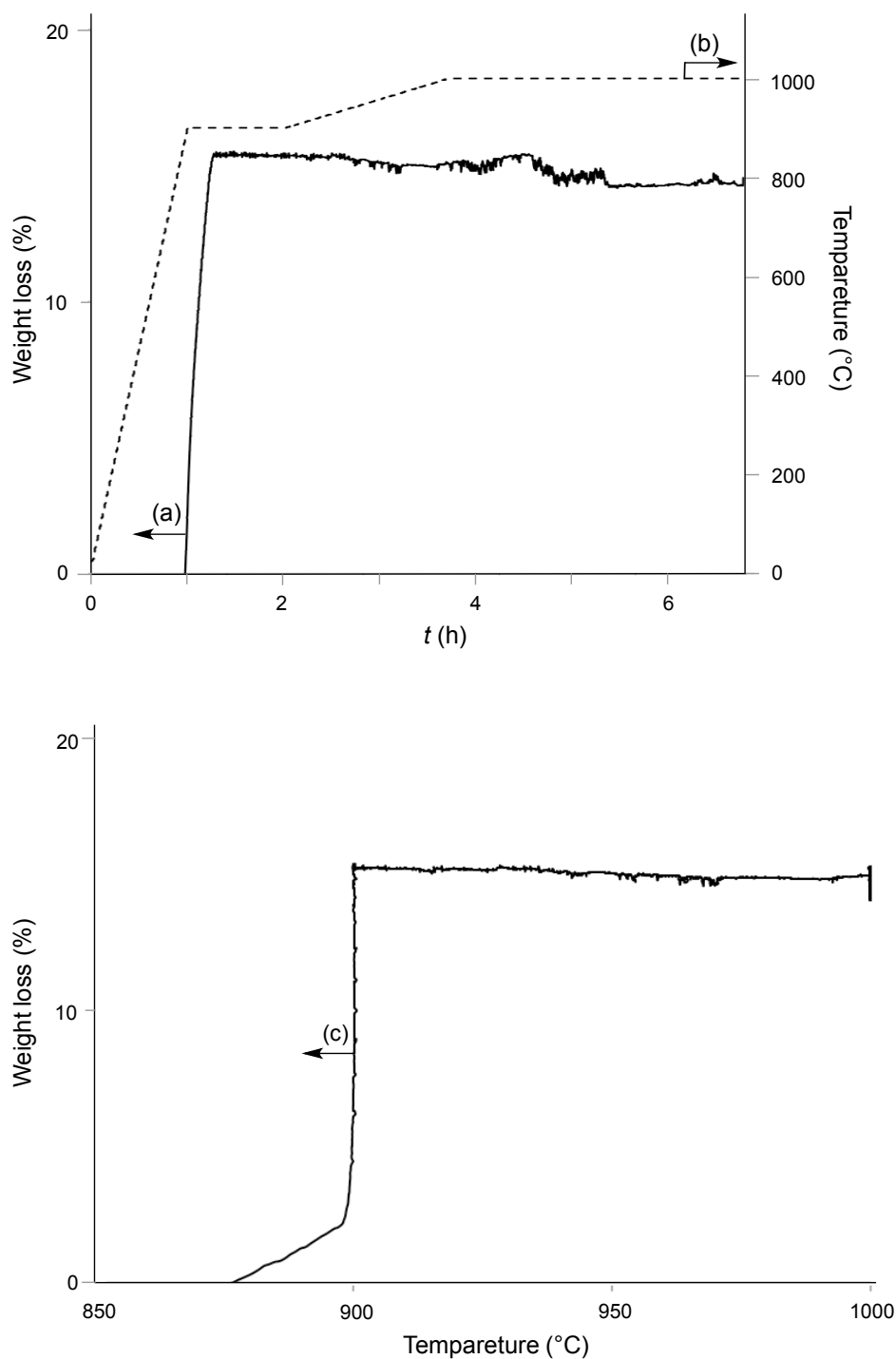


Figure 4.3. Weight loss of the mixture of SrCO₃, TiO₂ and Rh₂O₃ over a temperature range of 25 °C–1000 °C. (a) Weight loss as a function of time (b) Set temperatures during heating. Sample was heated from 25 °C to 900 °C at 14.6 °C min⁻¹ and held at 900 °C for 60 min, then heated from 900 °C to 1000 °C at 1 °C min⁻¹. (c) Weight loss of the sample as a function of temperature.

Liquid-phase reductive deposition of Ru on SrTiO₃:Rh using 2-butanol and aqueous methanol solution of RuCl₃·3H₂O provides Ru (0.7 wt %)/SrTiO₃:Rh. The SEM image of Ru/SrTiO₃:Rh shows Ru nanoparticles (10–30 nm) on the surface of SrTiO₃:Rh (*ca.* 100–300 nm, Figure 4.4). The morphology of SrTiO₃:Rh did not change during the reductive deposition of Ru.

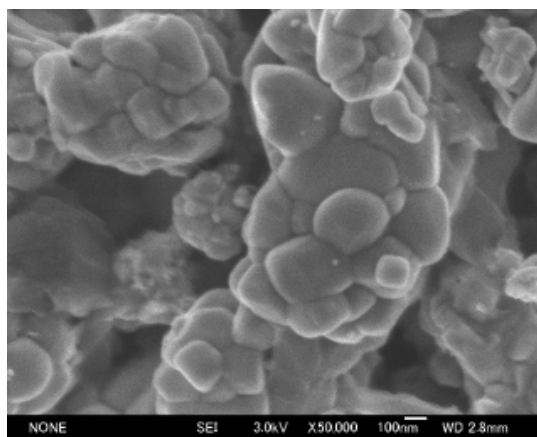
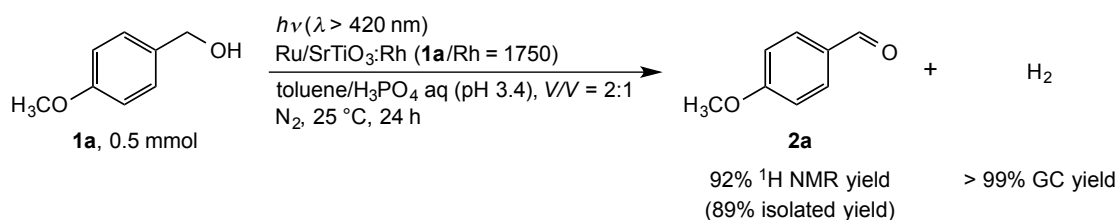


Figure 4.4. A SEM image of Ru/SrTiO₃:Rh prepared from SrTiO₃:Rh shown Figure 4.2(a).

Discovery of Ru/SrTiO₃:Rh-catalyzed dehydrogenation of alcohols to aldehydes

Visible-light responsible photocatalysts for the dehydrogenation of alcohols was screened using 4-methoxybenzyl alcohol (**1a**) as a model substrate because both **1a** and the desired aldehyde **2a** can be easily analyzed. Ru/SrTiO₃:Rh was found to be an effective photocatalyst for this purpose (Scheme 4.3). When a mixture of **1a** (0.5 mmol), toluene/H₃PO₄ aq (pH 3.4, 15 mL, *V/V* = 2:1) and Ru/SrTiO₃:Rh (**1a**/Rh = 1750, **1a**/Ru = 1362) was stirred at 25 °C for 24 h under visible light irradiation (> 420 nm), the corresponding aldehyde **2a** was obtained in 92% ¹H NMR yield (89% isolated yield). The yield of H₂ with respect to the initial amount of **1a** reached over 99%, as determined by a thermal conductivity detector coupled with gas chromatography (TCD-GC).



Scheme 4.3. Conversion of alcohol **1a** to aldehyde **2a** and molecular hydrogen under standard conditions.

Table 4.1. Conversion of alcohol **1a** to aldehyde **2a** and hydrogen under various conditions.^a

Entry	Changes from Scheme 4.3.	Yield (%)	
		Aldehyde (2a) ^b	H ₂ ^c
1	without Ru/SrTiO ₃ :Rh	< 1	< 1
2	SrTiO ₃ :Rh instead of Ru/SrTiO ₃ :Rh	2	< 1
3	Pt/SrTiO ₃ :Rh instead of Ru/SrTiO ₃ :Rh	3	< 1
4	without H ₃ PO ₄ aq	2	2
5	without toluene	77	80
6	hexane instead of toluene	68	67
7	CH ₂ Cl ₂ instead of toluene	26	21
8	CH ₃ CN instead of toluene	2	< 1
9	at 5 °C	60	55

^a Conditions: **1a** (0.5 mmol), toluene (10.0 mL), H₃PO₄ aq. (pH 3.4, 5 mL) and Ru/SrTiO₃:Rh (5.3 mg) under visible light irradiation (> 420 nm). ^b Determined by ¹H NMR spectroscopic measurements by using 1,1,2,2-tetrachloroethane as an internal standard. ^c Determined by TCD-GC.

The influence of the different reaction parameters was evaluated with alcohol **1a** (Table 4.1). The presence of Ru/SrTiO₃:Rh was found to be essential, with the reaction hardly proceeding without catalyst or using SrTiO₃:Rh or Pt/SrTiO₃:Rh instead (entries 1–3). Meanwhile, aqueous solvent was also found to be critical (entry 4). Reaction without toluene or with hexane instead of toluene did give aldehyde **2a** albeit in a lower yield than that under standard conditions (entries 5 and 6). In contrast, when polar solvents, such as dichloromethane and acetonitrile were used instead of toluene, the yield of aldehyde **2a** was significantly lower (entries 7 and 8). The reaction also proceeded at 5 °C and gave aldehyde **2a** in a moderated yield (entry 9).

Substrate scope

The scope of the Ru/SrTiO₃:Rh-catalyzed alcohol dehydrogenation is outlined in Table 4.2. The ΔG° of the reaction was estimated by using DFT calculation at M06-2X/6-311++G** level.^{20,21} Most reactions were predicted as endergonic ($\Delta G^\circ > 0$) indicating that the thermodynamic cost of the reaction needs to be supplied for promoting the reaction in a closed system. Various *p*-substituted benzyl alcohols could be converted to the corresponding aldehydes in good-to-excellent yields (entries 1–10). Dehydrogenation of alcohols bearing aryl silyl ether (**1c**), bromo (**1d**) and ester (**1e**) gave the desired aldehydes **2c–2e** in high yields. Although benzyl alcohol **1g** bearing an electron-withdrawing *p*-nitro group, was less active, desired product **2g** could be obtained in a moderated yield (entry 7). Interestingly, redox-sensitive functional groups, such as ketone, olefin, and alkyne moieties in **1h–1j** were tolerated under this reaction conditions despite the presence of H₂ in the reaction vessel (entries 8–10). *o*- or *m*-Substituted benzyl alcohols **1k–1m** could also be converted to the desired products **2k–2m** in excellent yields. Doubly dehydrogenated product **2n** was obtained from diol **1n** (entry 14). In the case of 1,4-diol **1o**, Ru/SrTiO₃ promotes the exothermic dehydrogenative lactonization⁶ and lactone **3o** was obtained in 82% NMR yield (68% isolated yield, entry 15). Saturated aliphatic alcohol **1p** showed lower reactivity than benzyl alcohols, yet gave aldehyde **2p** in 51% yield together with the corresponding carboxylic acid in 15% and molecular hydrogen in 82% yields (entry 16). Importantly, allylic olefins in alcohols **1q–1t** were tolerated under the reaction conditions and enals **2q–2t** were obtained in moderate to excellent yields with high preservation of the

stereochemical integrity (entries 17–20). Such chemoselectivity under the current conditions shows a stark contrast to the previously reported alcohol dehydrogenation under thermal conditions where olefin moieties are reduced by the co-produced H₂.^{4a,c,d}

Table 4.2. Catalytic conversion of primary alcohols **1** to aldehydes **2** or ester **3**.^a

$$\text{R-CH}_2\text{-OH} \xrightarrow[\text{N}_2, 25^\circ\text{C}, 24\text{ h}]{\begin{array}{l} h\nu (\lambda > 420\text{ nm}) \\ \text{Ru/SrTiO}_3\text{:Rh (1a/Rh = 700)} \\ \text{toluene/H}_3\text{PO}_4\text{ aq (pH 3.4)} \end{array}} \text{R-CHO} \quad \text{or} \quad \text{R}^1\text{-C(=O)-O-CH}_2\text{-R}^2 + \text{H}_2$$

1, 0.2 mmol 2 3

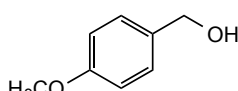
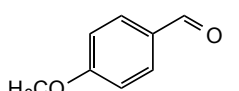
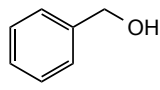
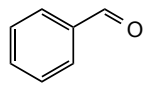
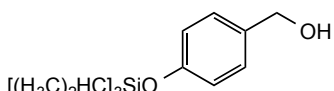
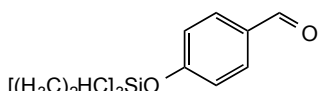
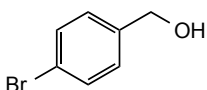
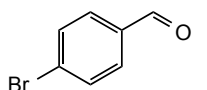
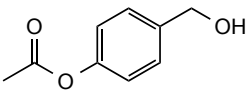
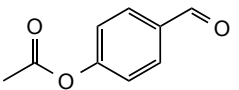
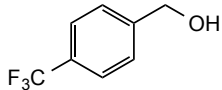
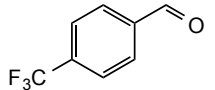
Entry	Alcohol (1)	Aldehyde (2) or ester (3)	Yield (%)		ΔG° (kJ mol ⁻¹)
			2 or 3 ^b	H ₂ ^c	
1			> 95 (89)	95	+18.9
2			> 95	88	+26.9
3			91 (80)	78	+17.6
4			> 95 (84)	> 99	+29.0
5			84	77	+25.0
6			86	> 99	+34.7

Table 4.2. *Continued.*^a

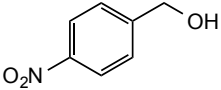
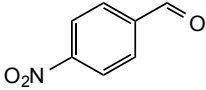
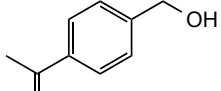
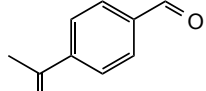
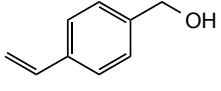
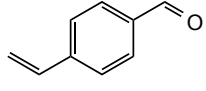
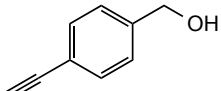
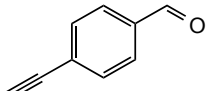
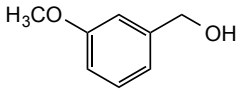
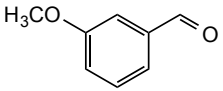
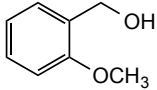
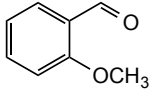
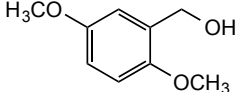
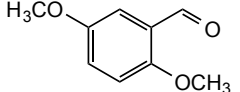
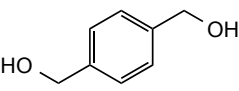
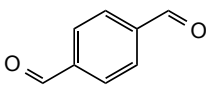
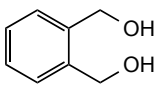
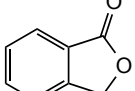
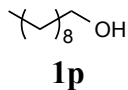
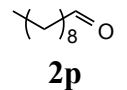
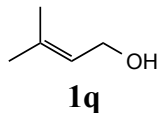
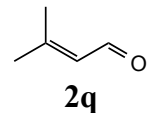
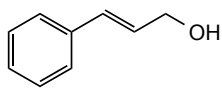
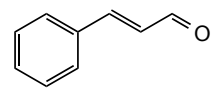
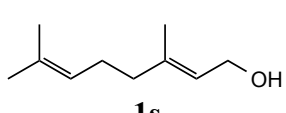
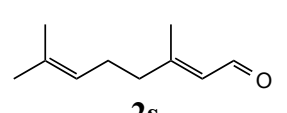
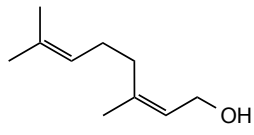
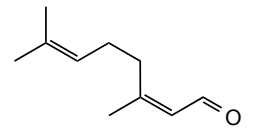
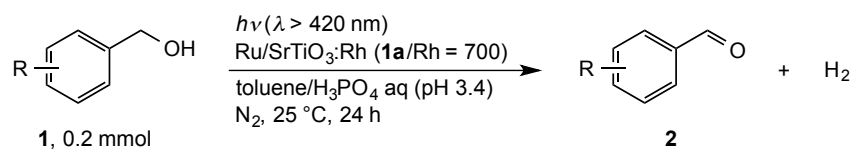
7			42	57	+39.6
	1g	2g			
8			> 95 (86)	98	+32.3
	1h	2h			
9			63	74	+23.9
	1i	2i			
10			90	98	+31.3
	1j	2j			
11			> 95	90	+27.6
	1k	2k			
12			> 95	93	+35.5
	1l	2l			
13			> 95	97	+16.4
	1m	2m			
14			92 (87)	> 99	+25.2
	1n	2n			
15			82 (68)	> 99	-9.7
	1o	3o			

Table 4.2. *Continued.*^a

16			51	82	–
17			57	57	+26.7
18			89	82	+9.6
19			> 95	> 99	+23.8
20			> 95	96	+19.7

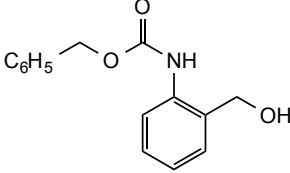
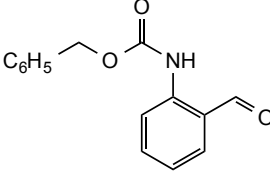
^a Conditions: **1** (0.2 mmol), toluene (10.0 mL), H₃PO₄ aq (pH 3.4, 5 mL) and Ru/SrTiO₃:Rh (5.3 mg) under visible light irradiation (> 420 nm). ^b Determined by ¹H NMR spectroscopic measurements by using 1,1,2,2-tetrachloroethane as an internal standard. Isolated yields are shown in parentheses. ^c Determined by TCD-GC.

Aminobenzaldehydes are one of the important compounds with various applications, such as polymer synthesis and visual colorimetric method for hydrazine.¹⁹ Whereas 4-(dimethylamino)benzyl alcohol (**1u**) showed low reactivity in this reaction (Table 4.3. entry 1), various *N*-protected benzyl alcohols **1v–1z** could be converted to the corresponding aldehydes in good-to-excellent yields (Table 4.3, entries 2–6). *N*-Acyl- and *N*-carbamoyl-amino group in these alcohols remained intact. *N*-Protected *o*-substituted aminobenzyl alcohols are less reactive, but *N*-acyl- or *N*-carbamoylalcohols **1y** and **1z** were converted to corresponding aldehydes **2y** and **2z** in moderate yields (entries 5 and 6).

Table 4.3. Catalytic conversion of *N*-protected benzyl alcohols **1** to benzaldehydes **2**.

Entry	Alcohol (1)	Aldehyde (2)	Isolated yield (%)	ΔG° (kJ mol ⁻¹)
1			8 ^b	+5.5
2			85	+26.3
3			51	+26.9
4			97	+23.4
5			79	+7.2

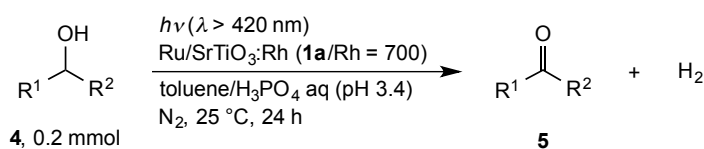
Table 4.3. *Continued.*^a

6	 <p>1z</p>	 <p>2z</p>	40	+11.3
---	--	--	----	-------

^a Conditions: **1** (0.2 mmol), toluene (10.0 mL), H₃PO₄ aq (pH 3.4, 5 mL) and Ru/SrTiO₃:Rh (5.3 mg) under visible light irradiation ($\lambda > 420$ nm). ^b Determined by ¹H NMR spectroscopic measurements by using 1,1,2,2-tetrachloroethane as an internal standard.

The Ru/SrTiO₃:Rh system was also applied to the dehydrogenation of secondary alcohols **4** to ketones **5**. Various aliphatic and aromatic ketones **5a–5d** were obtained in good-to-high yields (Table 4.4).

Table 4.4. Catalytic conversion of secondary alcohols **4** to ketones **5**.^a



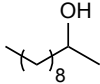
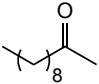
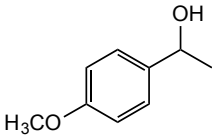
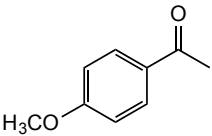
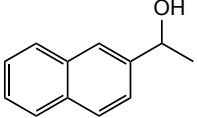
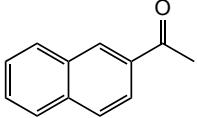
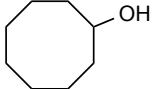
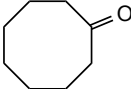
Entry	Alcohol (4)	Ketone (5)	Yield (%)		ΔG° (kJ mol ⁻¹)
			5 ^b	H ₂ ^c	
1	 <p>4a</p>	 <p>5a</p>	68	90	+23.6
2	 <p>4b</p>	 <p>5b</p>	88	115	+8.0

Table 4.4. *Continued.*^a

3			91	102	+30.2
	4c	5c			
4			96	99	+13.8
	4d	5d			

^a Conditions: **4** (0.2 mmol), toluene (10.0 mL), H₃PO₄ aq (pH 3.4, 5 mL) and Ru/SrTiO₃:Rh (5.3 mg) under visible light irradiation (> 420 nm). ^b Determined by ¹H NMR spectroscopic measurements by using 1,1,2,2-tetrachloroethane as an internal standard. Isolated yields are shown in parentheses. ^c Determined by TCD-GC.

Reaction profile

Nature of the Ru/SrTiO₃:Rh-catalyzed dehydrogenation under visible light irradiation has been discussed in Table 4.1. To evaluate the potential effectiveness of this reaction in organic synthesis as well as to obtain further mechanistic insights in this reaction, the author carried out a series of experiments using alcohol **1a** as model substrate. Conclusions are as follows:

(1) Formation of aldehyde **2a** and H₂ can most simply be described as an apparent dehydrogenation of alcohol **1a** promoted by the light irradiation. The yield of **2a** and H₂ were comparable throughout the reaction under light irradiation and remained unchanged under dark conditions (Figure 4.5).

(2) The reaction could be promoted with sunlight as an energy source. Alcohol **1a** was converted to aldehyde **2a** in 54% yield and H₂ in 62 % yield for 8 h under sunlight irradiation (Figure 4.6).

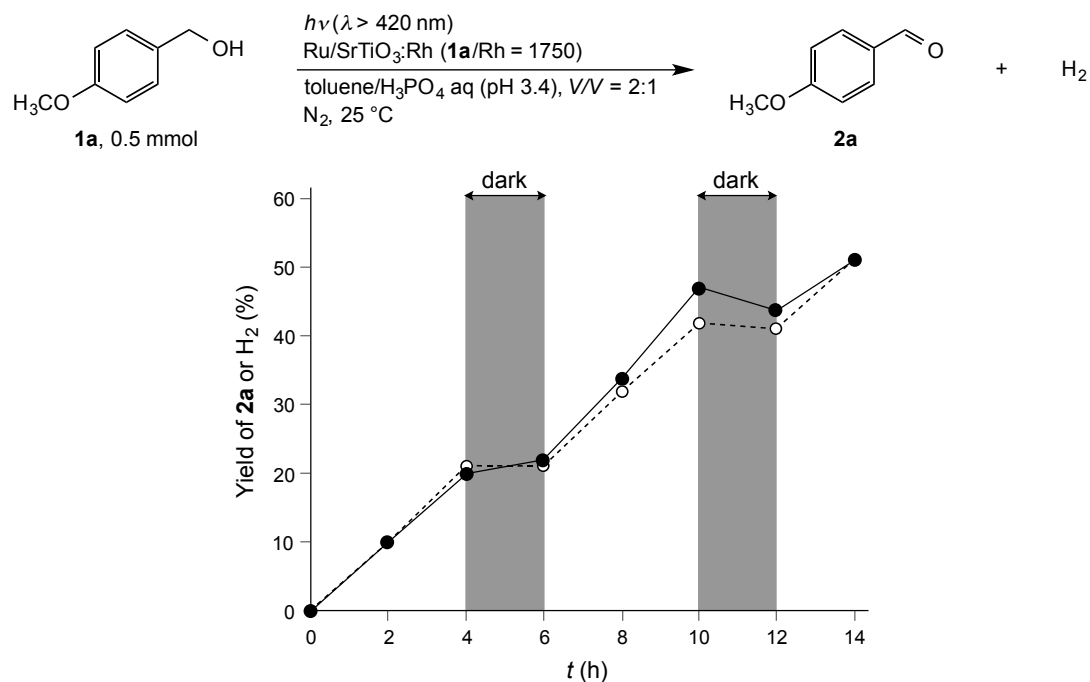


Figure 4.5. Reaction profile of the photocatalytic conversion of **1a** to **2a** (●) and H₂ (○).

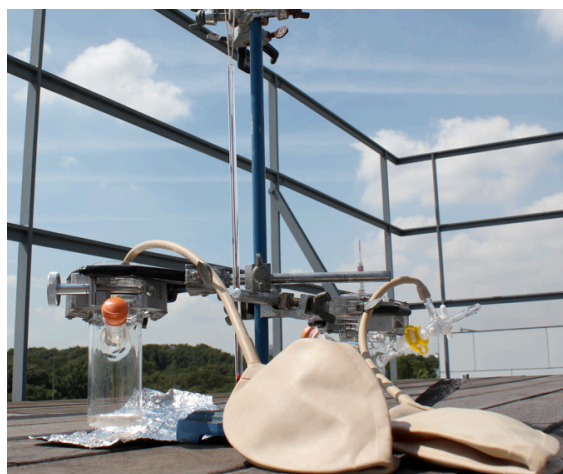
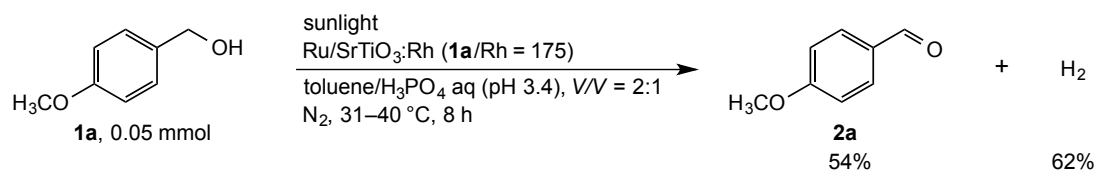


Figure 4.6. Conversion of **1a** to **2a** and H₂ under sunlight irradiation.

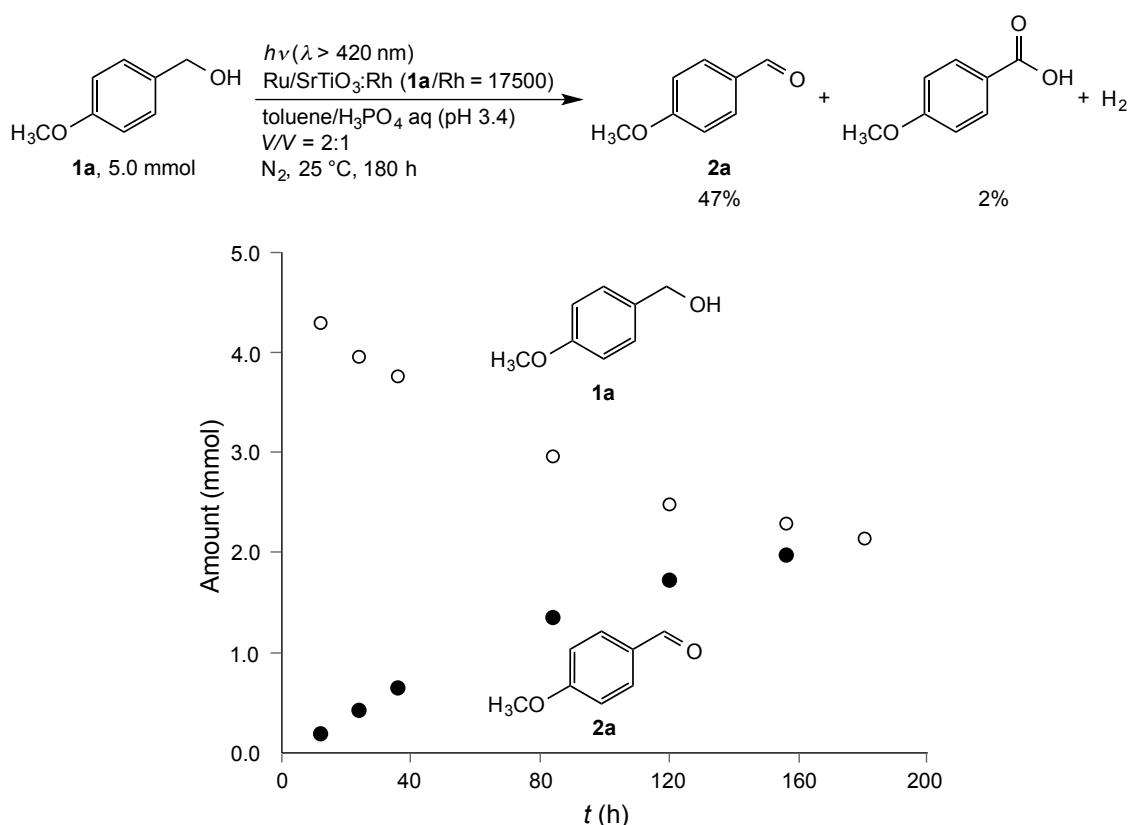
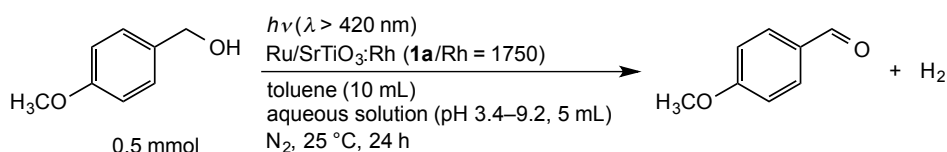


Figure 4.7. Amount of **1a** (○) and **2a** (●) in the dehydrogenation of **1a** for 180 h. Initial amount of **1a**: 5.0 mmol.

(3) The Ru/SrTiO₃:Rh catalyst is robust under continuous light irradiation. As shown in Figure 4.7, Ru/SrTiO₃:Rh showed the catalytic activity more than one week. When the 5.0 mmol of **1a** was used as substrate, Ru/SrTiO₃:Rh catalyzed the dehydrogenation of alcohol **1a** for 180 h and finally provided **2a** in 43% yield with 92% selectivity. The Rh-based turnover number reached 15,400.

(4) The photocatalyst operates with a wide range of pH values (Table 4.5). The reaction also proceeds under more neutral (entries 3 and 4) than standard conditions (pH 3.4) or basic conditions (entries 5–6). The results indicated that this system is potentially applicable to the dehydrogenation of various alcohols bearing acid- or base-sensitive functional groups by controlling pH of a reaction mixture.

Table 4.5. Dependence of the photocatalytic activity of Ru/SrTiO₃:Rh on pH values.^a

Entry	pH of buffer ^b	Yield (%)	
		Aldehyde ^c	H ₂ ^d
1	3.4	92	99
2	4.0	75	49
3	5.3	57	64
4	7.1	59	61
5	8.2	56	61
6	9.2	53	68

^a Conditions: **1a** (0.5 mmol), toluene (10.0 mL), buffer (pH 3.4–9.2, 5 mL) and Ru/SrTiO₃:Rh (5.3 mg) under visible light irradiation (> 420 nm). ^b pH adjusted with H₃PO₄ or K₂CO₃ aq. ^c Determined by ¹H NMR spectroscopic measurements by using 1,1,2,2-tetrachloroethane as an internal standard. ^d Determined by TCD-GC.

(5) The current reaction is promoted by the light-induced electronic transition from an impurity band of SrTiO₃:Rh provided by doped Rh³⁺ to a conduction band of SrTiO₃. Dehydrogenation of **1a** occurred under light irradiation with a longer wavelength, even at a wavelength around 500 nm (Figure 4.8). The band edge around 500 nm corresponds to electronic transitions from an Rh³⁺ electron donor level to a conduction band of SrTiO₃.^{17,18} The apparent quantum yield of dehydrogenation of **1a** was around 0.2% at 420 nm, calculated by the following equation (eq 1 and Scheme 4.4).

Apparent quantum yield (%)

$$\begin{aligned}
 &= [\text{Number of reacted electrons or holes}] / [\text{Number of incident photons}] \times 100\% \\
 &= [\text{Molecular number of aldehyde} \times 2] / [\text{Number of incident photons}] \times 100\% \quad (1)
 \end{aligned}$$

This value is broadly in line with those of photocatalytic reactions using SrTiO₃:Rh catalyst, such as H₂ evolution in water/methanol mixtures (5.2%),^{17a} Z-Scheme water splitting (0.3%)^{17b} and photoelectrochemical water splitting (0.18%).^{17d}

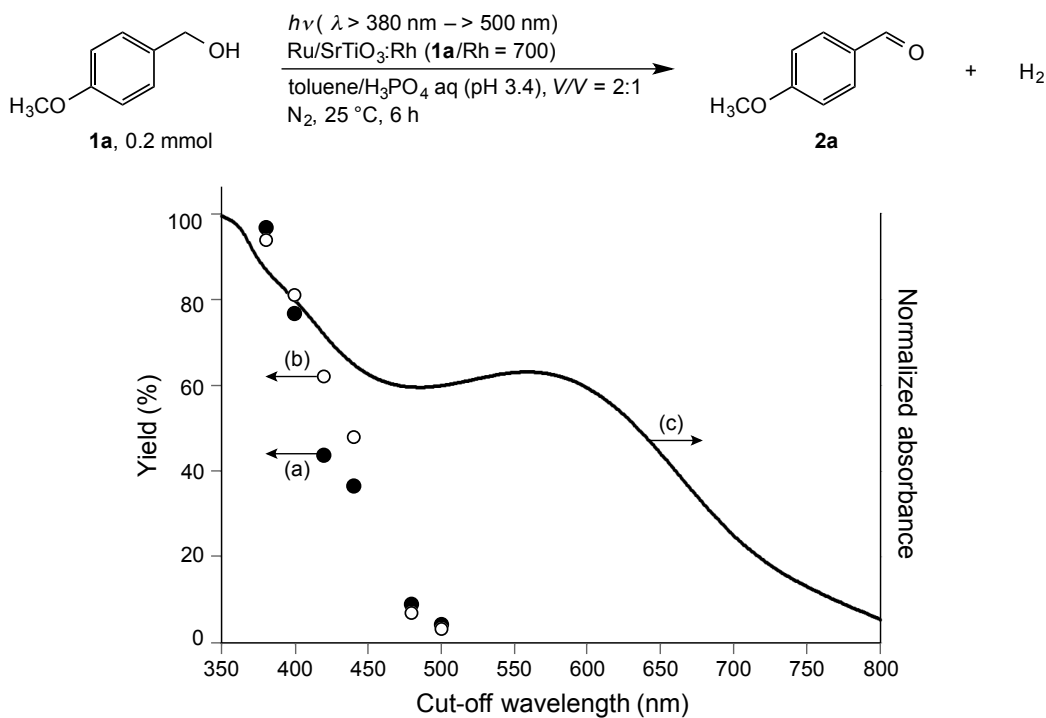
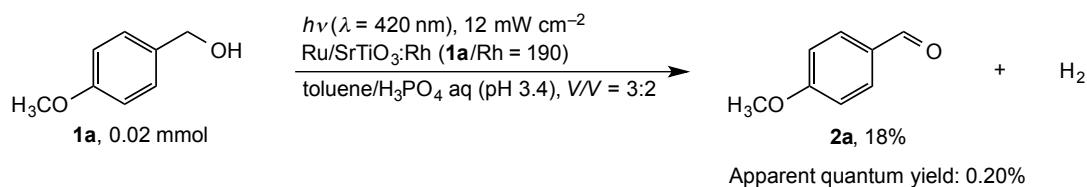


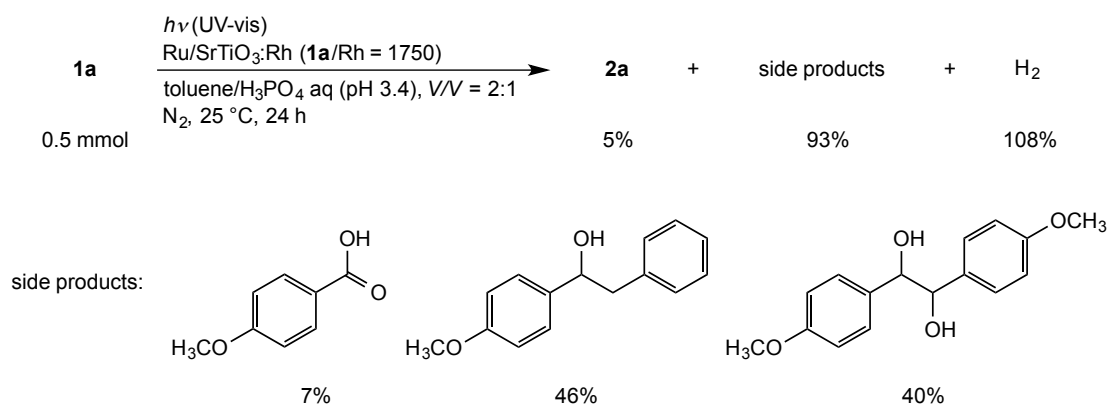
Figure 4.8. Photoresponse of the SrTiO₃:Rh in the dehydrogenation of **1a** to **2a**. (a,b) Yields of **2a**(●) and H₂ (○). (c) Diffuse reflectance spectrum of SrTiO₃:Rh; Light source: 300 W Xe lamp with cut off filters at the indicated wavelength.



Scheme 4.4. Apparent quantum yield of dehydrogenation of **1a**.

(6) The use of visible light is prerequisite for high selectivity. The reaction without a cut-off filter ($\lambda = 200\text{--}1100 \text{ nm}$) provided **2a** only in a lower yield (5% ¹H NMR

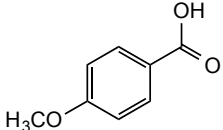
yield) and molecular hydrogen as high as in 108% yield. The reason of the low yield is due to side reactions, that produced 4-methoxybenzoic acid (7%), 1-(4-methoxyphenyl)-2-phenylethanol (46%) and 1,2-di(4-methoxyphenyl)ethanediol (40%) caused by UV light irradiation emitted from the Xe light source (Scheme 4.5).



Scheme 4.5. Dehydrogenation of **1a** under UV-visible light irradiation.

Table 4.6. Effect of the presence of alcohol **1a** on the selectivity ($\lambda > 420 \text{ nm}$).

$$\mathbf{1a} + \mathbf{2a} \xrightarrow[\text{N}_2, 25^\circ\text{C}, 24 \text{ h}]{\begin{array}{l} h\nu (\lambda > 420 \text{ nm}) \\ \text{Ru/SrTiO}_3:\text{Rh} (5.3 \text{ mg}) \\ \text{toluene/H}_3\text{PO}_4 \text{ aq (pH 3.4), V/V = 2:1} \end{array}} \mathbf{1a} + \mathbf{2a} + \text{4-methoxybenzoic acid} + \text{H}_2$$

Entry	Substrates (mmol)		Products (mmol)			
	1a	2a	1a	2a		H ₂
1	0.50	0	0.04	0.45	< 0.01	0.49
2	0	0.50	< 0.01	0.44	0.06	0.03
3	0.50	0.50	0.29	0.70	0.02	0.18

(7) The presence of alcohol in the reaction media suppress the overoxidation. As shown in Table 4.6, entry 1, dehydrogenation of **1a** (0.5 mmol) provides **2a** selectively, but irradiation of **2a** instead of **1a** results in a significant formation of the corresponding carboxylic acid (0.06 mmol, 12% based on **2a**, entry 2). This side reaction is effectively suppressed in the presence of alcohol **1a** (entry 3).

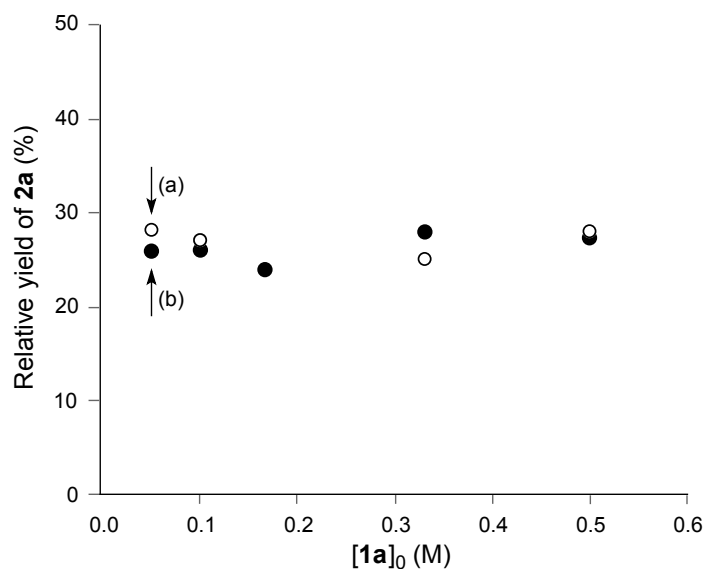
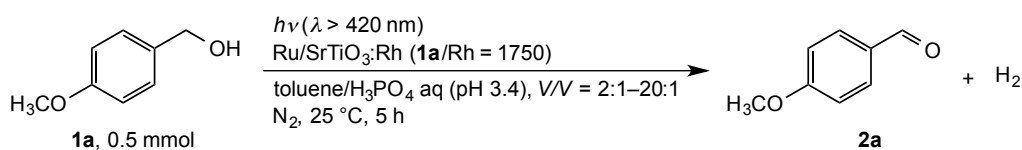


Figure 4.9. Dependence of yield on initial substrate concentrations. The relative yields of **2a** to **1a** were calculated by comparison of the peak area between **1a** and **2a** obtained by (a) GC-MS (●) and (b) ¹H NMR (○).

(8) The adsorption of substrate on the solid surface of Ru/SrTiO₃:Rh is not a rate-determining process under standard conditions. The initial alcohol concentration does not affect the yield of aldehyde (Figure 4.9). The result suggests that the reaction rate is 0th order with respect to the concentration of **1a**, which is consistent with the diffusion control.

Proposed reaction mechanism

With the above mechanistic insights in hand, a proposed reaction mechanism for the photocatalytic dehydrogenation of alcohols with Ru/SrTiO₃:Rh is shown in Figure 4.10. The reaction occurs at the photocatalyst dispersed in the interface of organic and aqueous phases. In such a biphasic system, alcohol and proton can be sufficiently adsorbed on the surface of catalyst. Visible light irradiation of the photocatalyst induces charge separation of holes (h⁺) and electrons (e⁻). The photoexcited electrons are transferred to the conduction band of SrTiO₃ and holes are generated in the impurity band of SrTiO₃:Rh.^{17a} The transferred electrons migrate from the conduction band (Ti⁴⁺_{3d}) to Ru nanoparticles loaded on the surface of SrTiO₃:Rh. The electrons in the Ru nanoparticles with protons (H⁺) generate molecular hydrogen (H₂).

Simultaneous to the reaction sequence with electrons, the photogenerated hole (Rh³⁺_{4d} or Rh⁴⁺_{4d}) abstracts electron from alcohol on the surface, giving protons the other way around. The oxidized alcohol, an α-hydroxyl carbon radical intermediate (HOĊR), is further converted to the aldehyde by liberating another e⁻ to the photocatalyst, as well as H⁺ to the reaction media. However the reaction intermediate would not be a “free” carbon radical, because no olefin isomerization proceeds with allylic substrates (Table 4.2, entries 17–20).

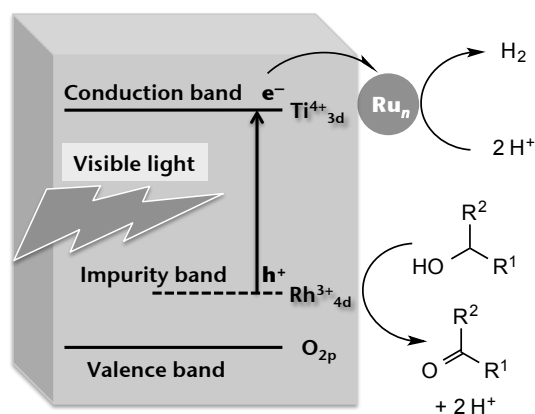


Figure 4.10. Proposed mechanism of dehydrogenation of alcohols.

4.4 Conclusions

Ru/SrTiO₃:Rh promotes the dehydrogenation of alcohols to aldehydes under visible-light irradiation. Ru/SrTiO₃:Rh is applicable to the dehydrogenation of a wide variety of alcohols, where the presence of redox- or base-sensitive functional groups, such as olefin, alkyne, ketone and amide or carbamates. In addition, various allylic olefin moieties in alcohols are also tolerated and corresponding products with high preservation of stereochemical integrity.

4.5 Experimental section

General comments

¹H and ¹³C NMR spectra were recorded on a JEOL ECA-600 (600 MHz for ¹H, 150 MHz for ¹³C) or a JEOL ECA-500 (500 MHz for ¹H, 125 MHz for ¹³C) at 25 °C. Chemical shifts are reported as δ in ppm and are internally referenced to tetramethylsilane (TMS, 0.00 ppm for ¹H), CD₂HSOCD₃ (2.50 ppm for ¹H), CDCl₃ (77.2 ppm for ¹³C) or dimethyl sulfoxide-*d*₆ (DMSO-*d*₆, 39.5 ppm for ¹³C). Infrared (IR) spectra were recorded on a FT-IR6100 (JASCO). High-resolution mass spectrometry (HRMS) was recorded with a JEOL JMS-T100GCV spectrometer. These analytical experiments were carried out at the Chemical Instrumental Center, Research Center for Materials Science, Nagoya University. Melting points were recorded on an OptiMelt automated melting point system (Stanford Research Systems). MS was conducted with an Agilent GC system (Agilent 5975) coupled with an MS system (Agilent 6850). Diffuse reflectance spectra (DRS) were recorded on UV-2450 (SHIMADZU) and were converted from reflection to absorbance by the Kubelka–Munk method. The amount of H₂ was determined by TCD-GC (Agilent 490) using argon as a carrier. X-ray diffraction (XRD) patterns were recorded on a Rigaku MiniFlex diffractometer using Cu Ka radiation. Scanning electron microscopy (SEM) images were recorded on a JEOL JSM-6700F. Thermogravimetric analysis (TGA) was carried out on a Shimadzu TGA-50. Photocatalytic reactions were performed in cylindrical Pyrex glass reaction vessel (diameter: 50 mm, height: 130 mm) with a top window made of Pyrex (diameter: 50 mm) unless otherwise noted. The cylindrical vessels were heated at 230–300 °C under

vacuum for 24 h prior to the reaction.²² The light source was a 300 W Xe lamp (Ushino: BA-x300/ES1 Technology; CERMAX PE300BF) equipped with cold mirror and cutoff filters (HOYA L42) to control the wavelength of the incident light. For the determination of apparent quantum yield, reaction was carried out in 5 mL-Pyrex glass reaction tube with a top window made of Pyrex (diameter: 10 mm), using a 300 W Xe lamp (Ushino Technology; CERMAX LX-300F) equipped with a cutoff filter (HOYA), a band-pass filter (Asahi Spectra Co. 420 nm), and fiber optics. The number of incident photons was measured by a photodiode (OPHIR; PD300-UV-ROHS head and Nova power monitor). DFT calculations were carried out using the Gaussian 09 program package.²⁰ Geometries were optimized at the M06-2X/6-311++G** level of theory.²¹ Free energies (ΔG°) were computed at the same level.

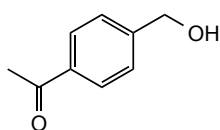
Materials

SrCO₃, TiO₂, Rh₂O₃, RuCl₃•3H₂O, 4-methoxybenzyl alcohol (**1a**), benzyl alcohol (**1b**), 4-bromobenzyl alcohol (**1d**), 4-trifluoromethylbenzyl alcohol (**1f**), 4-nitrobenzyl alcohol (**1g**), 3-methoxybenzyl alcohol (**1k**), 2-methoxybenzyl alcohol (**1l**), 2,5-methoxybenzyl alcohol (**1m**), 1,4-benzenedimethanol (**1n**), 1,2-benzenedimethanol (**1o**), 1-decanol (**1p**), 3-methyl-2-buten-1-ol (**1q**), cinnamyl alcohol (**1r**), geraniol (**1s**), nerol (**1t**), 2-decanol (**4a**), 1-(4-methoxyphenyl)ethanol (**4b**), 1-(2-naphthyl)ethanol (**4c**) and cyclooctanol (**4d**) were purchased from Aldrich, Furuya Metal Co., Ltd., TCI or Wako, and used without further purification. 4-(Triisopropylsilyloxy)phenylmethanol (**1c**),²³ 4-(hydroxymethyl)phenyl acetate (**1e**),²⁴ (9*H*-fluoren-9-yl)methyl [4-(hydroxymethyl)phenyl]carbamate (**1w**),²⁵ *N*-(2-formylphenyl)acetamide (**1y**),²⁶ were prepared according to the literature procedures. 1-[4-(Hydroxymethyl)phenyl]ethanone (**1h**) and 4-vinylbenzyl alcohol (**1i**), 4-ethynylbenzyl alcohol (**1j**), 4-(dimethylamino)benzyl alcohol (**1u**), 4-acetamidobenzyl alcohol (**1v**), 4-(Cbz-amino)benzyl alcohol (**1x**), *N*-(2-formylphenyl)acetamide (**1y**) and (2-hydroxymethyl-phenyl)-carbamic acid benzyl ester (**1z**) were synthesized as shown in below by modifying the literature procedures.

Catalyst Preparation

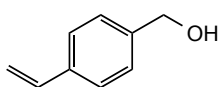
A typical procedure for the preparation of Ru/SrTiO₃:Rh. SrTiO₃:Rh (1 wt % Rh) was prepared by SrCO₃ powder (1524.0 mg, 10.3 mmol) treated in air at 300 °C for 1 h before use, TiO₂ (791.7 mg, 9.9 mmol) and Rh₂O₃ (12.8 mg, 0.05 mmol) followed by calcination in air at 1000 °C for 10 h using an alumina crucible. To a 300 mL round-bottom flask, SrTiO₃:Rh (400 mg), the aqueous solution of RuCl₃•3H₂O (36 mM, 770 μL) and 2-butanol were added. The mixture was heated at 110 °C for 3 h, and filtered. The solid was washed with water and acetone and dried under air atmosphere overnight to afford Ru/SrTiO₃:Rh as gray powder.

Synthesis of alcohols



1-[4-(Hydroxymethyl)phenyl]ethanone (1h).²⁸ To a solution of 4-ethynylbenzyl alcohol (233 mg, 1.76 mmol) in methanol (4 mL), Co^{III}TPPSCI²⁷ (16.1 mg, 0.9 mol %) and water (10 mL) were added.

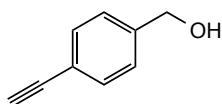
The solution was heated to 100 °C under air in the dark for 30 min. After having been cooled to rt, the mixture was extracted with ethyl acetate. The organic layers were collected and dried over Na₂SO₄. The product **1h** was purified by column chromatography on silica gel (hexane/ethyl acetate = 1:1). White solid, 0.25 g, 94% yield. Mp 56.7–58 °C (lit.²⁸ 51–54 °C). ¹H NMR (600 MHz, CDCl₃) δ 2.60 (s, 1H), 4.78 (s, 2H), 7.46 (d, *J* = 8.2 Hz, 2H), 7.95 (d, *J* = 8.2 Hz, 2H); ¹³C{¹H} NMR (600 MHz, CDCl₃) δ 26.7, 64.7, 126.7, 128.7, 136.5, 146.3, 197.9.



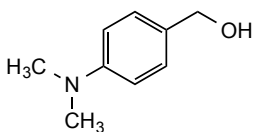
4-Vinylbenzyl alcohol (1i).²⁹ To a degassed mixture of terephthalaldehyde (0.81 g, 6.0 mmol) and methyltriphenylphosphonium iodide (2.02 g, 5.0 mmol) in *N,N*-dimethylformamide (DMF, 10 mL), anhydride potassium carbonate (2.9 g, 20 mmol)

was added. The mixture was refluxed under a N₂ atmosphere for 1 h, then cooled to rt and filtered. The filtrate was poured into 150 mL water and extracted with ethyl acetate. The organic layer was washed with brine, dried over Na₂SO₄, and concentrated. Aldehyde **2i** was purified by column chromatography on silica gel (hexane only). Colorless oil, 0.49 g, 75% yield. ¹H NMR (600 MHz, CDCl₃) δ 5.43 (d, *J* = 11.0 Hz, 1H), 5.91 (d, *J* = 17.9 Hz, 1H), 6.77 (dd, *J* = 11.0, 17.9 Hz, 1H), 7.54 (d, *J* = 8.2 Hz, 2H), 7.84 (d, *J* = 7.6 Hz, 2H), 9.99 (s, 1H). ¹³C{¹H} NMR (600 MHz, CDCl₃) δ 117.5, 126.8,

130.1, 135.7, 135.9, 143.5, 191.8. The oil was dissolved in 10 mL methanol, and the solution was cooled to 0–5 °C in an ice bath. NaBH₄ (222 mg, 6.0 mmol) was added in three portions within 1 h. Then the solution was stirred at rt for another 1 h. The solvent was removed in a rotary evaporator, the residue was dissolved in NH₄Cl aq, and the solution was extracted with ethyl acetate. The organic layers were collected and dried over Na₂SO₄. The product **1i** was purified by column chromatography on silica gel (hexane/ethyl acetate = 3:1–1:1). Colorless oil, 0.46 g, 92% yield. ¹H NMR (600 MHz, DMSO-*d*₆) δ 4.48 (d, *J* = 5.5 Hz, 2H), 5.16–5.22 (m, 2H), 5.78 (d, *J* = 18.0 Hz, 1H), 6.77 (dd, *J* = 11.0 Hz, 17.9 Hz, 1H), 7.28 (d, *J* = 8.3 Hz, 2H), 7.41 (d, *J* = 7.6 Hz, 2H); ¹³C{¹H} NMR (600 MHz, DMSO-*d*₆) δ 63.2, 114.1, 126.3, 127.1, 136.1, 137.0, 142.8.

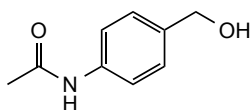


4-Ethynylbenzyl alcohol (1j).³⁰ To a solution of CuI (19 mg, 0.1 mmol, 1 mol %), PdCl₂[P(C₆H₅)₃]₂ (70 mg, 0.1 mmol, 1 mol %), and 4-bromobenzyl alcohol (1.89 g, 10.0 mmol) in N(CH₂CH₃)₃ (15 mL), trimethylsilyl acetylene (0.98 g, 10.0 mmol) was added. The mixture was degassed and heated at 70 °C for 36 h under a N₂ atmosphere. The resulting dark brown mixture was filtered and concentrated *in vacuo*. Crude product was purified by column chromatography on silica gel (hexane/ethyl acetate = 5:1) to obtain coupling product **M1**. White solid, 1.1 g, 54% yield. Mp 71.6–72.6 °C (lit.³¹ 66 °C). ¹H NMR (600 MHz, DMSO-*d*₆) δ 4.49 (d, *J* = 5.5 Hz, 2H), 5.25 (t, *J* = 5.5 Hz, 1H), 7.29 (d, *J* = 8.2 Hz, 2H), 7.39 (d, *J* = 7.6 Hz, 2H); ¹³C{¹H} NMR (600 MHz, DMSO-*d*₆) δ 0.44, 63.0, 94.0, 105.9, 120.9, 127.0, 131.9, 144.2. **M1** (0.75 g, 3.7 mmol) was dissolved in THF (10 mL), and TBAF (1 M THF solution, 0.4 mL, 0.4 mmol, 9 mol %) was added. The mixture was stirred at room temperature for 30 min and then the solvent was removed under reduced pressure. The residue was purified by silica gel column chromatography (hexane/ethyl acetate = 4:1–1:1 gradient) to afford the alkyne **1j** quantitatively. A white solid was obtained after recrystallization (from hexane), 0.48 g, 98% yield. Mp 40.6–41.9 °C (lit.³⁰ 37–38.5 °C). ¹H NMR (600 MHz, DMSO-*d*₆) δ 4.08 (s, 1H), 4.50 (d, *J* = 5.5 Hz, 2H), 5.26 (t, *J* = 4.2 Hz, 1H), 7.31 (d, *J* = 9.6 Hz, 2H), 7.41 (d, *J* = 10.3 Hz, 2H); ¹³C{¹H} NMR (600 MHz, DMSO-*d*₆) δ 63.0, 80.6, 84.1, 120.4, 127.0, 132.0, 144.1.

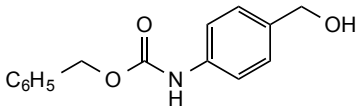


4-(Dimethylamino)benzyl alcohol (1u).³² To a solution of 4-(dimethylaminobenzyl) aldehyde (0.75 g, 3.4 mmol) in CH₃OH, NaBH₄ (0.2 g, 5.3 mmol) was added. The mixture was stirred for 2 h at 0–5 °C. After removed methanol, the residue was dissolved in NH₄Cl aq and

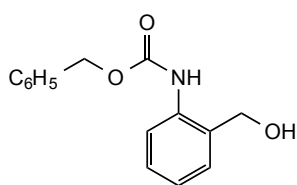
extracted with ethyl acetate. The organic layer was concentrated and crude product was purified by column chromatography on silica gel (hexane/ethyl acetate = 1:3) to afford the alcohol **1u**. 0.5 g, 66% yield. ¹H NMR (600 MHz, CDCl₃) δ 1.53 (s, 1H), 2.94 (s, 6H), 4.54–4.58 (m, 2H), 6.72 (d, *J* = 8.94 Hz, 2H), 7.24 (d, *J* = 8.94 Hz, 2H); ¹³C{¹H} NMR (150 MHz, CDCl₃) δ 40.6 (2C), 65.3, 112.6 (2C), 128.6 (2C), 128.9, 150.3.



4-Acetamidobenzyl alcohol (1v).³³ To a solution of 4-aminobenzyl alcohol (0.50 g, 4.1 mmol) and N(CH₂CH₃)₃ (2.5 mL) in CH₃COOCH₂CH₃ (10 mL), acetyl chloride (1.0 mL, 14 mmol) was added at 0 °C. The mixture was stirred at 0 °C for 2 h and quenched with ice water. The organic layer was separated and concentrated. Crude product was purified by column chromatography on silica gel (hexane/ethyl acetate = 1:1–1:1.5 gradient) to obtain white solid. The solid was dissolved in CH₃OH, and KOH aq were added. The mixture was stirred at rt for 3 h and then CH₃OH was removed under reduced pressure. The crude mixture was extracted with ethyl acetate and the organic layer was combined and concentrated to afford the alcohol **1v**. Light yellow powder, 0.35 g, 47% yield. Mp 118–121 °C. ¹H NMR (600 MHz, CDCl₃) δ 1.59 (s, 1 H), 2.18 (s, 3H), 4.66 (s, 1H), 7.17 (s, 1H), 7.33 (d, *J* = 8.22 Hz, 2H), 7.49 (d, *J* = 8.28 Hz, 2H); ¹³C{¹H} NMR (150 MHz, CDCl₃) δ 24.6, 65.0, 119.9 (2C), 127.8 (2C), 136.8, 137.3, 168.2.



4-(Cbz-amino)benzyl alcohol (1x). To a solution of 4-aminobenzyl alcohol (0.37 g, 3.0 mmol), THF (10 mL) and NaHCO₃ aq, phenylchloroformate (0.4 mL, 3.2 mmol) was added at 5–10 °C. The mixture was stirred for 20 min at 5–10 °C. The organic layer was separated and concentrated. Crude product was purified by column chromatography on silica gel (hexane/ethyl acetate = 1:1) to afford the alcohol **1x**. White solid, 0.59 g, 81% yield. Mp 98–100 °C. IR (KBr) 1243, 1533, 1704, 3313 cm⁻¹; ¹H NMR (600 MHz, DMSO-*d*₆) δ 4.43 (d, *J* = 6.18 Hz, 2H), 5.08 (t, *J* = 3.51 Hz, 1H), 5.15 (s, 2H), 7.23 (d, *J* = 8.28 Hz, 2H), 7.34 (t, *J* = 6.18 Hz, 1H), 7.45–7.38 (m, 6H), 9.71 (br, 1H); ¹³C{¹H} NMR (150 MHz, DMSO-*d*₆) δ 62.6, 65.7, 117.9 (2C), 127.0 (2C), 128.0, 128.1 (2C), 128.4 (2C), 136.56, 136.64, 137.7, 153.4; HRMS (EI) *m/z* calcd for C₁₅H₁₅NO₃ 257.1052, found 257.1048.

**(2-Hydroxymethyl-phenyl)-carbamic acid benzyl ester**

(1z).³² To a solution of *o*-aminobenzyl alcohol (0.37 g, 3.0 mmol), THF (10 mL) and NaHCO₃ aq, phenylchloroformate (0.5 mL, 3.3 mmol) was added at 0 °C. The mixture was stirred for 20 min at 0 °C. The organic layer was separated and concentrated. Crude product was purified by column chromatography on silica gel (hexane/ethyl acetate = 1:1) to afford the alcohol **1z**. White solid, 0.56 g, 72% yield. Mp 88–90 °C. ¹H NMR (600 MHz, CDCl₃) δ 2.02 (t, *J* = 6.18 Hz, 1H), 4.69 (d, *J* = 5.52 Hz, 2H), 5.20 (s, 2H), 7.03 (t, *J* = 7.56 Hz, 1H), 7.16 (d, *J* = 7.56 Hz, 1H), 7.36–7.30 (m, 2H), 7.38 (t, *J* = 6.74 Hz, 2H), 7.42 (d, *J* = 6.84 Hz, 2H), 7.96 (s, 2H); ¹³C{¹H} NMR (150 MHz, CDCl₃) δ 64.4, 67.0, 120.6, 123.4, 128.3 (3C), 128.6 (2C), 128.8, 129.3, 136.1, 137.7, 138.8, 153.9.

Dehydrogenation of alcohols**A typical procedure for dehydrogenation of alcohols: 4-methoxybenzaldehyde (2a, Table 4.2, entry 1).**

Alcohol **1a** (0.20 mmol), Ru/SrTiO₃: Rh (5.3 mg), H₃PO₄ aq (pH 3.4, 5.0 mL) and toluene (10.0 mL) were added successively to a cylindrical Pyrex glass reaction vessel (diameter: 50 mm, height: 130 mm with a top window made of Pyrex) connected to a balloon. The catalyst assembled in the interface of toluene and aqueous layers after shaking. Then the vessel was sealed and covered with aluminum foil except the top window. The atmosphere was replaced with nitrogen by means of five evacuate-fill sequences, then the vessel was immersed in a water bath (kept at 25 °C using a cooling circulator) and was irradiated with a 300 W Xe lamp (Ushino: BA-x300/ES1 Technology; CERMAX PE300BF) equipped with cold mirror and cutoff filters (HOYA L42) for 24 h. The H₂ evolution was checked by means of micro-GC (Agilent 490, Ar carrier) before the suspension was filtered using a Millipore membrane filter (0.45 μm) with a syringe. The organic layer was separated, and the aqueous layer was extracted with ethyl acetate. The organic layers were combined, and concentrated. ¹H NMR analysis of this crude mixture using 1,1,2,2-tetrachloroethane as an internal standard indicated the formation of amide **2a** in 95% yield.

The identity of aldehydes **2** was confirmed by comparing the ¹H NMR spectra with the reported data or those of commercial samples. ¹H NMR data of **2c**,³⁵ **2e**,³⁶ **2h**,³⁷ **2i**,³⁸

2j,³⁹ **2m**,⁴⁰ **2q**,⁴¹ **2s**,⁴² **2t**,⁴² **2v**,⁴³ **2w**,²⁵ **2x**,⁴⁴ **2y**,⁴⁵ **2z**,³⁴, **5a**,⁴⁶ and **5d**⁴⁷ are available in literatures. Aldehydes **2a**, **2b**, **2d**, **2f**, **2g**, **2k**, **2l**, **2n**, **2p**, **2r**, **2u**, **3o**, **5b** and **5c** are commercially available. The yields of **2b**, **2f**, **2q** and **5c** were determined by directly monitoring the toluene layer of the reaction mixture using ¹H NMR because of their low boiling point.

Reaction profile of the photocatalytic conversion of 1a to 2a and H₂ (Figure 4.5). As per the above-mentioned typical procedure, the mixture including alcohol **1a** (0.50 mmol) and 1,1,2,2-tetrachloroethane (20 μL) were irradiated with a 300 W Xe lamp equipped with cold mirror and cutoff filters (HOYA L42) for 24 h.

Conversion of 1a to 2a and H₂ under sunlight irradiation (Figure 4.6). The reaction mixture (**1a**, 0.05 mmol) was exposed to sunlight on the roof of the building without stirring from 10:00 am to 6:00 pm on July 18th, 2012, at Nagoya, Japan.

Dehydrogenation using 5 mmol of 1 for 180 h (Figure 4.7). As per the above-mentioned typical procedure, the mixture including alcohol **1a** (5.0 mmol) was irradiated with a 300 W Xe lamp equipped with cold mirror and cutoff filters (HOYA L42) for 24 h.

Photoresponse of the SrTiO₃:Rh in the dehydrogenation of 1a to 2a. (Figure 4.8). As per the above-mentioned typical procedure, the reaction mixture was irradiated with a 300 W Xe lamp equipped with cold mirror and cutoff filters (HOYA L38, L40, L42, L44, L48 and L50) for 6 h.

Dependence of yield on initial substrate concentration (Figure 4.9). As per the above-mentioned typical procedure, the mixture including alcohol **1a** (0.50 mmol) and the different amount of toluene (1, 3, 5 and 10 mL) were irradiated with a 300 W Xe lamp equipped with cold mirror and cutoff filters (HOYA L42) for 24 h. The relative yields of were calculated by comparison of the peak area between **1a** and **2a** obtained by GC-MS and ¹H NMR.

4.6. References and notes

- 1 a) J. D. Holladay, J. Hu, D. L. King and Y. Wang, *Catal. Today*, 2009, **139**, 244–260. b) G. E. Dobereiner and R. H. Crabtree, *Chem. Rev.*, 2010, **110**, 681–703. c) C. Gunanathan and D. Milstein, *Science*, 2013, **341**, 249–260. d) M. Trincado, D. Banerjee and H. Grützmacher, *Energy Environ. Sci.*, 2014, **7**, 2464–2503.
- 2 a) T. Matsumoto, M. Ueno, N. Wang and S. Kobayashi, *Chem. Asian J.*, 2008, **3**, 196–214. b) *Oxidation of Alcohols to Aldehydes and Ketones. Basic Reactions in Organic Synthesis*, ed. G. Tojo and M. Fernández, Springer, New York, 2010.
- 3 a) S. Musa, I. Shaposhnikov, S. Cohen and D. Gelman, *Angew. Chem. Int. Ed.*, 2011, **50**, 3533–3537. b) G. Zeng, S. Sakaki, K. Fujita, H. Sano and R. Yamaguchi, *ACS Catal.*, 2014, **4**, 1010–1020.
- 4 a) K. Fujita, T. Yoshida, Y. Imori and R. Yamaguchi, *Org. Lett.*, 2011, **13**, 2278–2281. b) A. Prades, E. Peris and M. Albrecht, *Organometallics*, 2011, **30**, 1162–1167. c) R. Kawahara, K. Fujita and R. Yamaguchi, *J. Am. Chem. Soc.*, 2012, **134**, 3643–3646. d) R. Kawahara, K. Fujita and R. Yamaguchi, *Angew. Chem. Int. Ed.*, 2012, **51**, 12790–12794.
- 5 a) J. Zhao and J. F. Hartwig, *Organometallics*, 2005, **24**, 2441–2446. b) J. Zhang, G. Leitus, Y. B.-David and D. Milstein, *J. Am. Chem. Soc.*, 2005, **127**, 10840–10841. c) J. Zhang, E. Balaraman, G. Leitus and D. Milstein, *Organometallics*, 2011, **30**, 5716–5724. d) A. Sølvhøj and R. Madsen, *Organometallics*, 2011, **30**, 6044–6048.
- 6 K. Fujita, W. Ito and R. Yamaguchi, *ChemCatChem*, 2014, **6**, 109–112.
- 7 a) F. H. A. Bolder, *Ind. Eng. Chem. Res.*, 2008, **47**, 7496–7500. b) Y. Mikami, K. Ebata, T. Mitsudome, T. Mizugaki, K. Jitsukawa and K. Kaneda, *Heterocycles*, 2010, **80**, 855–861.
- 8 C. Gunanathan, L. J. W. Shimon and D. Milstein, *J. Am. Chem. Soc.*, 2009, **131**, 3146–3147.
- 9 W. Fang, J. Chen, Q. Zhang, W. Deng and Y. Wang, *Chem. Eur. J.*, 2011, **17**, 1247–1256.
- 10 a) J. B. Pedley, R. D. Naylor, S. P. Kirby, *Thermochemical Data of Organic Compounds Ed. 2*, Chapman & Hall, London, 1986. b) Z. Jin, Q. Li, X. Zheng, C. Xi, C. Wang, H. Zhang, L. Feng, H. Wang, Z. Chen, Z. Jiang, *J. Photochem. Photobiol. A*, 1993, **71**, 85–96.

- 11 a) Y. Shiraishi and T. Hirai, *J. Photochem. Photobiol. C*, 2008, **9**, 157–170. b) M. Zhang, C. Chen, W. Ma and J. Zhao, *Angew. Chem. Int. Ed.*, 2008, **47**, 9730–9733. c) H. Schmaderer, P. Hilgers, R. Lechner and B. König, *Adv. Synth. Catal.*, 2009, **351**, 163–174. d) S. Higashimoto, K. Okada, T. Morisugi, M. Azuma, H. Ohue, T. H. Kim, M. Matsuoka and M. Anpo, *Top. Catal.*, 2010, **53**, 578–583. e) V. Augugliaro and L. Palmisano, *ChemSusChem*, 2010, **3**, 1135–1138. f) G. Palmisano, E. G.-López, G. Marci, V. Loddo, S. Yurdakal, V. Augugliaro and L. Palmisano, *Chem. Commun.*, 2010, **46**, 7074–7089. g) F. Su, S. C. Smitha, G. Lipner, X. Fu, M. Antonietti, S. Blechert and X. Wang, *J. Am. Chem. Soc.*, 2010, **132**, 16299–16301. h) N. Zhang, Y. Zhang, X. Pan, X. Fu, S. Liu and Y. Xu, *J. Phys. Chem. C*, 2011, **115**, 23501–23511. i) S. Higashimoto, K. Okada, M. Azuma, H. Ohue, T. Terai and Y. Sakata, *RSC Adv.*, 2012, **2**, 669–676. j) N. Zhang, S. Liu, X. Fu and Y. Xu, *J. Mater. Chem.*, 2012, **22**, 5042–5052. k) D. Tsukamoto, Y. Shiraishi, Y. Sugano, S. Ichikawa, S. Tanaka and T. Hirai, *J. Am. Chem. Soc.*, 2012, **134**, 6309–6315. l) A. Tanaka, K. Hashimoto and H. Kominami, *J. Am. Chem. Soc.*, 2012, **134**, 14526–14533. m) L. Shen, S. Liang, W. Wu, R. Lianga and L. Wu, *Dalton Trans.*, 2013, **42**, 13649–13657. n) Y. Zhang and Y.-J. Xu, *RSC Adv.*, 2014, **4**, 2904–2910. o) M. Xie, X. Dai, S. Meng, X. Fu and S. Chen, *Chem. Eng. J.*, 2014, **245**, 107–116. p) S. Furukawa, T. Shishido, K. Teramura and T. Tanaka, *ChemPhysChem*, 2014, **15**, 2665–2667.
- 12 W. Zhai, S. Xue, A. Zhu, Y. Luo and Y. Tian, *ChemCatChem*, 2011, **3**, 127–130.
- 13 T. Mitkina, C. Stanglmair, W. Setzer, M. Gruber, H. Kisch and B. König, *Org. Biomol. Chem.*, 2012, **10**, 3556–3561.
- 14 T. P. A. Ruberu, N. C. Nelson, I. I. Slowing and J. Vela, *J. Phys. Chem. Lett.*, 2012, **3**, 2798–2802.
- 15 S. Sarina, S. Bai, Y. Huang, C. Chen, J. Jia, E. Jaatinen, G. A. Ayoko, Z. Bao and H. Zhu, *Green Chem.*, 2014, **16**, 331–341.
- 16 Z. Liu, J. Caner, A. Kudo, H. Naka and S. Saito, *Chem. Eur. J.*, 2013, **19**, 9452–9456.
- 17 a) R. Konta, T. Ishii, H. Kato and A. Kudo, *J. Phys. Chem. B*, 2004, **108**, 8992–8995. b) Y. Sasaki, A. Iwase, H. Kato and A. Kudo, *J. Catal.*, 2008, **259**, 133–137. c) A. Kudo and Y. Miseki, *Chem. Soc. Rev.*, 2009, **38**, 253–278. d) K. Iwashina and

- A. Kudo, *J. Am. Chem. Soc.*, 2011, **133**, 13272–13275. e) S. Kawasaki, K. Akagi, K. Nakatsuji, S. Yamamoto, I. Matsuda, Y. Harada, J. Yoshinobu, F. Komori, R. Takahashi, M. Lippmaa, C. Sakai, H. Niwa, M. Oshima, K. Iwashina and A. Kudo, *J. Phys. Chem. C*, 2012, **116**, 24445–24448. f) S. Kawasaki, K. Nakatsuji, J. Yoshinobu, F. Komori, R. Takahashi, M. Lippmaa, K. Mase and A. Kudo, *Appl. Phys. Lett.*, 2012, **101**, 033910. g) Y. Sasaki, H. Kato and A. Kudo, *J. Am. Chem. Soc.*, 2013, **135**, 5441–5449. Morphology and DRS images of Ru/SrTiO₃:Rh before and after its usage, and its energy band gap between valence and conduction bands are shown in refs. 17c–e.
- 18 a) Y. Sasaki, H. Nemoto, K. Saito and A. Kudo, *J. Phys. Chem. C*, 2009, **113**, 17536–17542. b) A. Kudo, *MRS Bull.*, 2011, **36**, 32–38.
- 19 a) M. Heinenberg and H. Ritter, *Macromol. Chem. Phys.*, 1999, **200**, 1792–1805. b) P. G. W. Scott, *J. Pharm. Pharmacol.*, 1952, **4**, 681–686.
- 20 Gaussian 09, Revision B.01, M. J. Frisch, G. W. Trucks, H. B. Schlegel, G. E. Scuseria, M. A. Robb, J. R. Cheeseman, G. Scalmani, V. Barone, B. Mennucci, G. A. Petersson, H. Nakatsuji, M. Caricato, X. Li, H. P. Hratchian, A. F. Izmaylov, J. Bloino, G. Zheng, J. L. Sonnenberg, M. Hada, M. Ehara, K. Toyota, R. Fukuda, J. Hasegawa, M. Ishida, T. Nakajima, Y. Honda, O. Kitao, H. Nakai, T. Vreven, J. A. Montgomery, Jr., J. E. Peralta, F. Ogliaro, M. Bearpark, J. J. Heyd, E. Brothers, K. N. Kudin, V. N. Staroverov, T. Keith, R. Kobayashi, J. Normand, K. Raghavachari, A. Rendell, J. C. Burant, S. S. Iyengar, J. Tomasi, M. Cossi, N. Rega, J. M. Millam, M. Klene, J. E. Knox, J. B. Cross, V. Bakken, C. Adamo, J. Jaramillo, R. Gomperts, R. E. Stratmann, O. Yazyev, A. J. Austin, R. Cammi, C. Pomelli, J. W. Ochterski, R. L. Martin, K. Morokuma, V. G. Zakrzewski, G. A. Voth, P. Salvador, J. J. Dannenberg, S. Dapprich, A. D. Daniels, O. Farkas, J. B. Foresman, J. V. Ortiz, J. Cioslowski, and D. J. Fox, Gaussian, Inc., Wallingford CT, 2010.
- 21 Y. Zhao and D. G. Truhlar, *Acc. Chem. Res.*, 2008, **41**, 157–167.
- 22 A. S. D'Souza and C. G. Pantano, *J. Am. Ceram. Soc.*, 2002, **85**, 1499–1504.
- 23 J. Katzhendler, Y. Klauzner, I. Beylis, M. Mizhiritskii, Y. Shpernat, B. Ashkenazi, and D. Fridland, US2008/0221303.
- 24 H. J. Jessen, T. Schulz, J. Balzarini and C. Meier, *Angew. Chem. Int. Ed.*, 2008, **47**, 8719–8722.

- 25 T. Schadendorf, C. Hoppmann and K. Rück-Braun, *Tetrahedron Lett.*, 2007, **48**, 9044–9047.
- 26 C. Z. Gómez-Castro, I. I. Padilla-Martínez, F. J. Martínez-Martínez and E. V. García-Báeza, *ARKIVOC*, 2008, v, 227–244.
- 27 T. Tachinami, T. Nishimura, R. Ushimaru, R. Noyori and H. Naka, *J. Am. Chem. Soc.*, 2013, **135**, 50–53.
- 28 C. F. Nutall and G. W. Cribble, *Tetrahedron Lett.*, 1983, **24**, 4287–4290.
- 29 L.-J. Zhao, C. K.-W. Kwong, M. Shia and P. H. Toy, *Tetrahedron*, 2005, **61**, 12026–12032.
- 30 S. V. Klyatskaya, E. V. Tretyakov and S. F. Vasilevsky, *Russ. Chem. Bull.*, 2002, **51**, 128–134.
- 31 S. Hiraoka, K. Hirata and M. Shionoya, *Angew. Chem. Int. Ed.*, 2004, **43**, 3814–3818.
- 32 N. S. Shaikh, K. Junge and M. Beller, *Org. Lett.*, 2007, **9**, 5429–5432.
- 33 D. Das, S. Roy and P. K. Das, *Org. Lett.*, 2004, **6**, 4133–4136.
- 34 M. Waibel and J. Hasserodt, *Tetrahedron Lett.*, 2009, **50**, 2767–2769.
- 35 M. A. Ischay, Z. Lu and T. P. Yoon, *J. Am. Chem. Soc.*, 2010, **132**, 8572–8574.
- 36 O. Khersonsky and D. S. Tawfik, *Biochem.*, 2005, **44**, 6371–6382.
- 37 J. Mo, L. Xu and J. Xiao, *J. Am. Chem. Soc.*, 2005, **127**, 751–760.
- 38 T. M. Gøgsig, L. S. Søbjerg, A. T. Lindhardt, K. L. Jensen and T. Skrydstrup, *J. Org. Chem.*, 2008, **73**, 3404–3410.
- 39 M. A. Fazio, O. P. Lee and D. L. Schuster, *Org. Lett.*, 2008, **10**, 4979–4982.
- 40 M. J. Piggott, *Tetrahedron*, 2006, **62**, 3550–3556.
- 41 X. Wang, R. Liu, Y. Jin and X. Liang, *Chem. Eur. J.*, 2008, **14**, 2679–2685.
- 42 a) S. Velusamy, M. Ahamed and T. Punniyamurthy, *Org. Lett.*, 2004, **6**, 4821–4824.
b) M. W. Lodewyk, V. G. Lui and D. J. Tantillo, *Tetrahedron Lett.*, 2010, **51**, 170–173.
- 43 SDBSWeb: <http://sdb.sdb.aist.go.jp/> (National Institute of Advanced Industrial Science and Technology, accessed November 2014) SDBS No. 6315.
- 44 S. D. Straight, J. Andréasson, G. Kodis, A. L. Moore, T. A. Moore and D. Gust, *J. Am. Chem. Soc.*, 2005, **127**, 2717–2724.

- 45 K. Ahmad, N. F. Thomas, M. R. Mukhtar, I. Noorbacha, J.-F. F. Weber, M. A. Nafiah, S. S. Velu, K. Takeya, H. Morita, C.-G. Lim, A. H. A. Hadi and K. Awang, *Tetrahedron*, 2009, **65**, 1504–1516.
- 46 R. Chowdhury and S. K. Ghosh, *Org. Lett.*, 2009, **11**, 3270–3273.
- 47 H. Tanaka, J. Kubota, S. Miyahara and M. Kuroboshi, *Bull. Chem. Soc. Jpn.*, 2005, **78**, 1677–1684.

List of Publications

(副論文)

1. Why *p*-Cymene? Conformational Effect in Asymmetric Hydrogenation of Aromatic Ketones with a η^6 -Arene/ Ruthenium(II) Catalyst
Aki Matsuoka, Christian A. Sandoval, Masanobu Uchiyama, Ryoji Noyori and Hiroshi Naka
Chem. Asian J., 2015, **10**, 112–115.
2. Hydration of Nitriles to Amides by a Chitin-supported Ruthenium Catalyst
Aki Matsuoka, Takahiro Isogawa, Yuna Morioka, Benjamin R. Knappett, Andrew E. H. Wheatley, Susumu Saito and Hiroshi Naka
RSC Adv., 2015, **5**, 12152–12160.

(参考論文)

1. Chiral η^6 -Arene/*N*-Tosylethylenediamine–Ruthenium(II) Complexes: Solution Behavior and Catalytic Activity for Asymmetric Hydrogenation
Christian A. Sandoval, Fusheng Bie, Aki Matsuoka, Yoshiki Yamaguchi, Hiroshi Naka, Yuehui Li, Koichi Kato, Noriyuki Utsumi, Kunihiko Tsutsumi, Takeshi Ohkuma, Kunihiko Murata and Ryoji Noyori
Chem. Asian J., 2010, **5**, 806–816.
2. Acetals of *N,N*-Dimethylformamides: Ambiphilic Behavior in Converting Carbon Dioxide to Dialkyl Carbonates
Yuki Takada, Aki Matsuoka, Ya Du, Hiroshi Naka and Susumu Saito
Chem. Lett., 2013, **42**, 146–147.